Oscillations and Waves

1 Simple Harmonic Oscillation

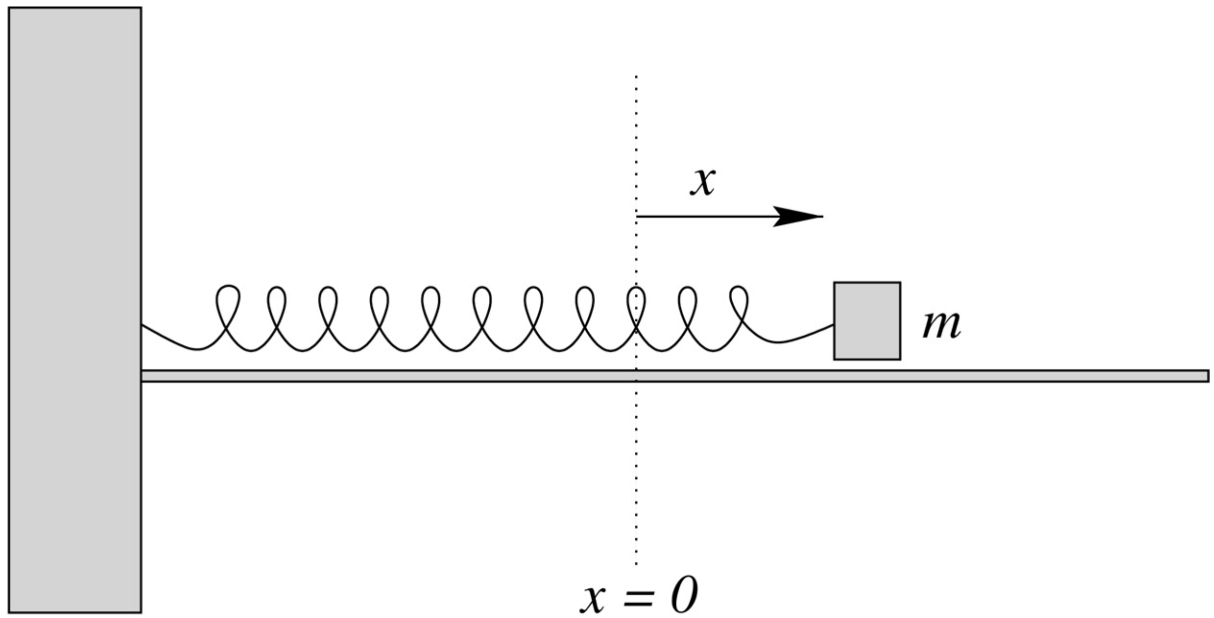

FIGURE 1.1
Mass on a spring.

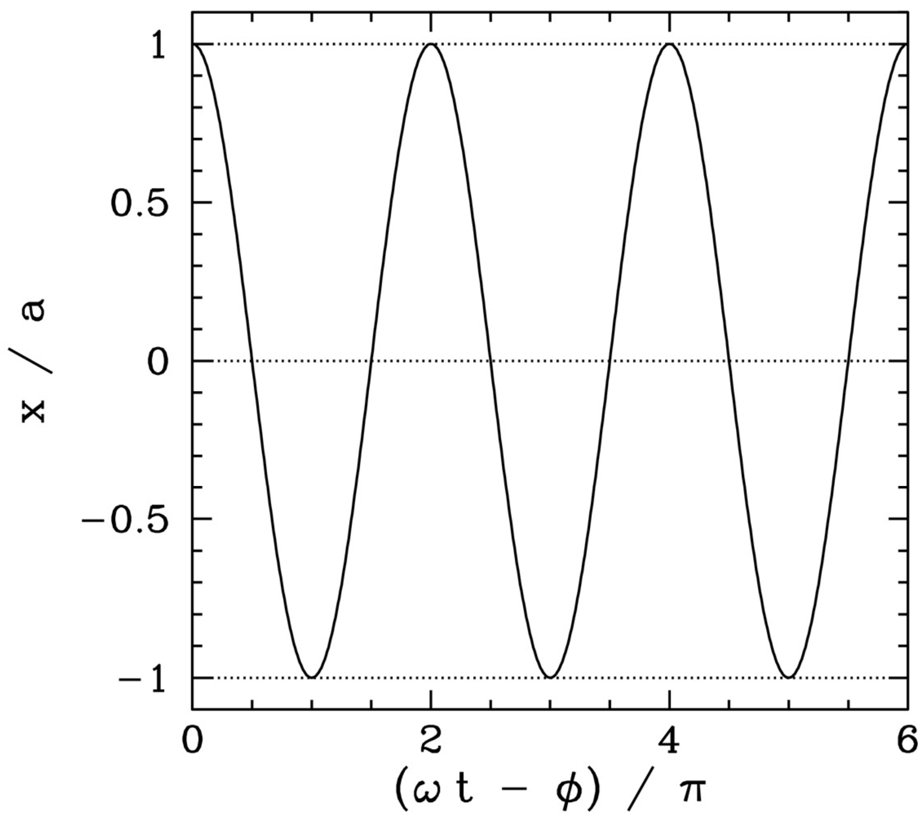

FIGURE 1.2
Simple harmonic oscillation.

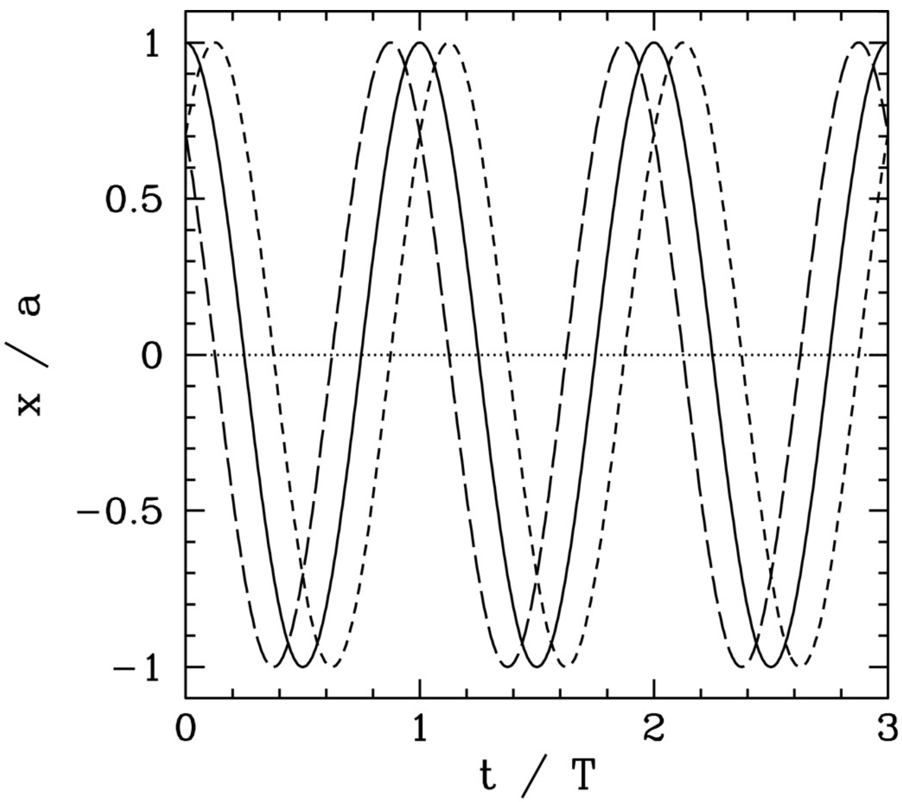

FIGURE 1.3
Simple harmonic oscillation. The solid, short-dashed, and long-dashed curves correspond to $\phi = 0$, $+\pi/4$, and $-\pi/4$, respectively.

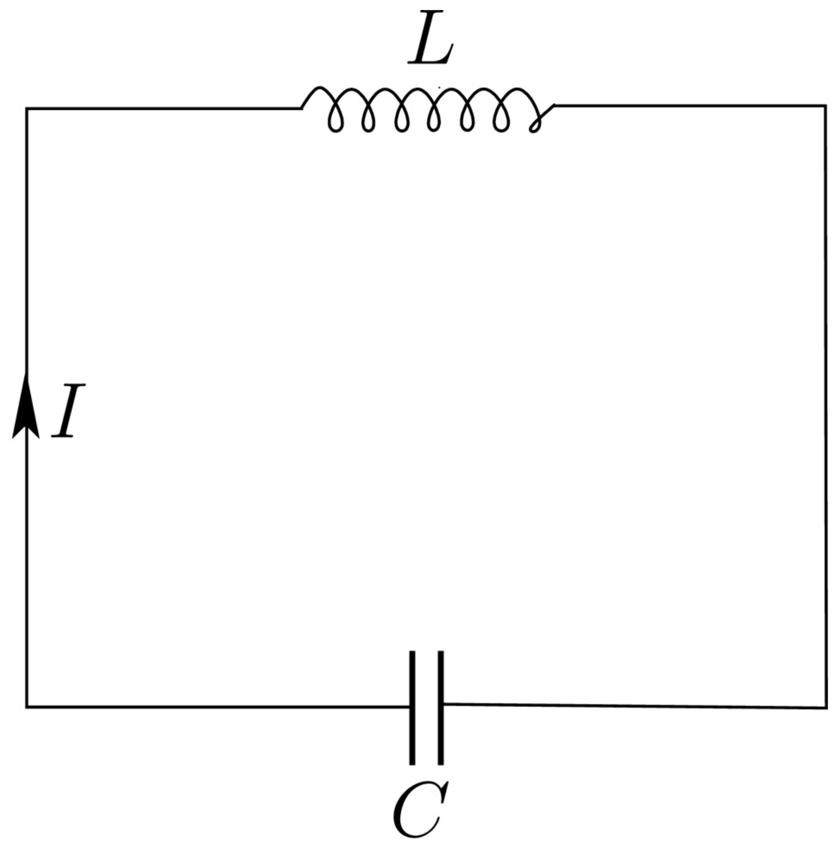

FIGURE 1.4
An LC circuit.

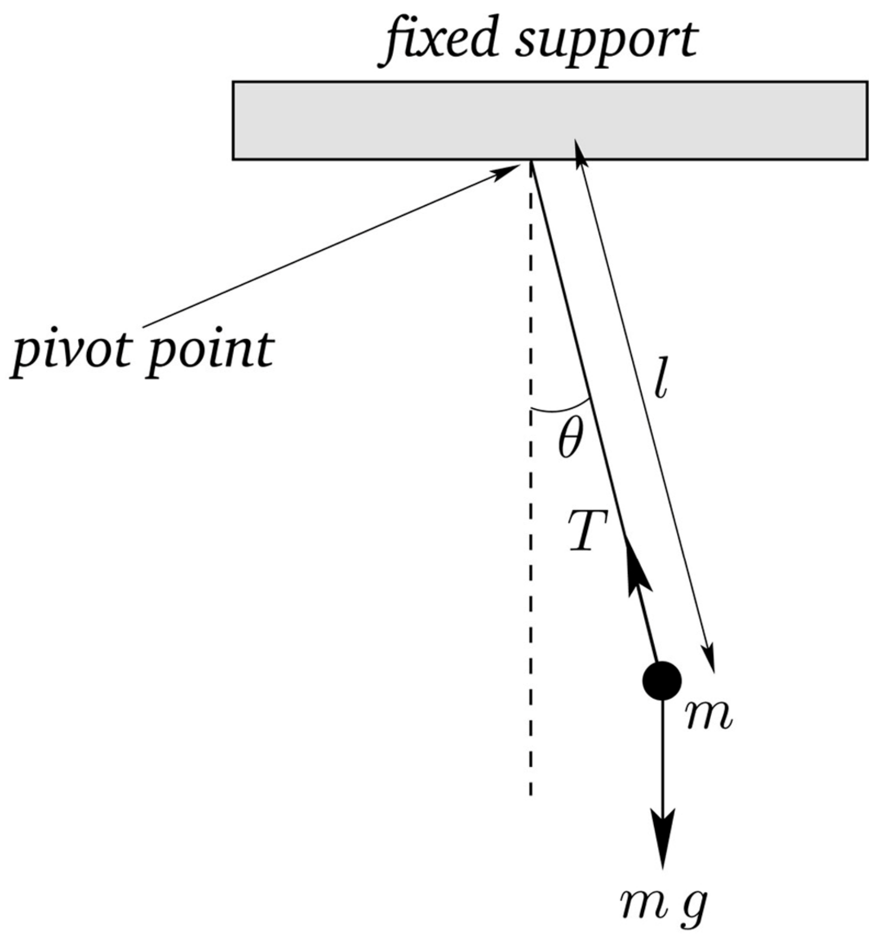

FIGURE 1.5
A simple pendulum.

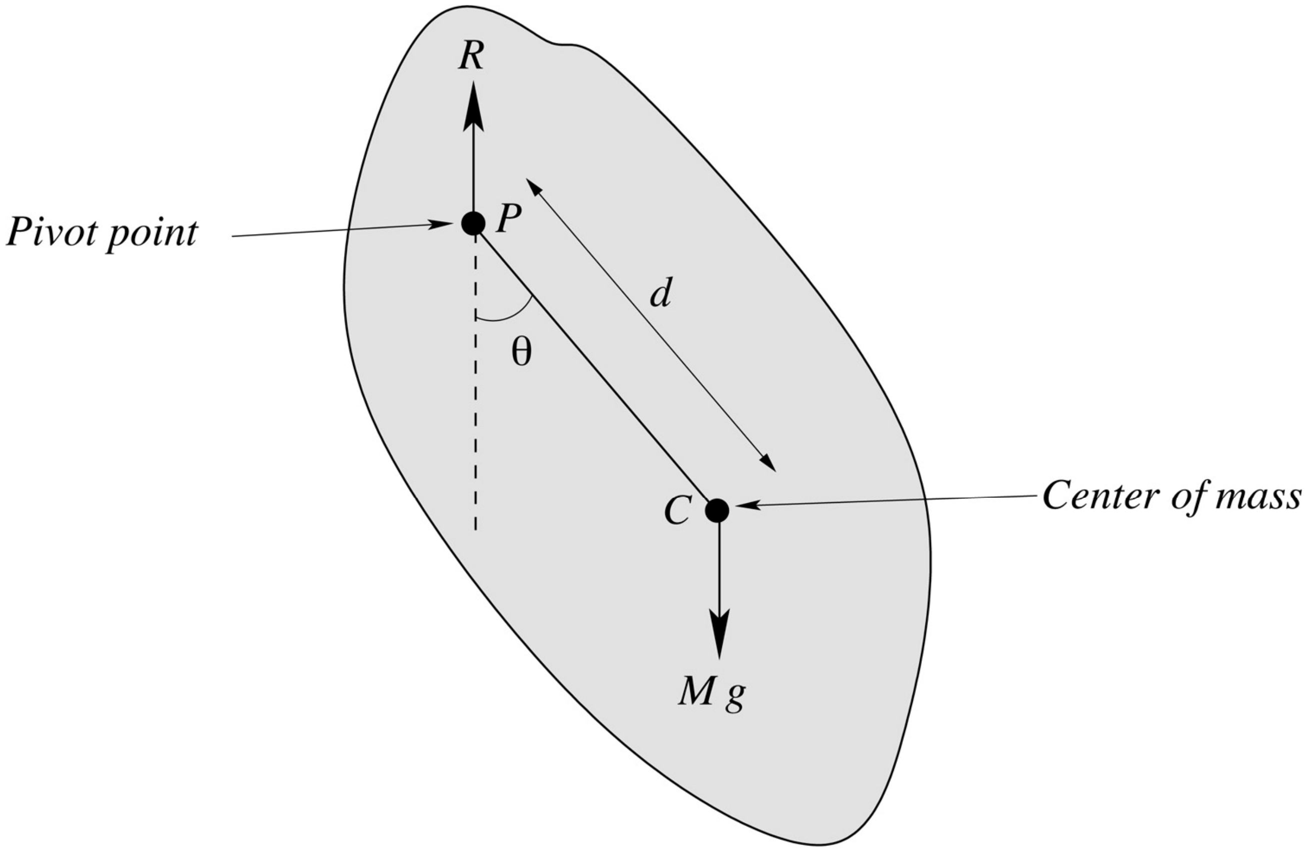

FIGURE 1.6
A compound pendulum.

Oscillations and Waves

2 Damped and Driven Harmonic Oscillation

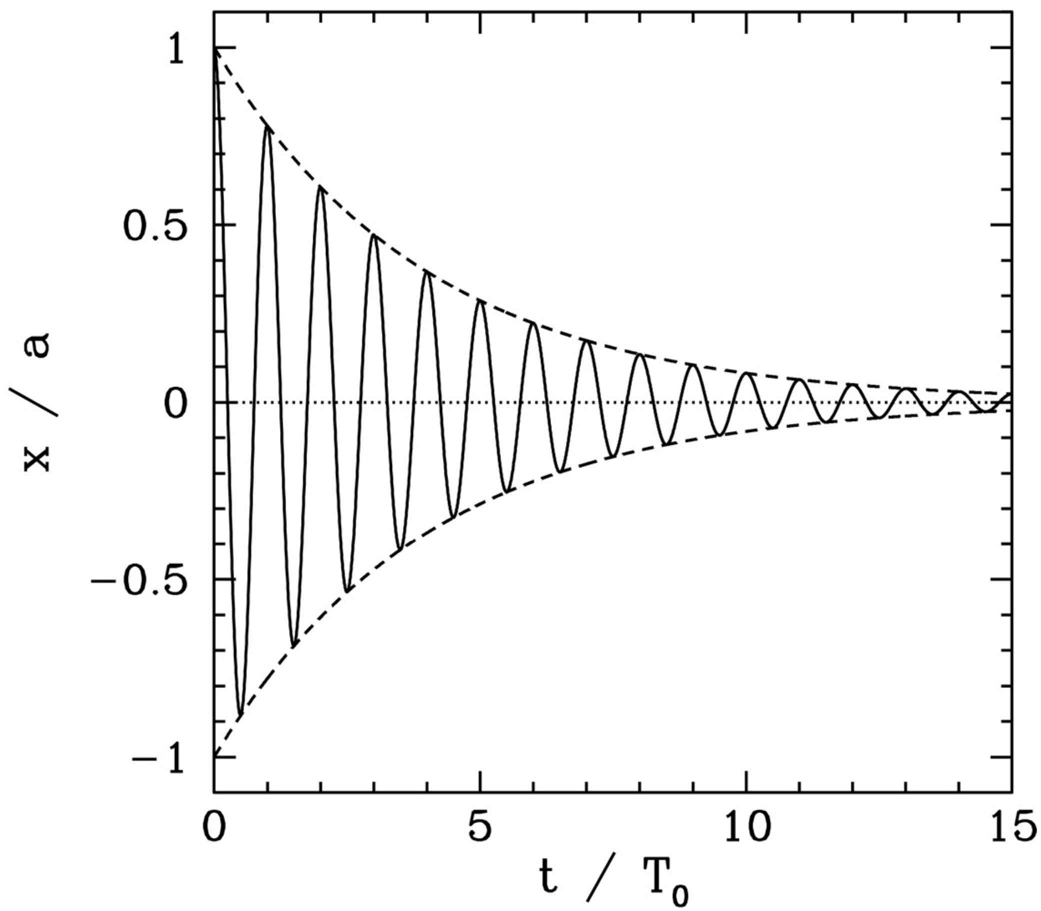

FIGURE 2.1
Damped harmonic oscillation.

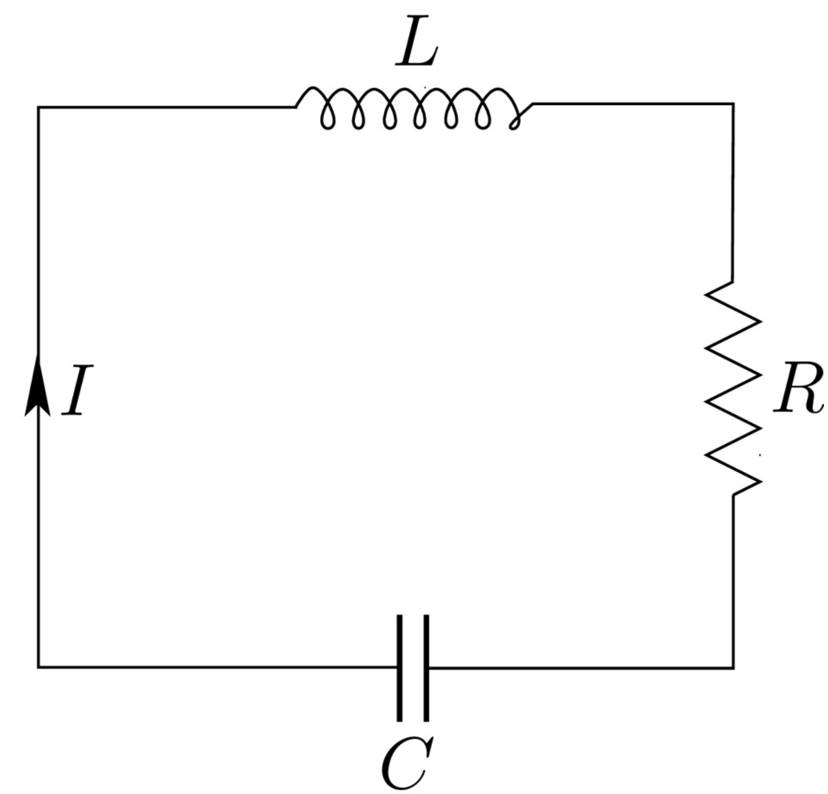

FIGURE 2.2
An LCR circuit.

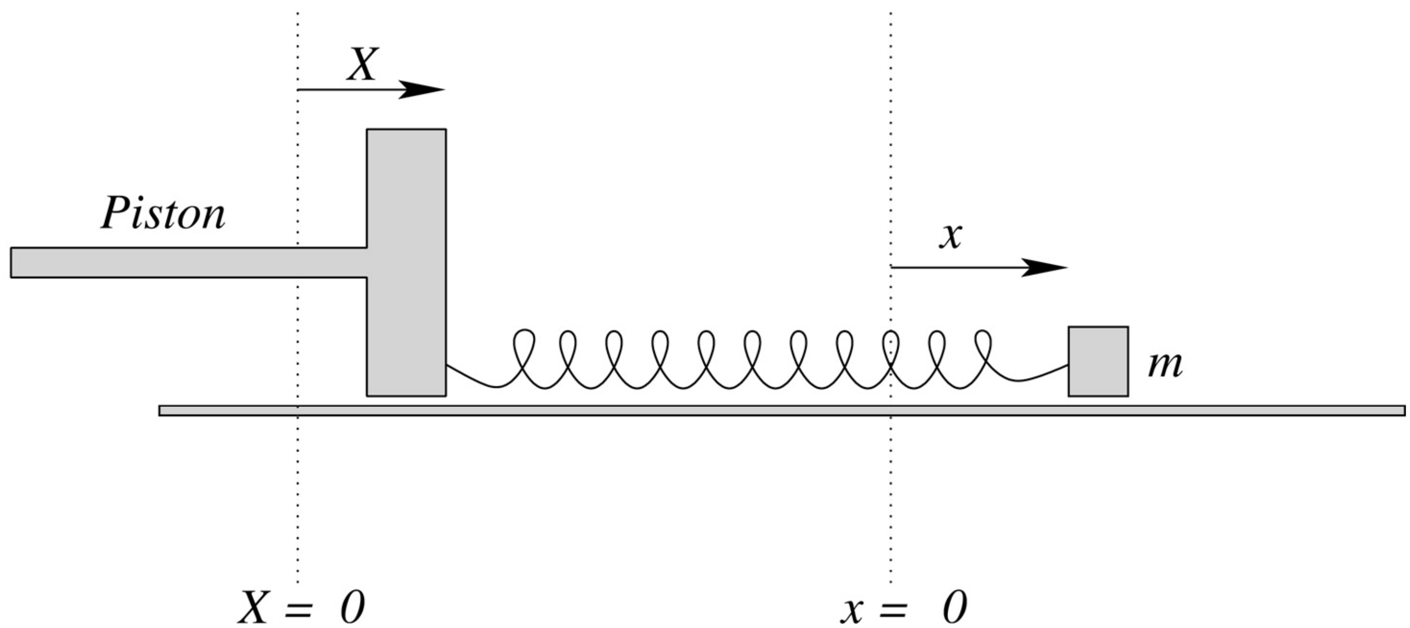

FIGURE 2.3
A driven oscillatory system

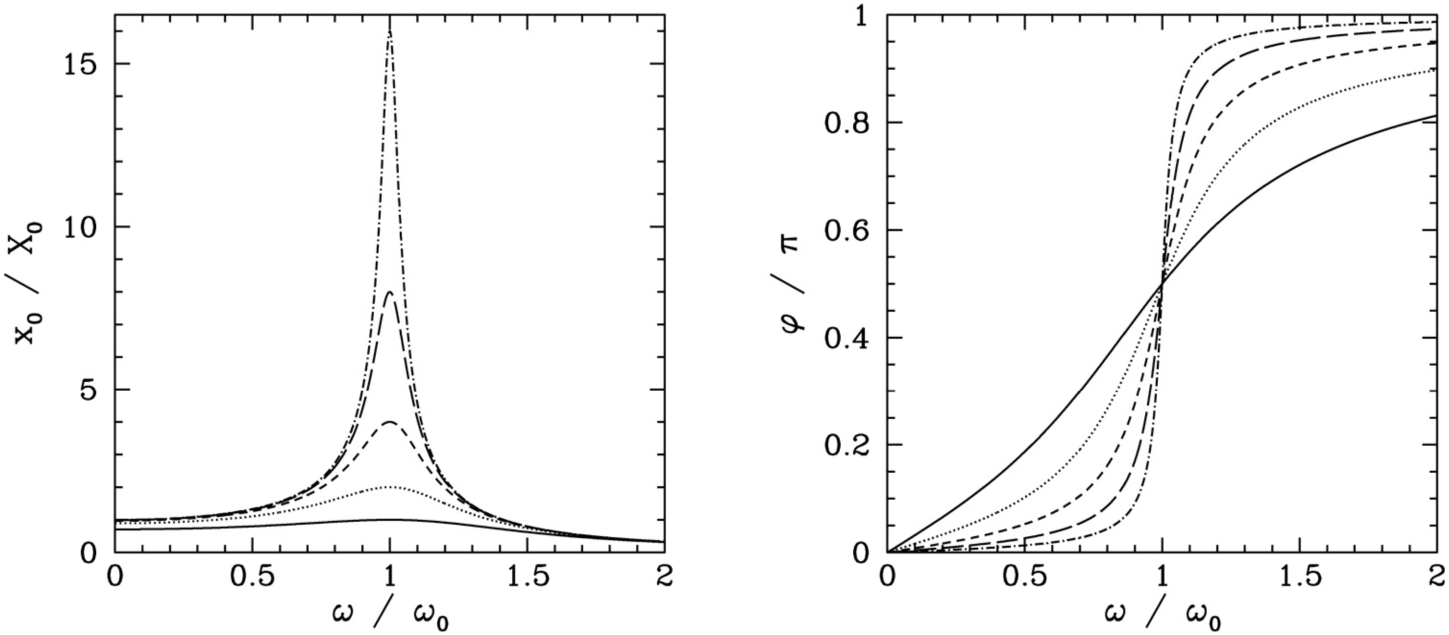

FIGURE 2.4
Driven harmonic motion.

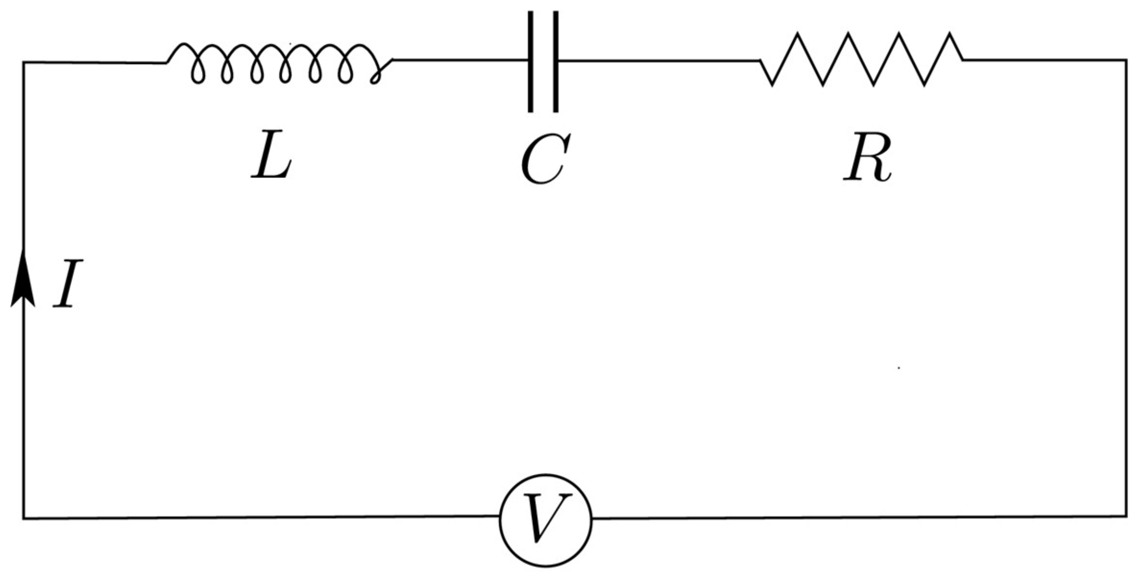

FIGURE 2.5
A driven LCR circuit.

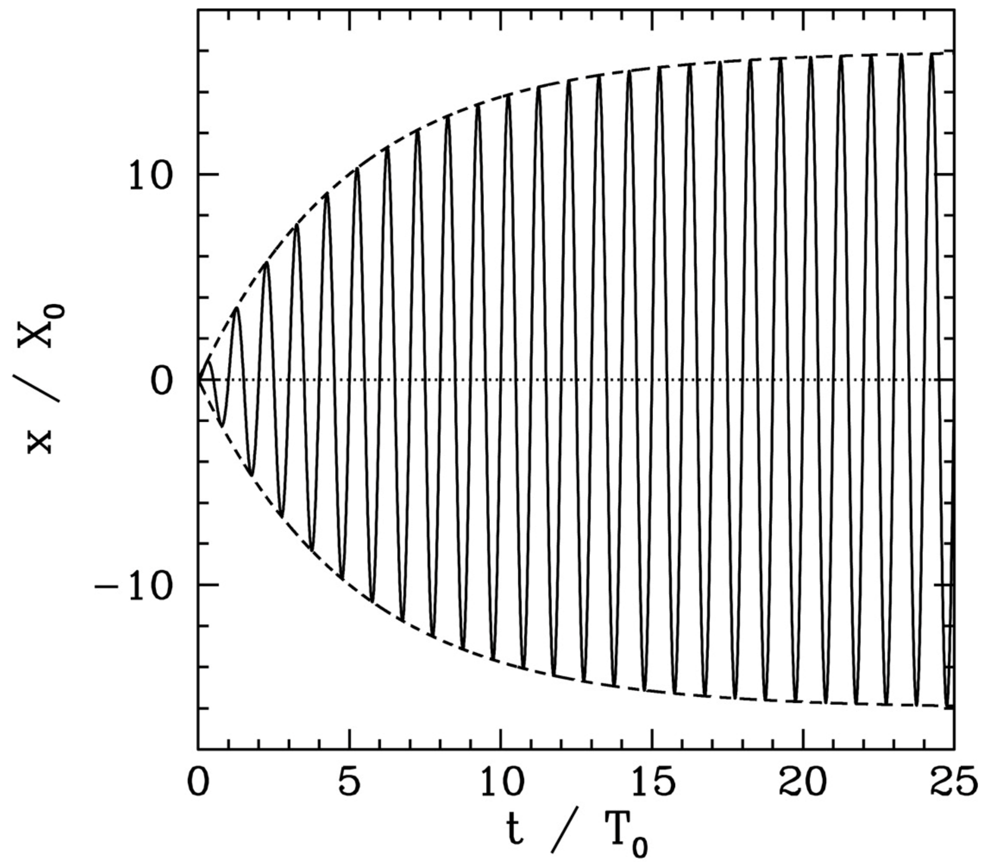

FIGURE 2.6
Resonant response of a driven damped harmonic oscillator.

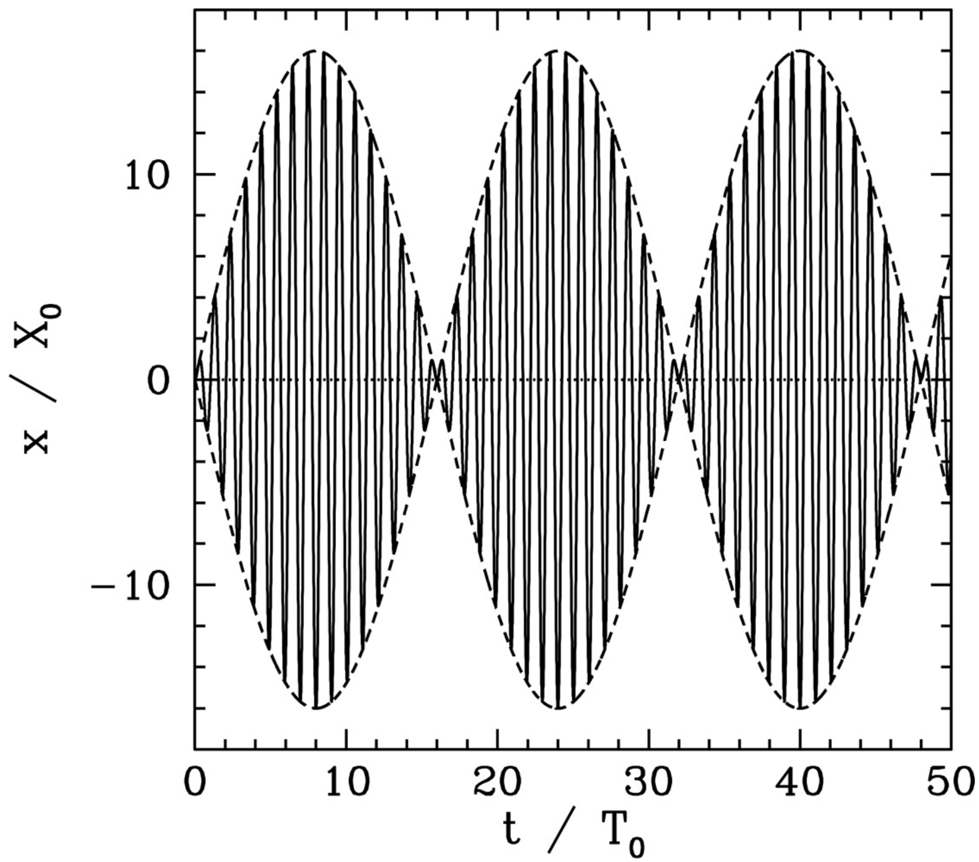

FIGURE 2.7
Off-resonant response of a driven undamped harmonic oscillator.

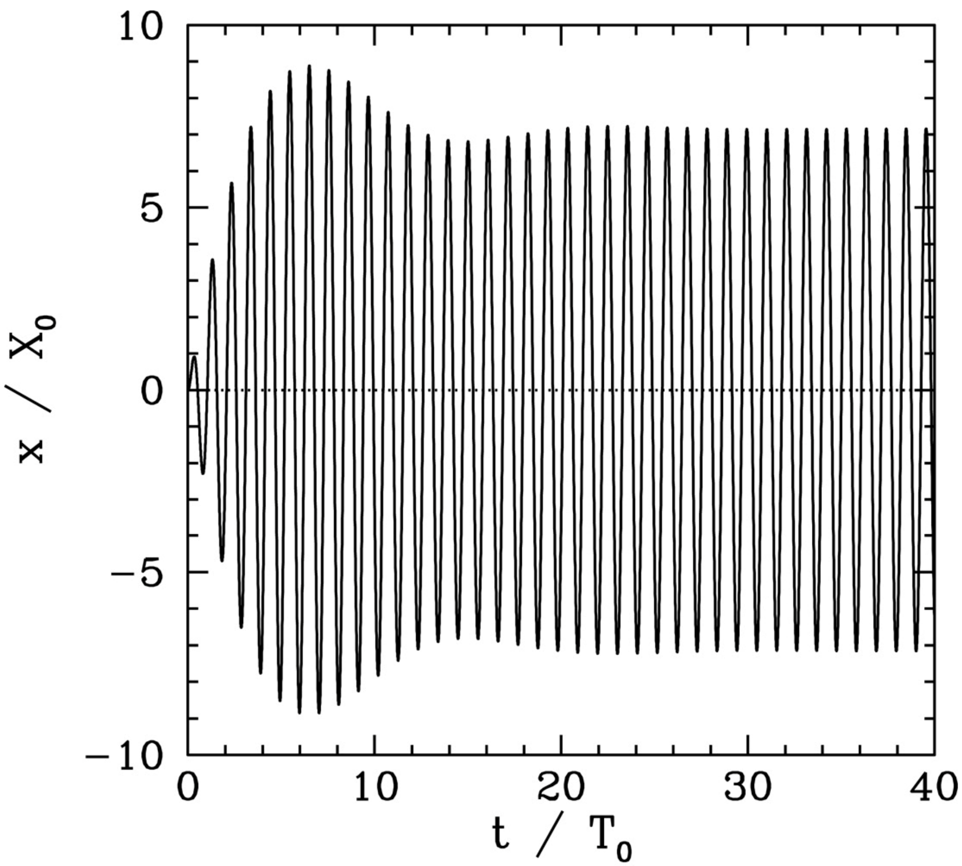

FIGURE 2.8
Nonresonant response of a driven damped harmonic oscillator.

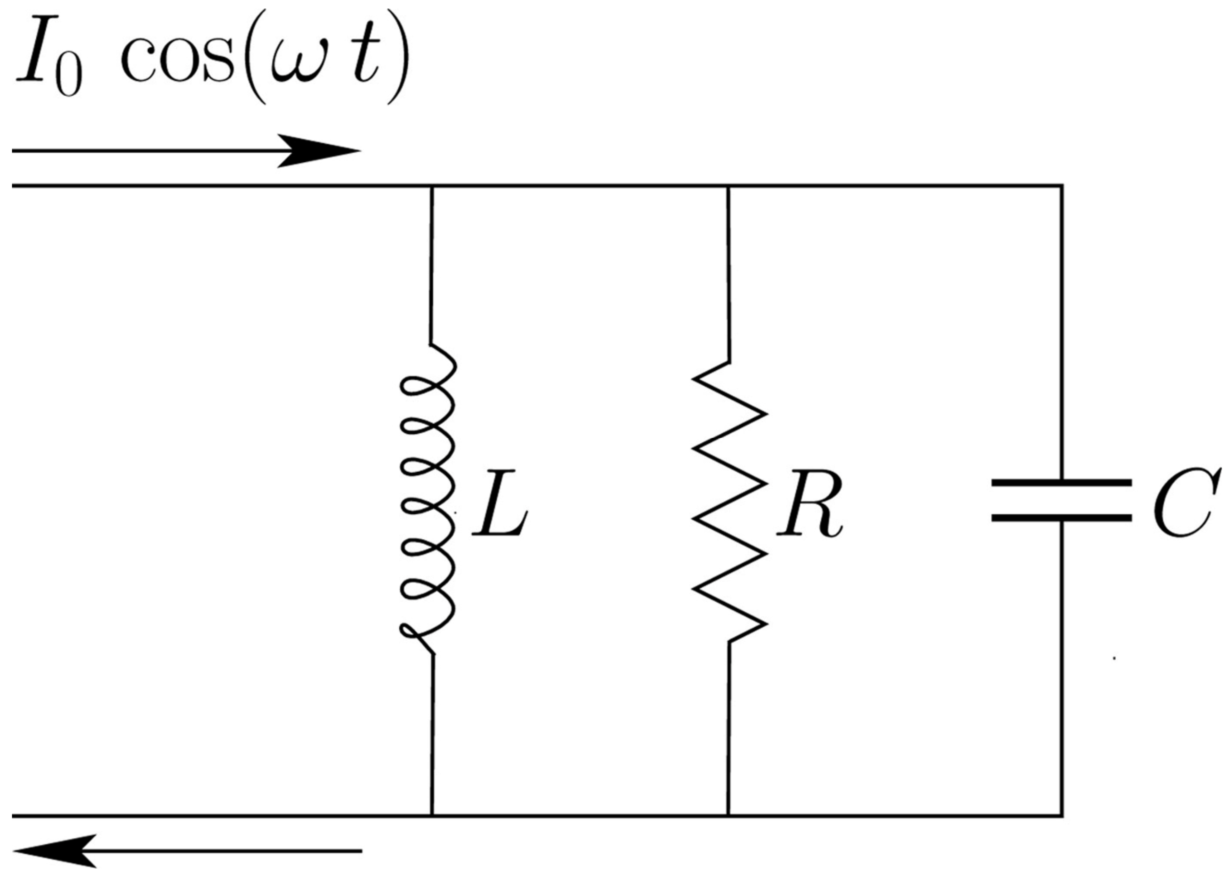
$I_0 \cos(\omega t)$
L
R
C

Oscillations and Waves

3 Coupled Oscillations

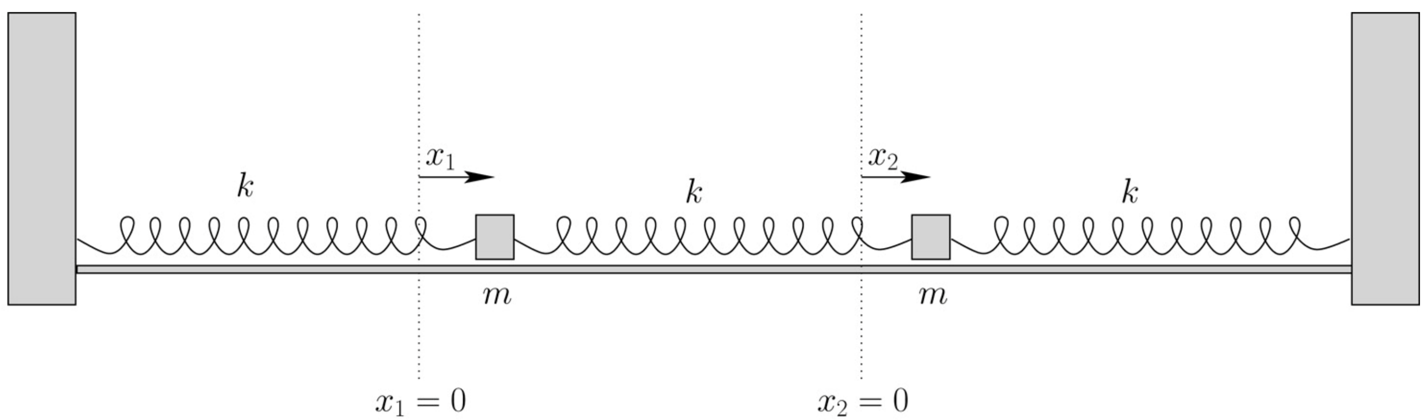

FIGURE 3.1
Two degree of freedom mass-spring system.

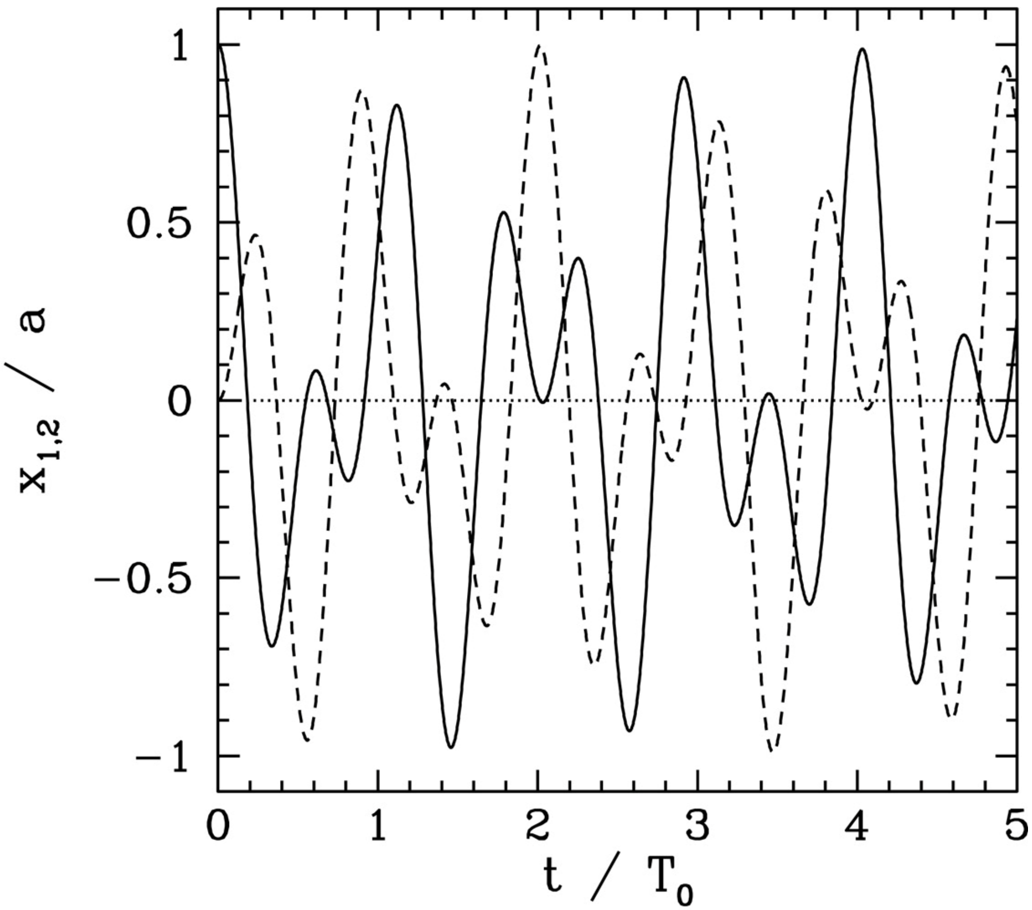

FIGURE 3.2
Coupled oscillations in a two degree of freedom mass-spring system.

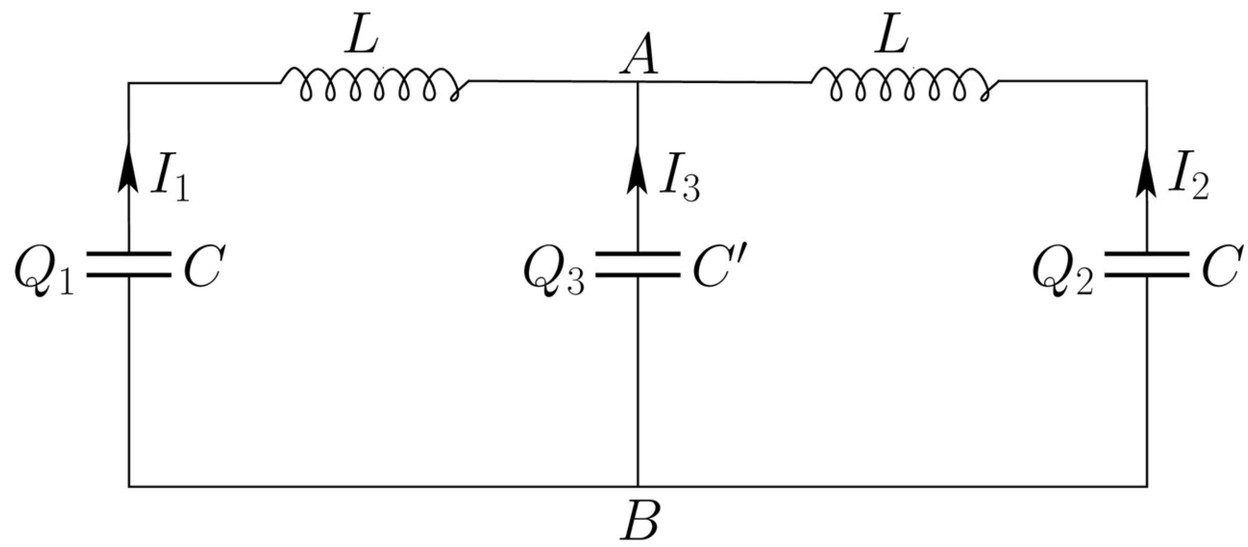

FIGURE 3.3
A two degree of freedom LC circuit.

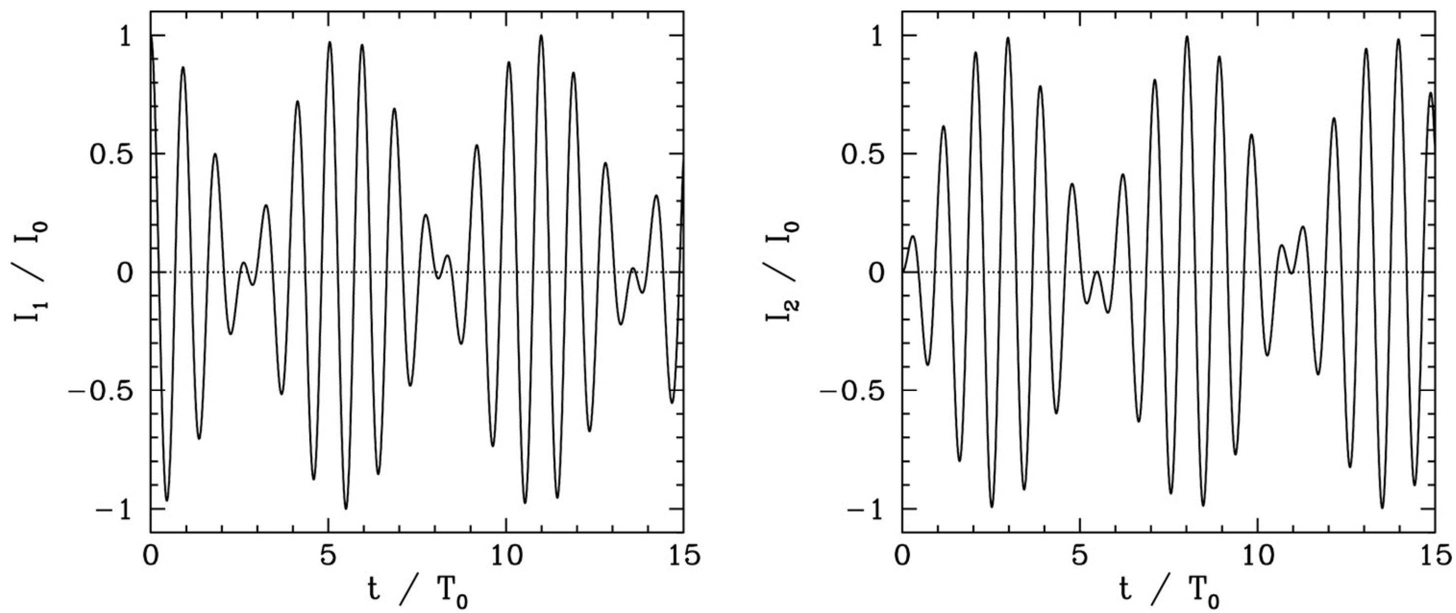

FIGURE 3.4
Coupled oscillations in a two degree of freedom *LC* circuit.

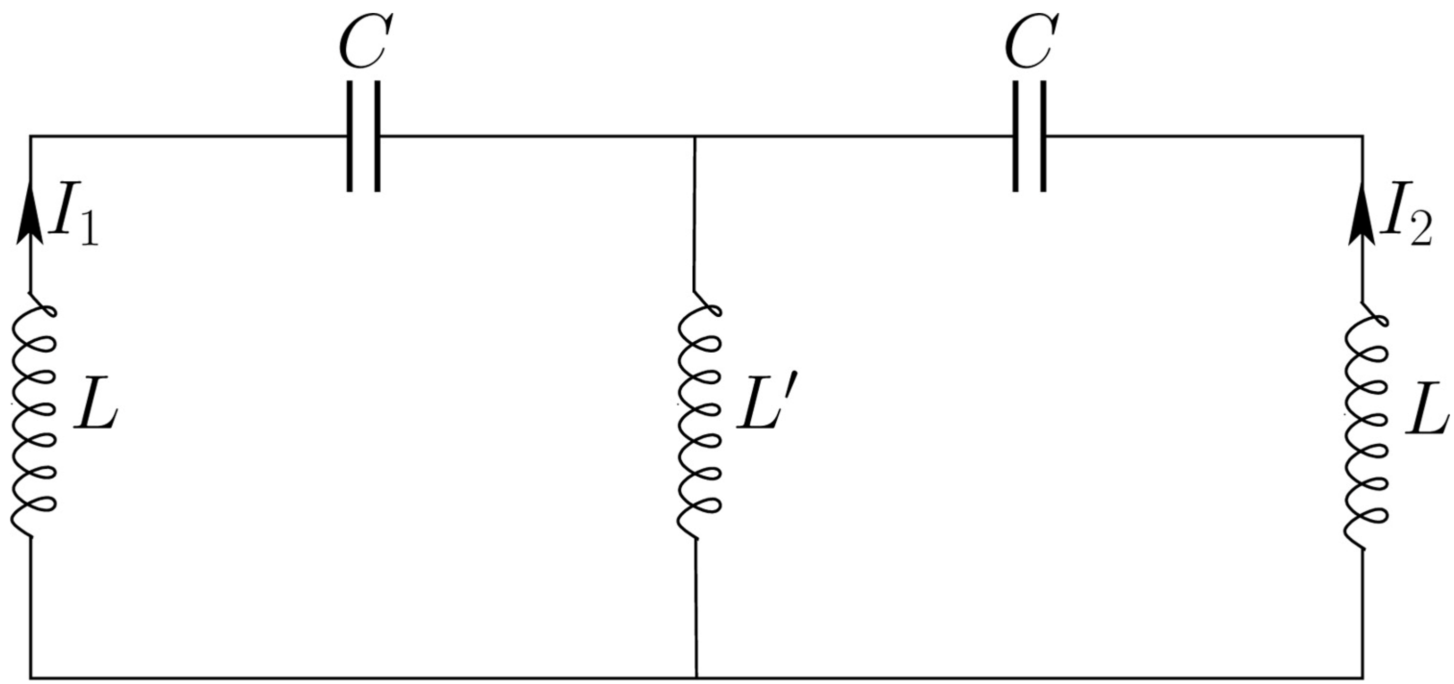
C
C
I_1
I_2
L
L′
L

Oscillations and Waves

4 Transverse Standing Waves

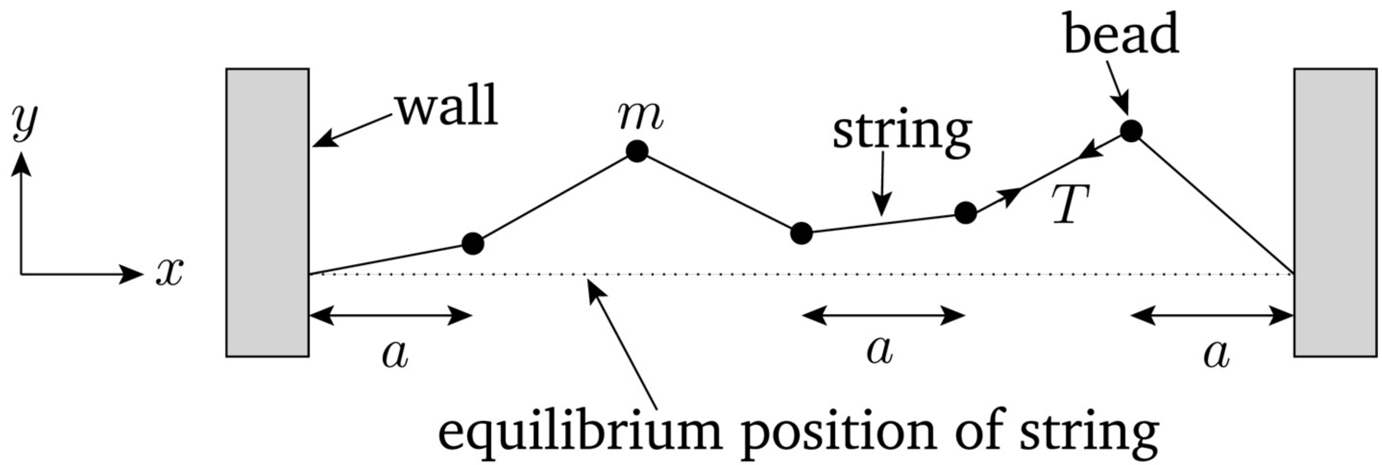

FIGURE 4.1
A beaded string.

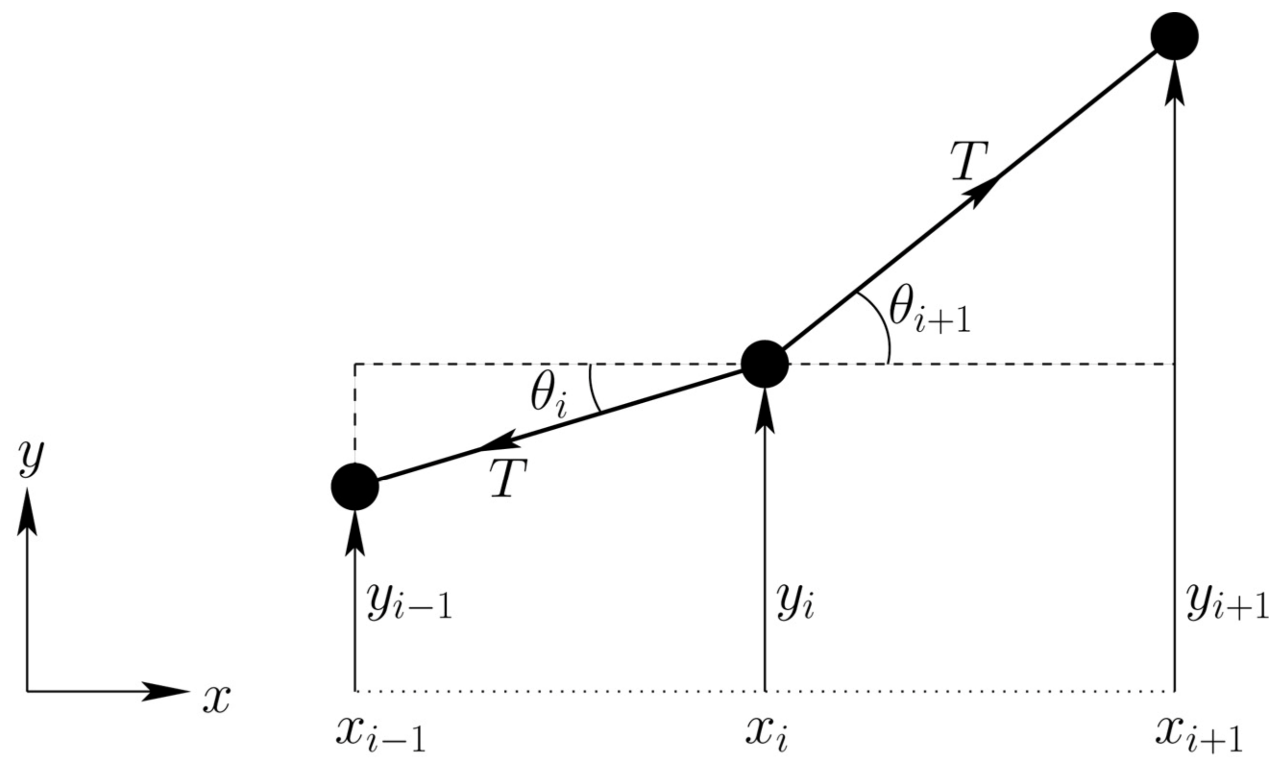

FIGURE 4.2
A short section of a beaded string.

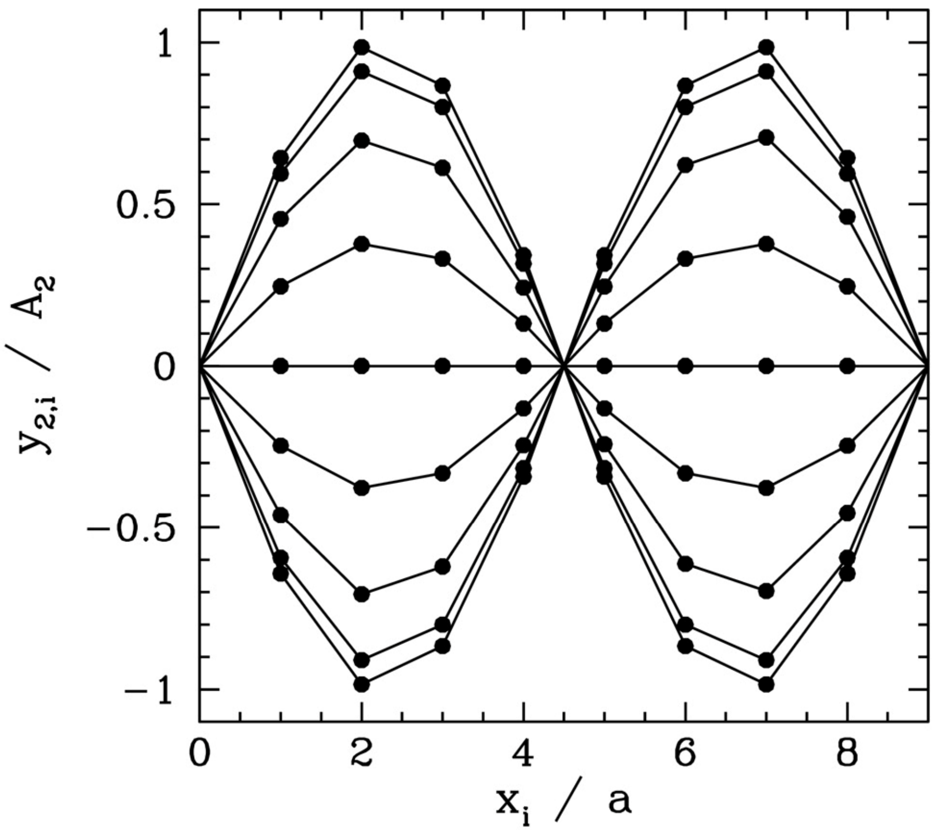

FIGURE 4.3
Time evolution of the $n = 2$ normal mode of a beaded string with eight equally spaced beads.

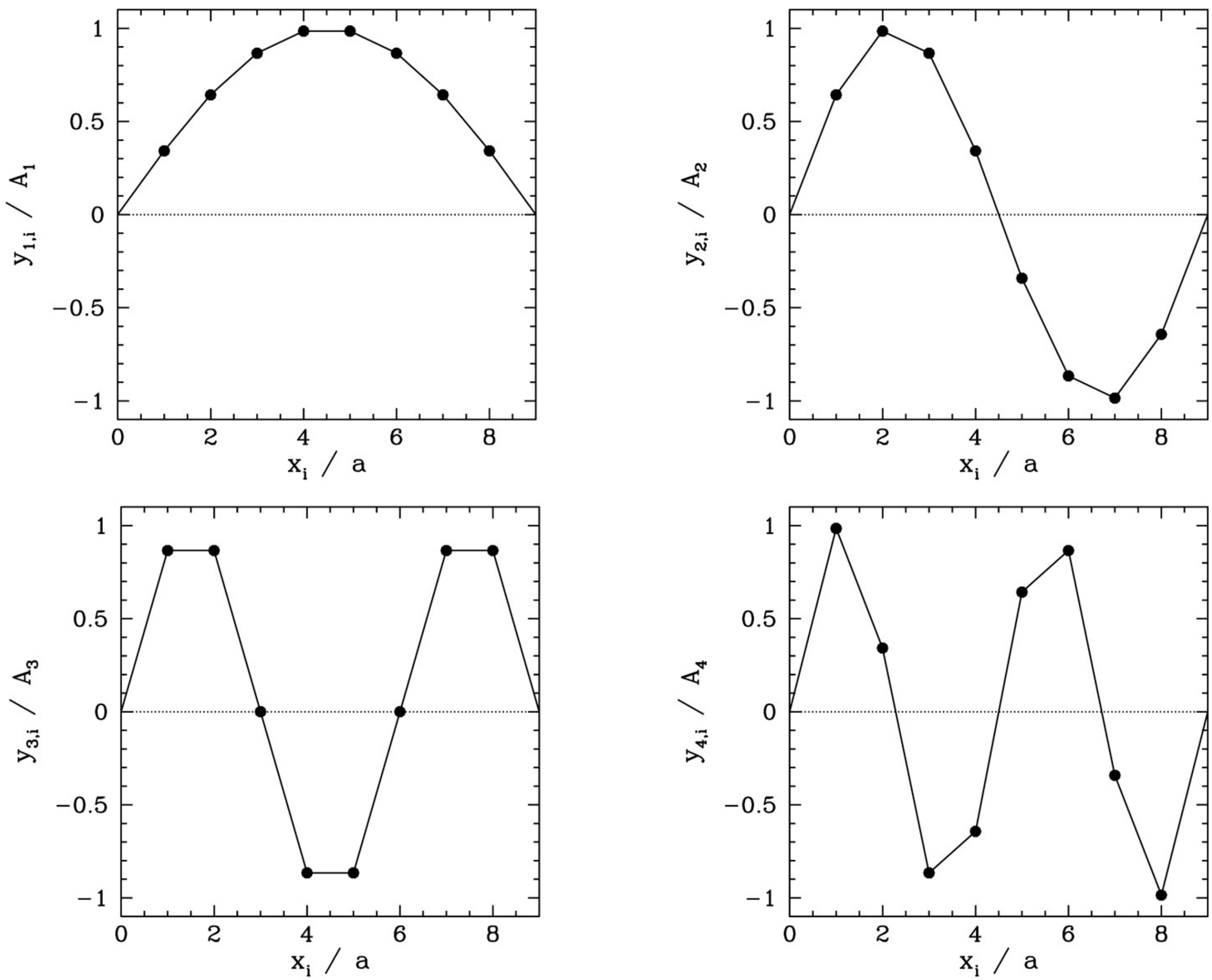

$y_{1,i}$ / A_1
x_i / a
$y_{2,i}$ / A_2
x_i / a
$y_{3,i}$ / A_3
x_i / a
$y_{4,i}$ / A_4
x_i / a

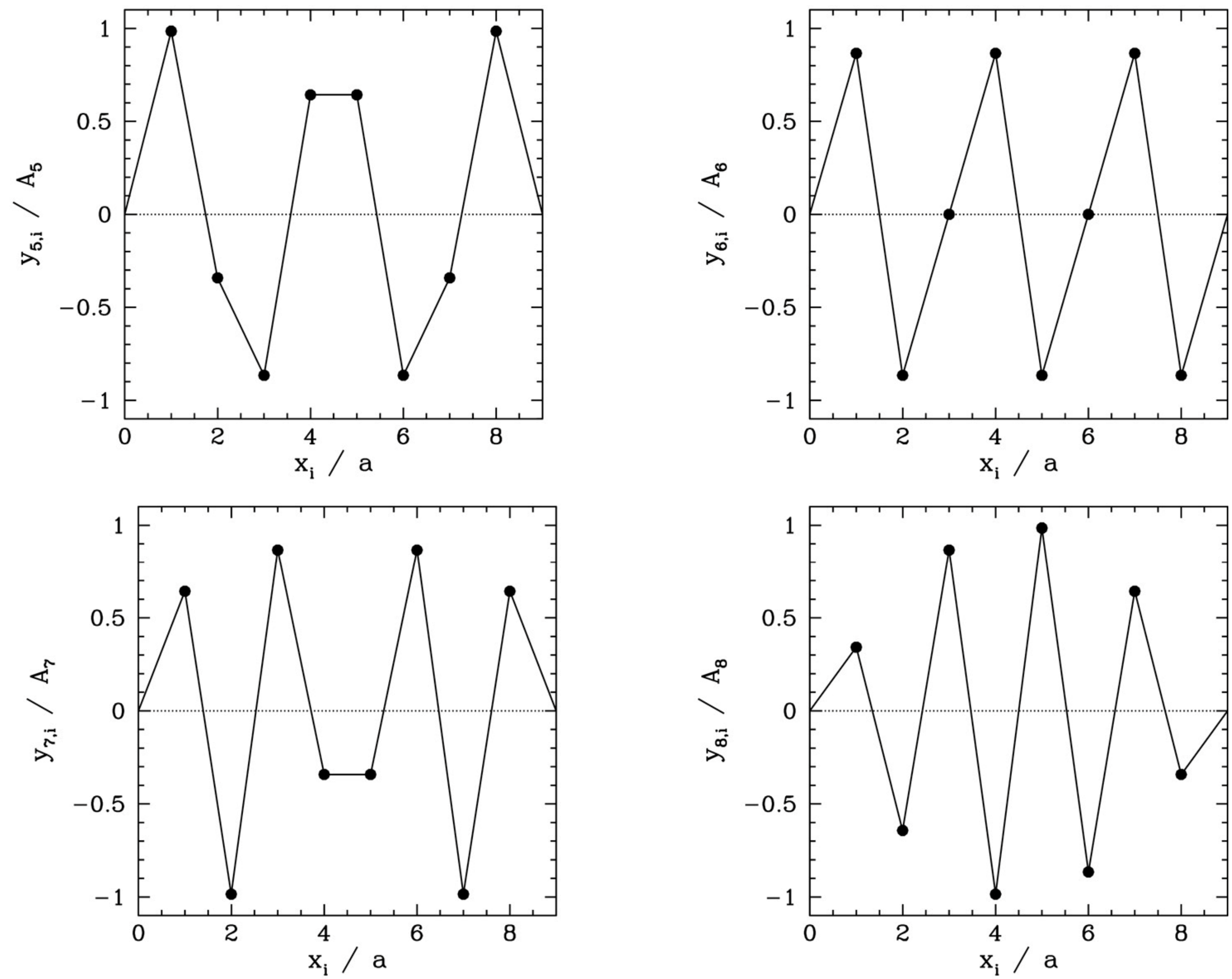

FIGURE 4.4
Normal modes of a beaded string with eight equally spaced beads.

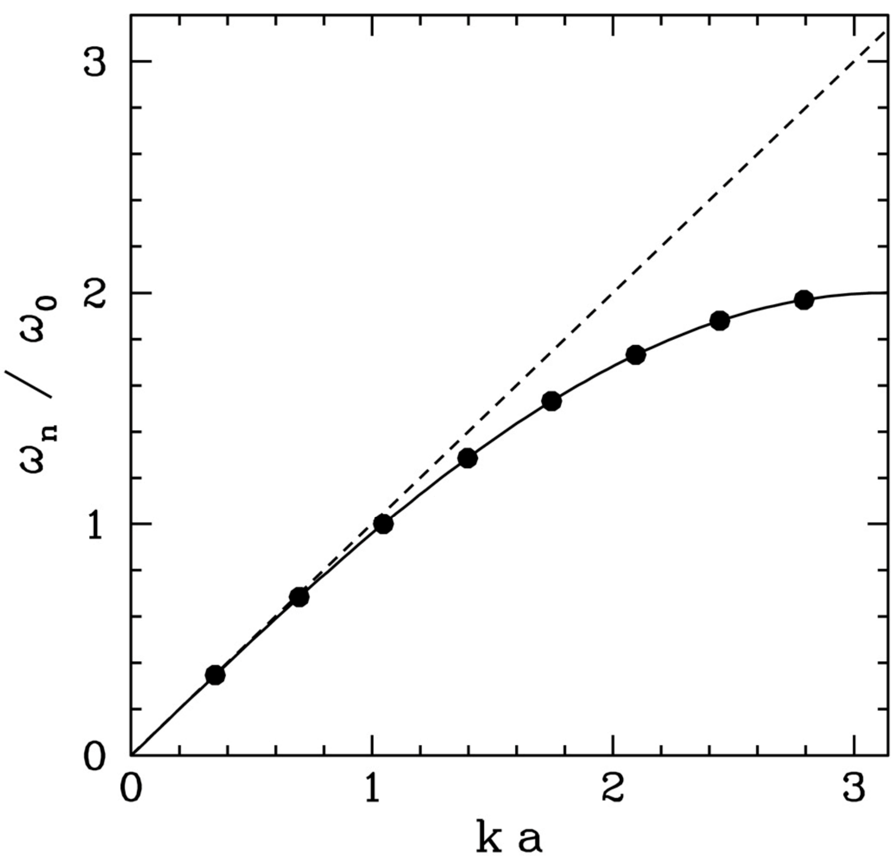

FIGURE 4.5
Normal frequencies of a beaded string with eight equally spaced beads.

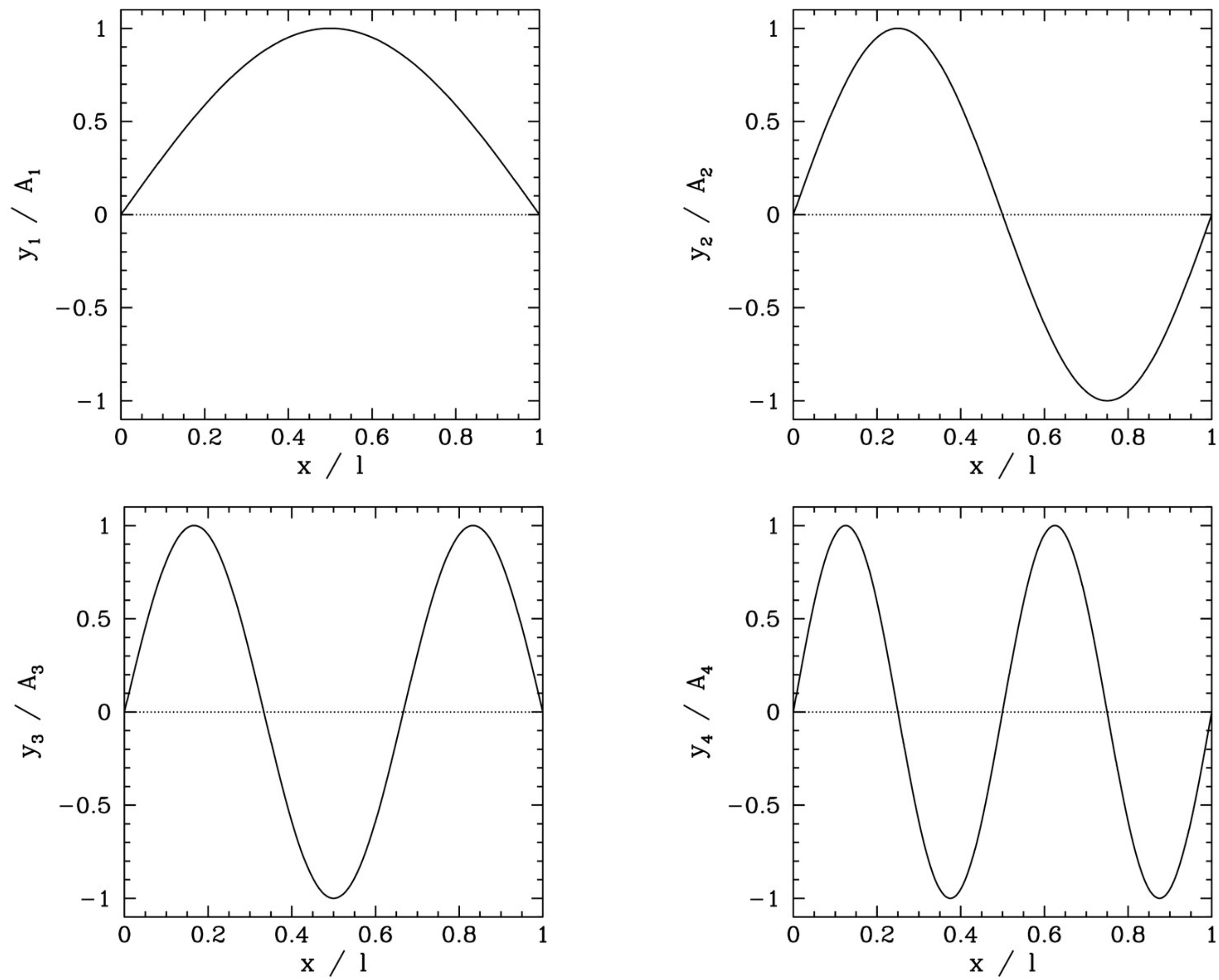
y_1 / A_1
y_2 / A_2
y_3 / A_3
y_4 / A_4
x / l
1
0.5
0
−0.5
−1
0
0.2
0.4
0.6
0.8
1

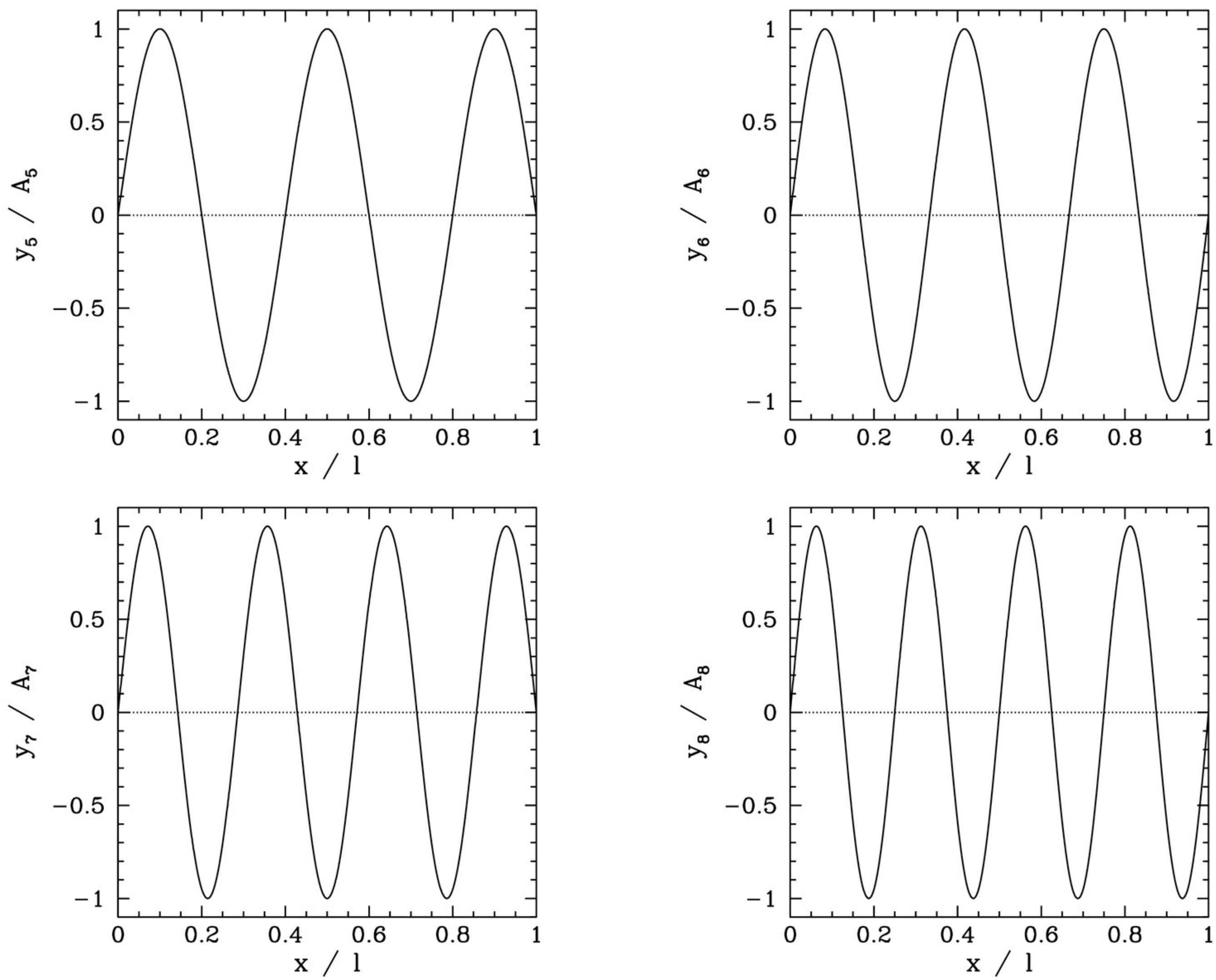

FIGURE 4.6
First eight normal modes of a uniform string.

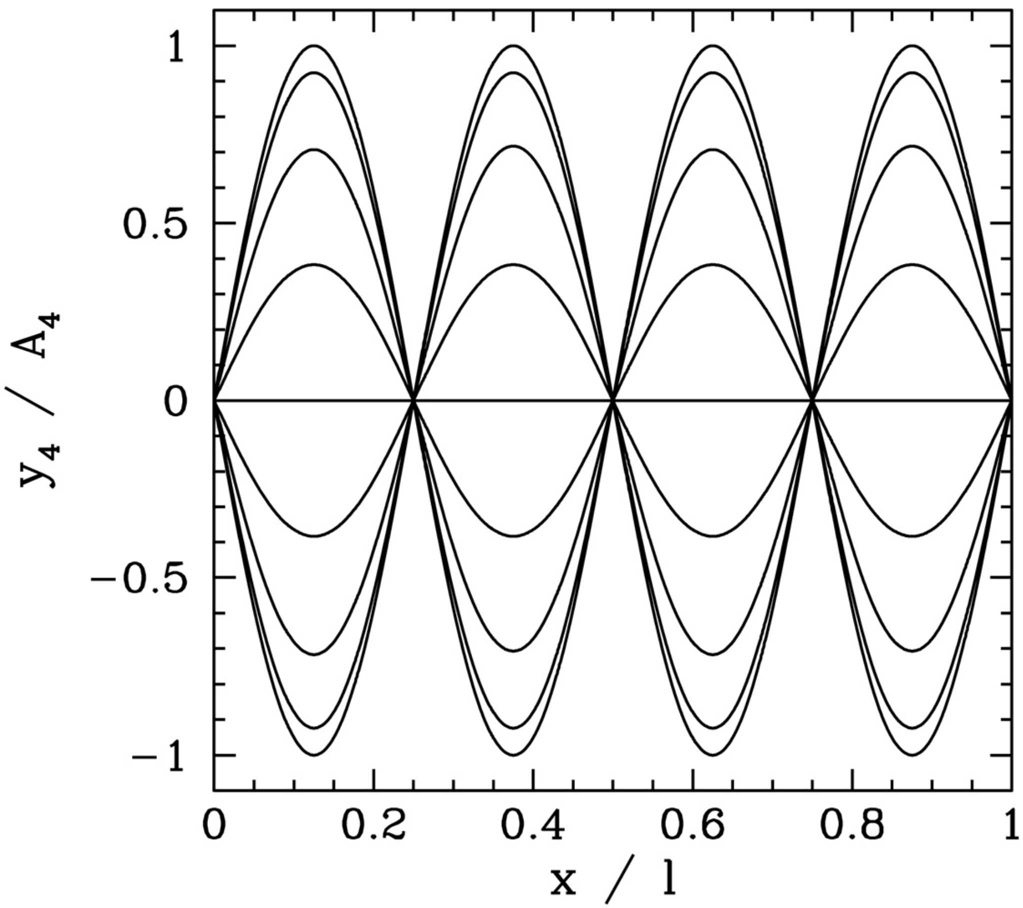

FIGURE 4.7
Time evolution of the $n = 4$ normal mode of a uniform string.

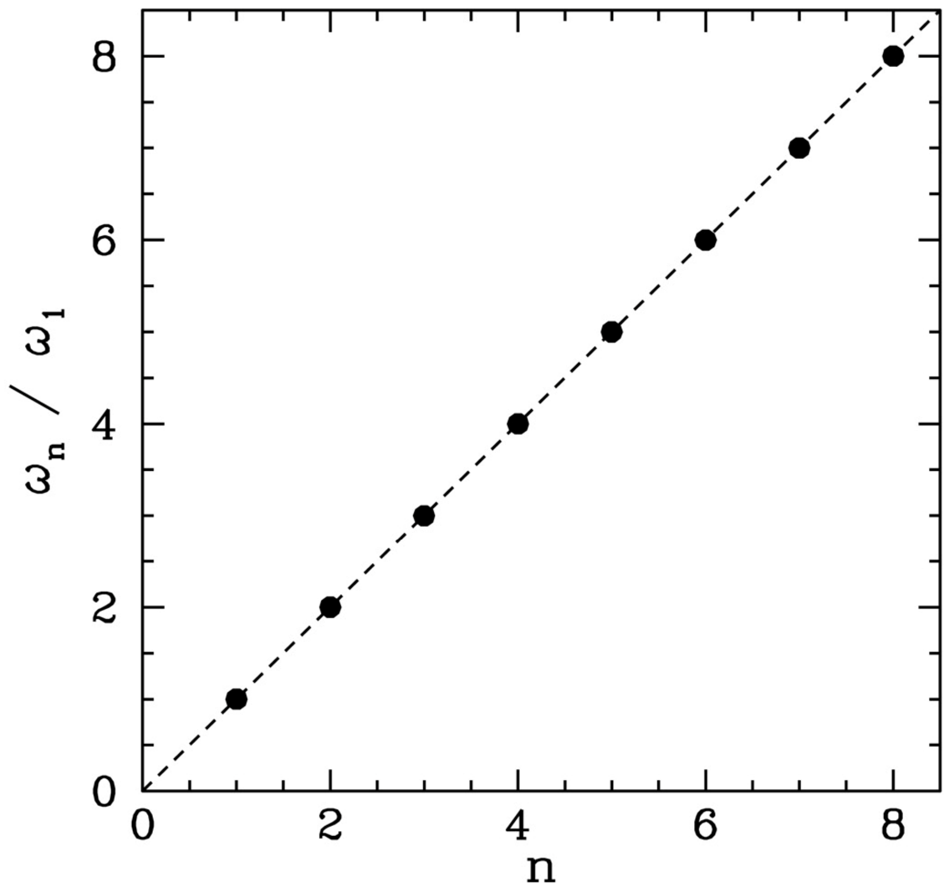

FIGURE 4.8
Normal frequencies of the first eight normal modes of a uniform string.

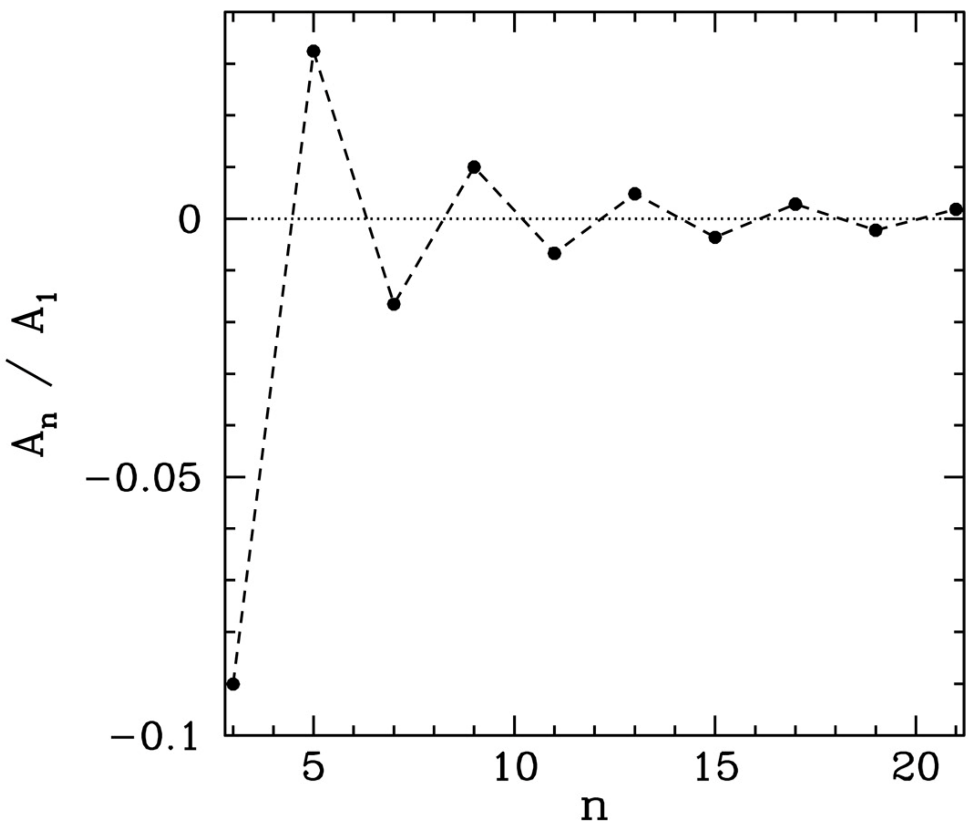

FIGURE 4.9
Relative amplitudes of the overtone harmonics of a uniform guitar string plucked at its midpoint.

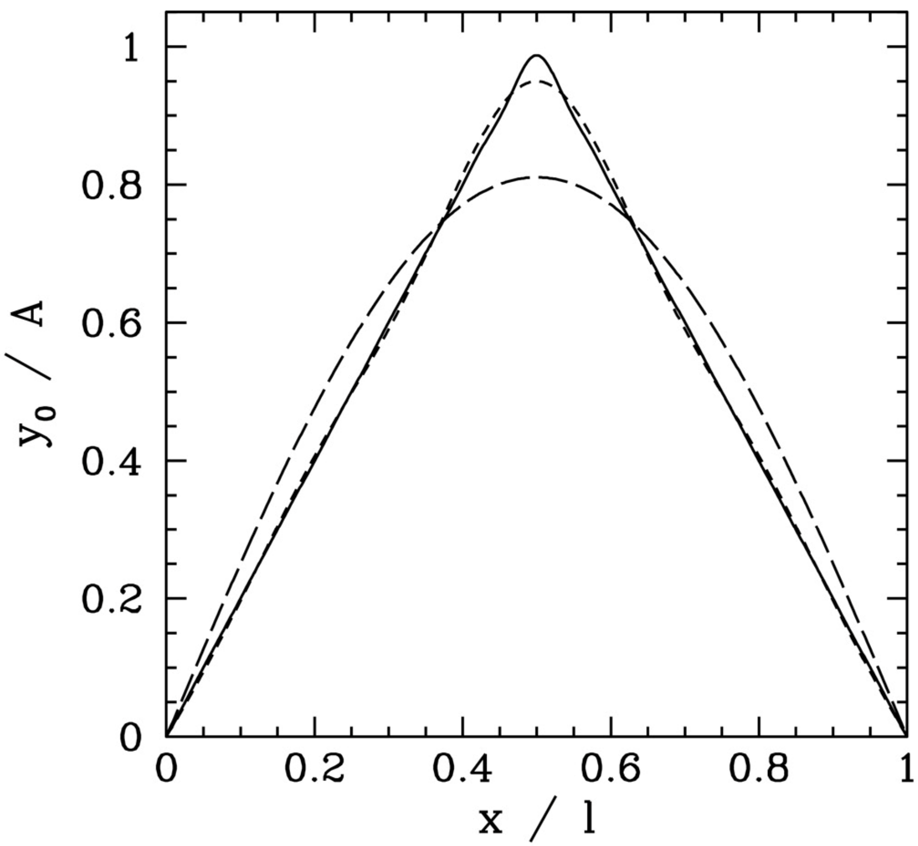

FIGURE 4.10
Reconstruction of the initial displacement of a uniform guitar string plucked at its midpoint.

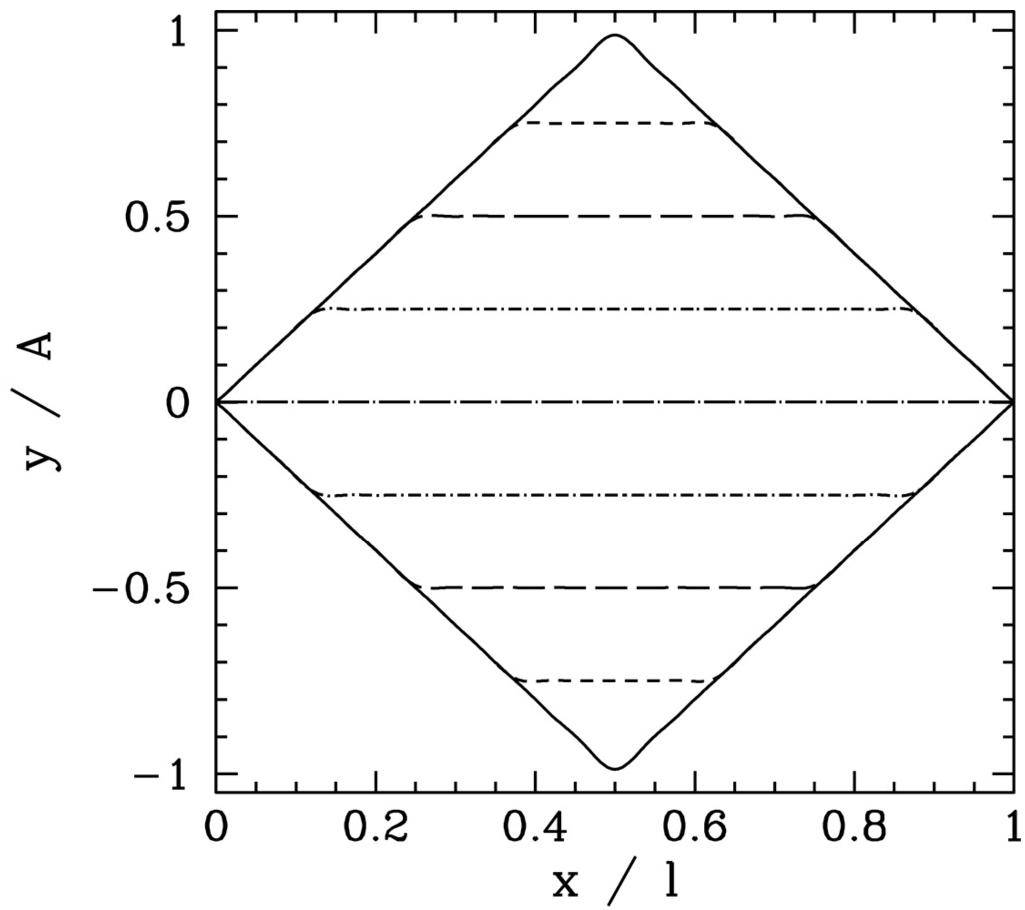

FIGURE 4.11
Time evolution of a uniform guitar string plucked at its midpoint.

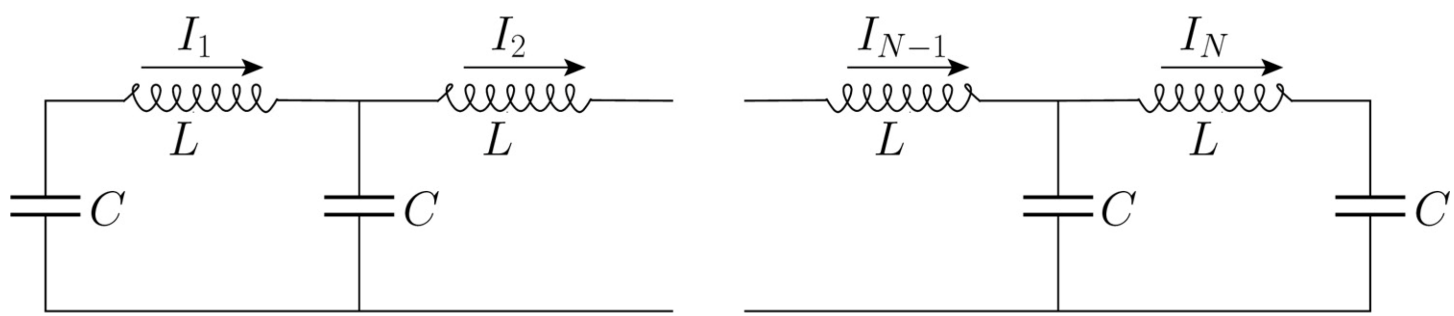
I_1
I_2
I_{N-1}
I_N
L
L
L
L
C
C
C
C

Oscillations and Waves

5 Longitudinal Standing Waves

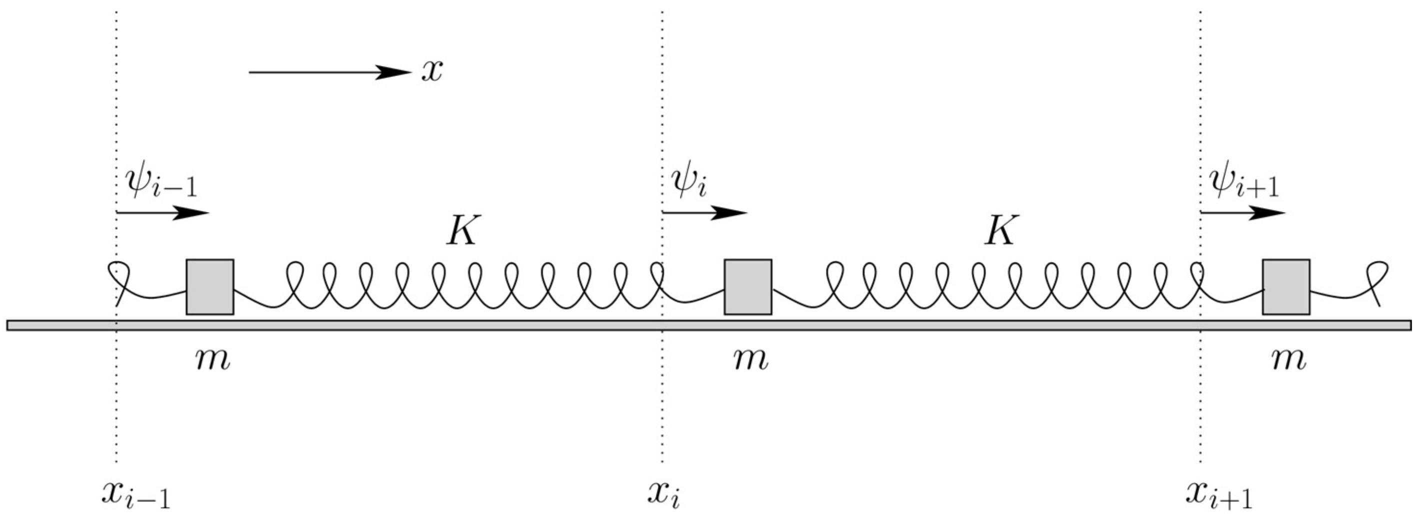

FIGURE 5.1
Detail of a system of spring-coupled masses.

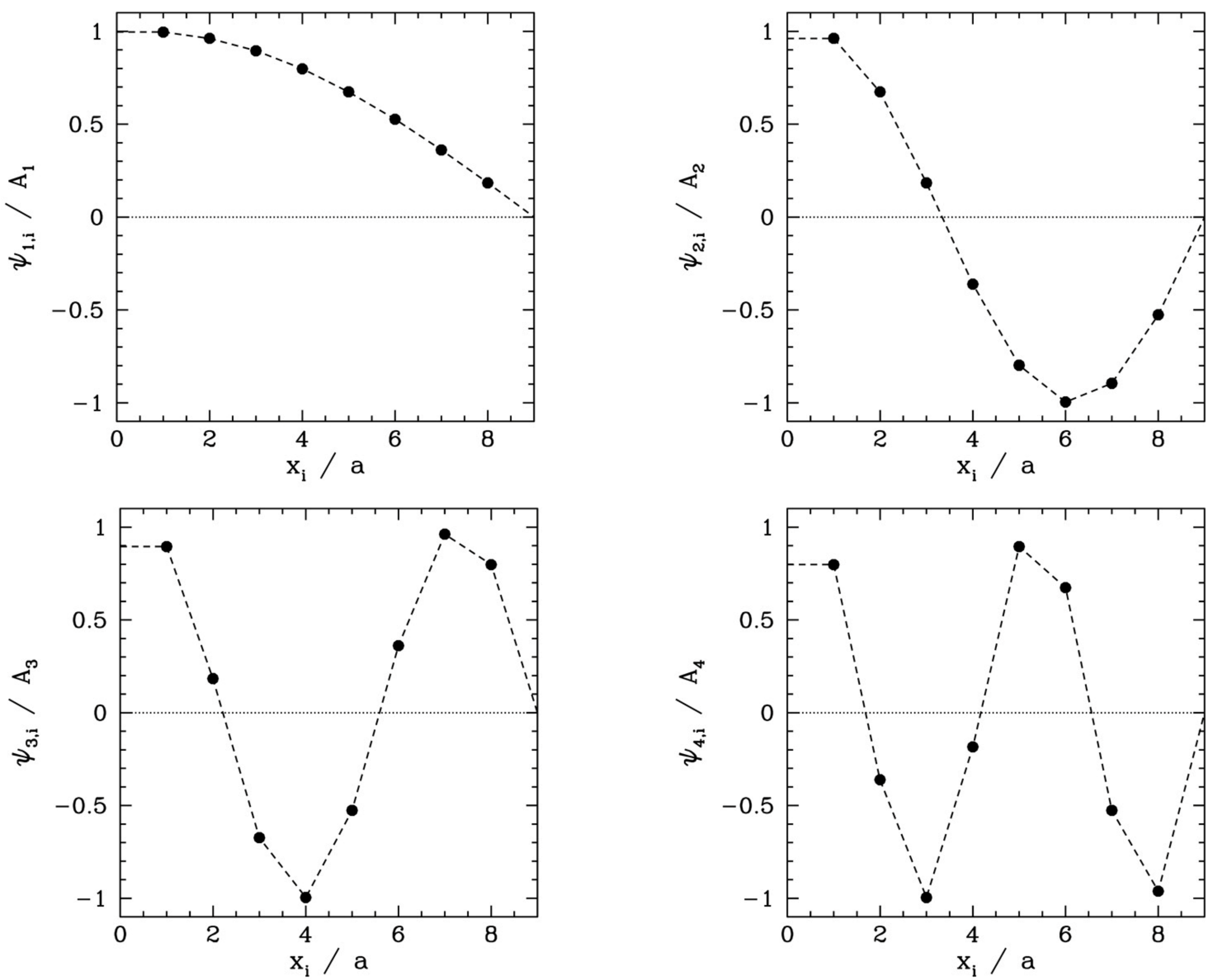

$\psi_{1,i}$ / A_1
x_i / a
$\psi_{2,i}$ / A_2
x_i / a
$\psi_{3,i}$ / A_3
x_i / a
$\psi_{4,i}$ / A_4
x_i / a

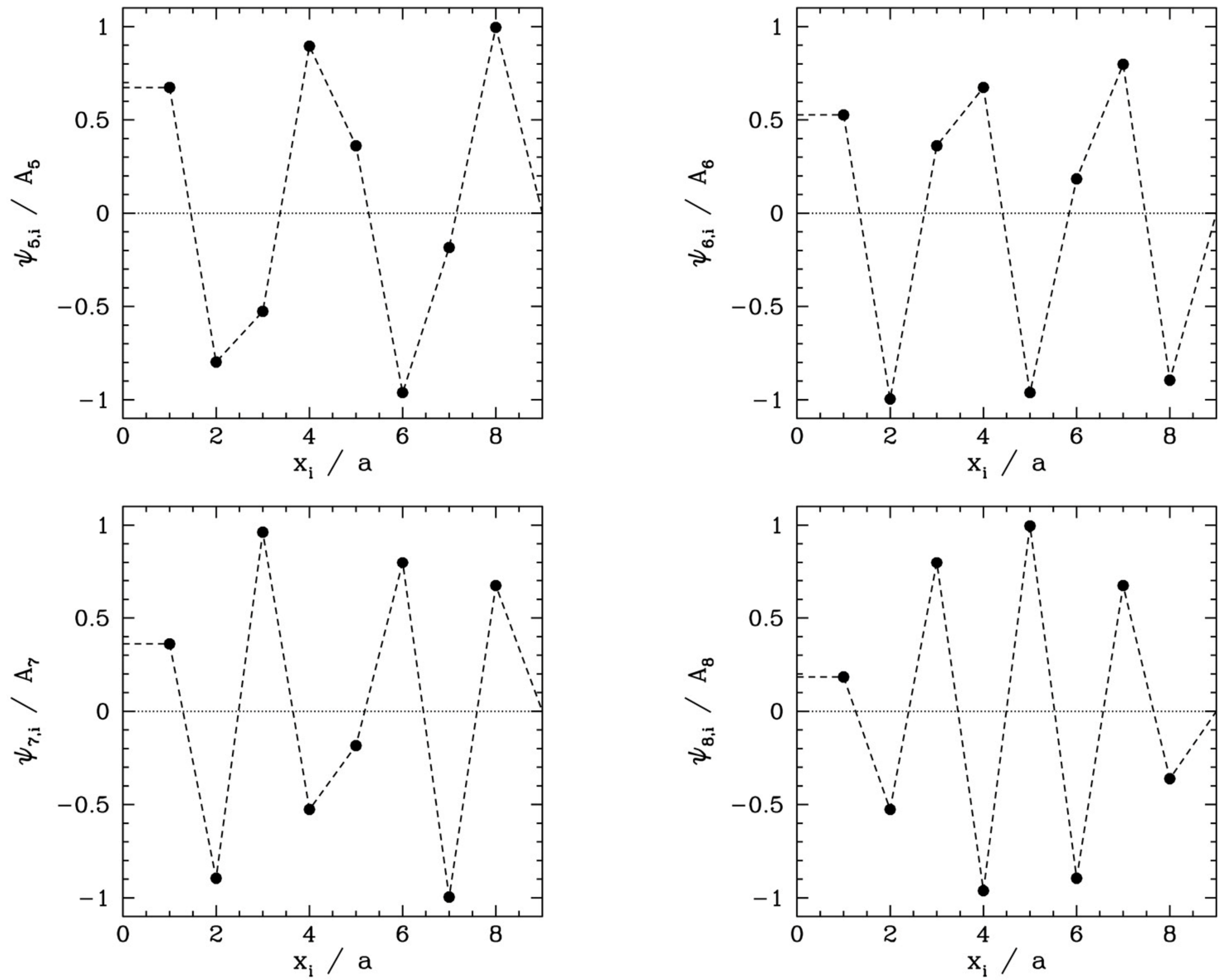

FIGURE 5.2
Normal modes of a system of eight spring-coupled masses.

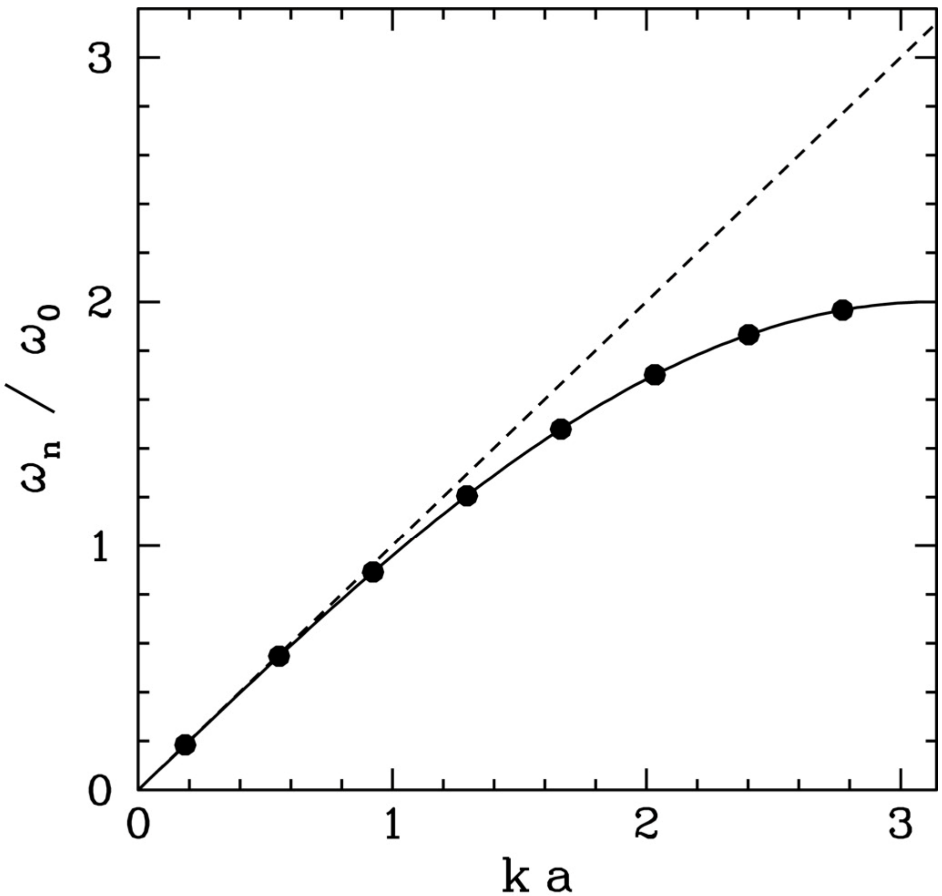

FIGURE 5.3
Normal frequencies of a system of eight spring-coupled masses.

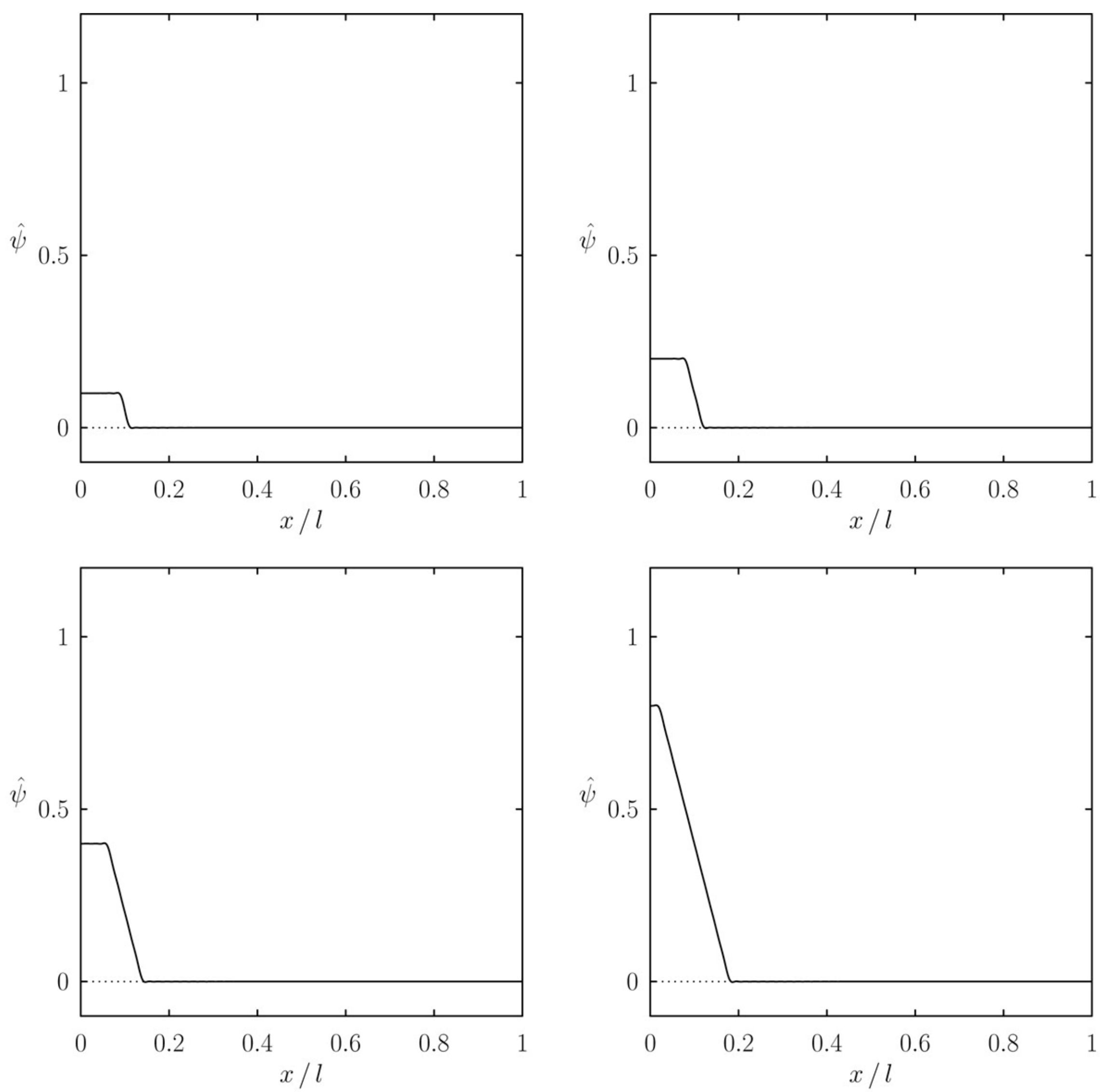

$\hat{\psi}$
1
0.5
0
0
0.2
0.4
0.6
0.8
1
$x\,/\,l$

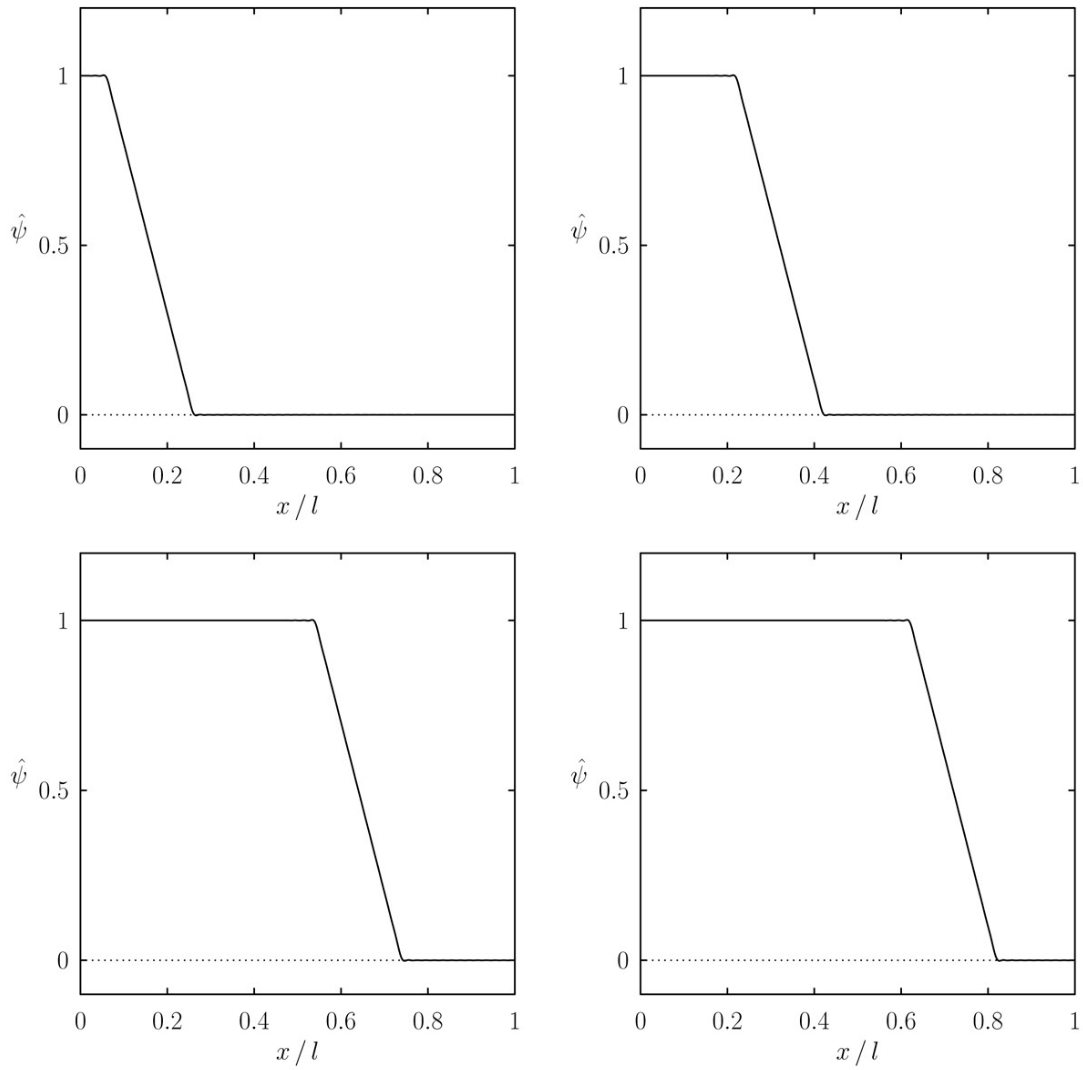

FIGURE 5.4
Time evolution of the normalized longitudinal displacement of a thin elastic rod.

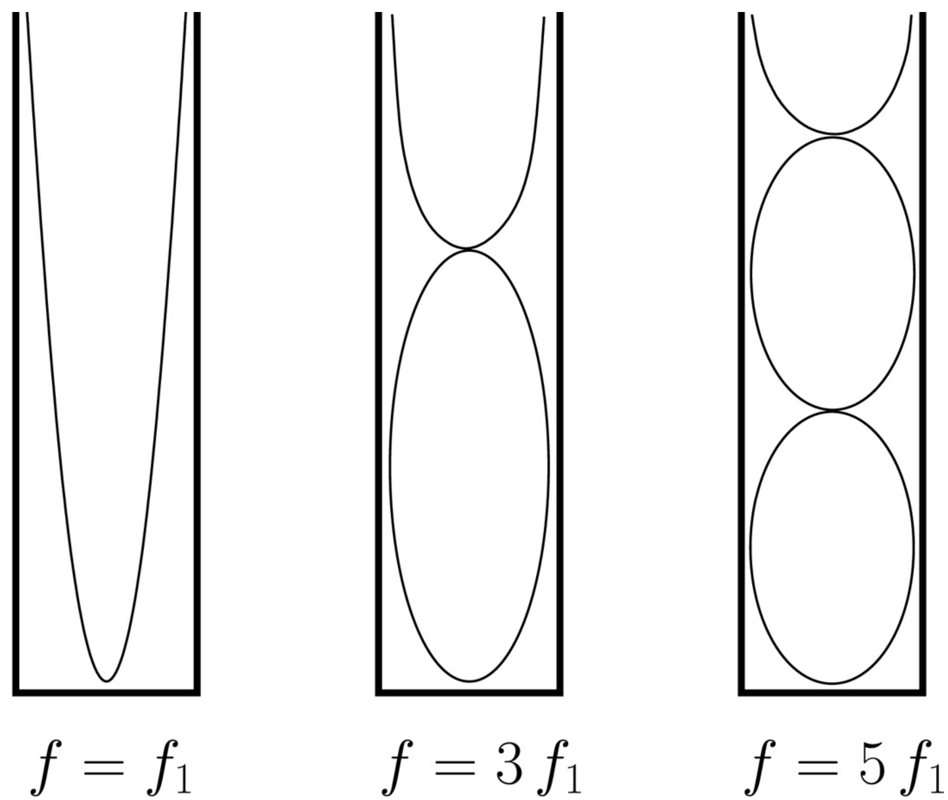

FIGURE 5.5
First three normal modes of an organ pipe (schematic).

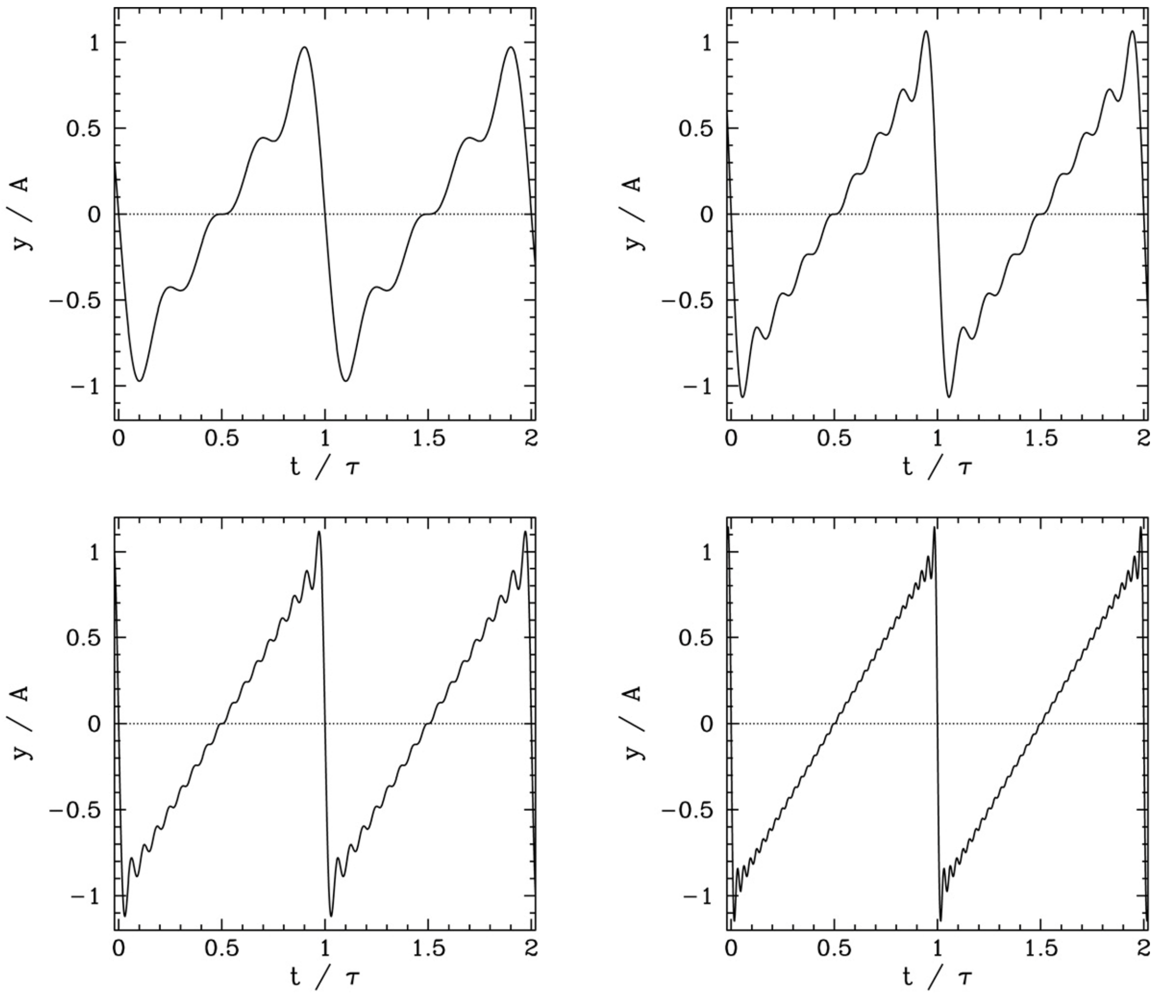

FIGURE 5.6
Fourier reconstruction of a periodic sawtooth waveform.

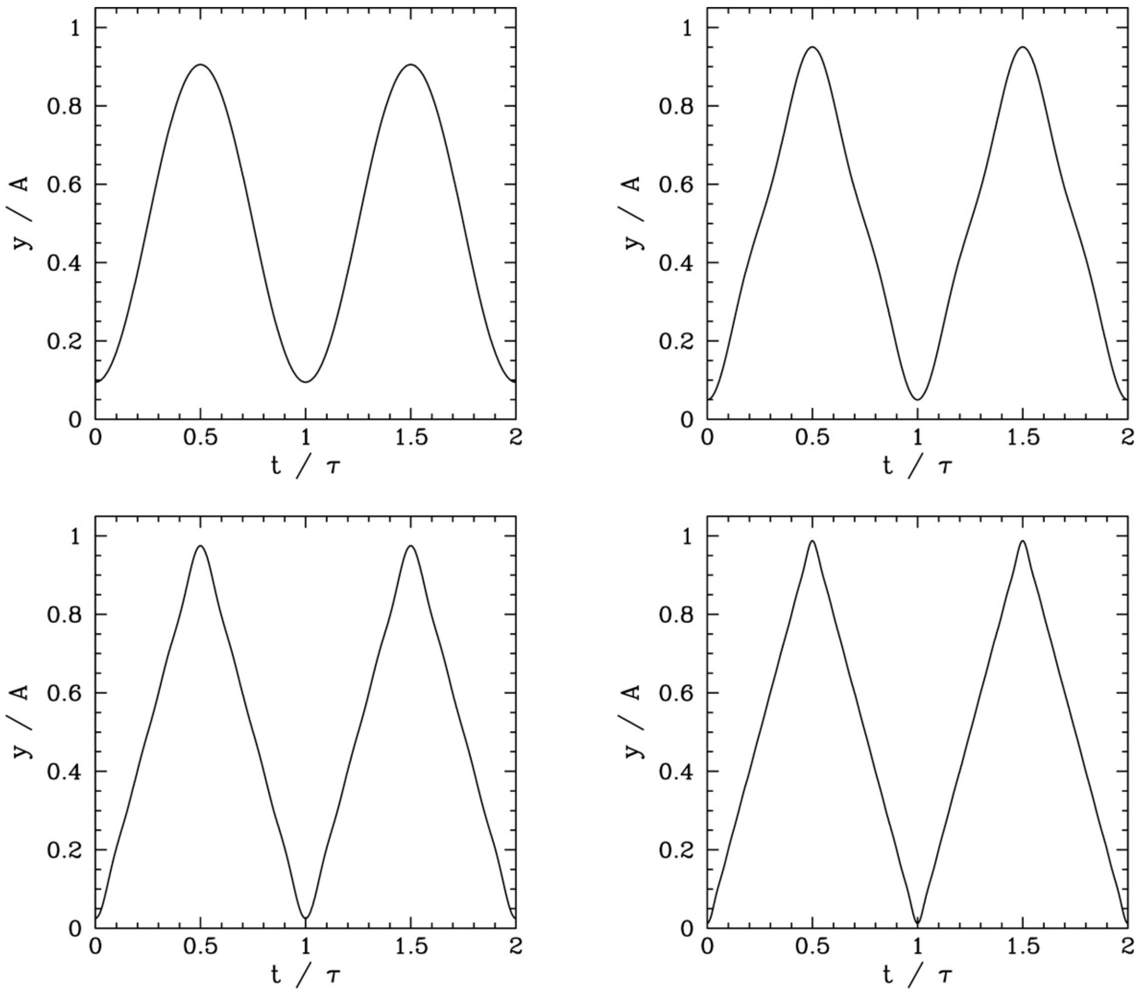

FIGURE 5.7
Fourier reconstruction of a periodic “tent” waveform.

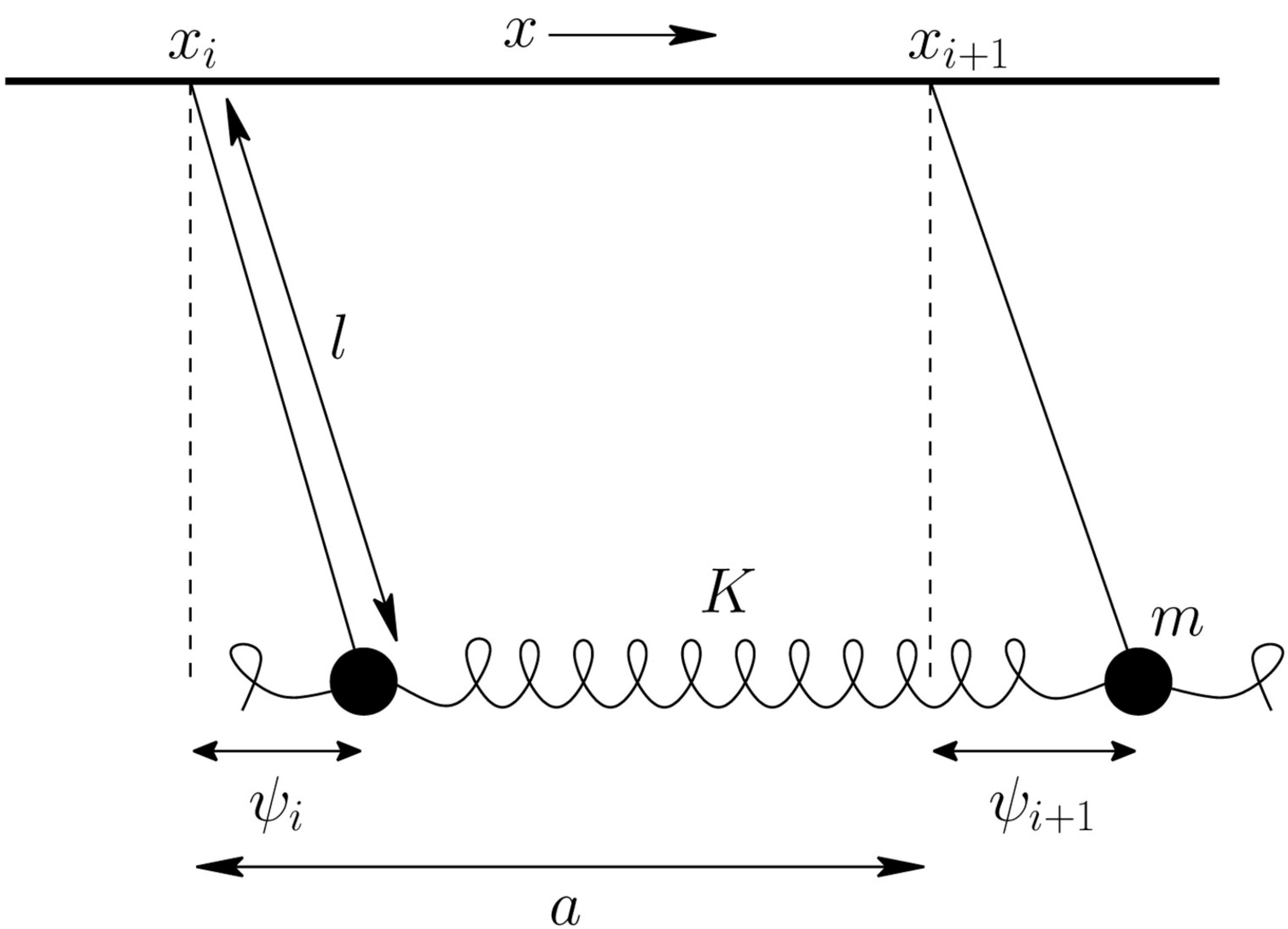

x_i
x
x_{i+1}
l
K
m
ψ_i
ψ_{i+1}
a

Oscillations and Waves

6 Traveling Waves

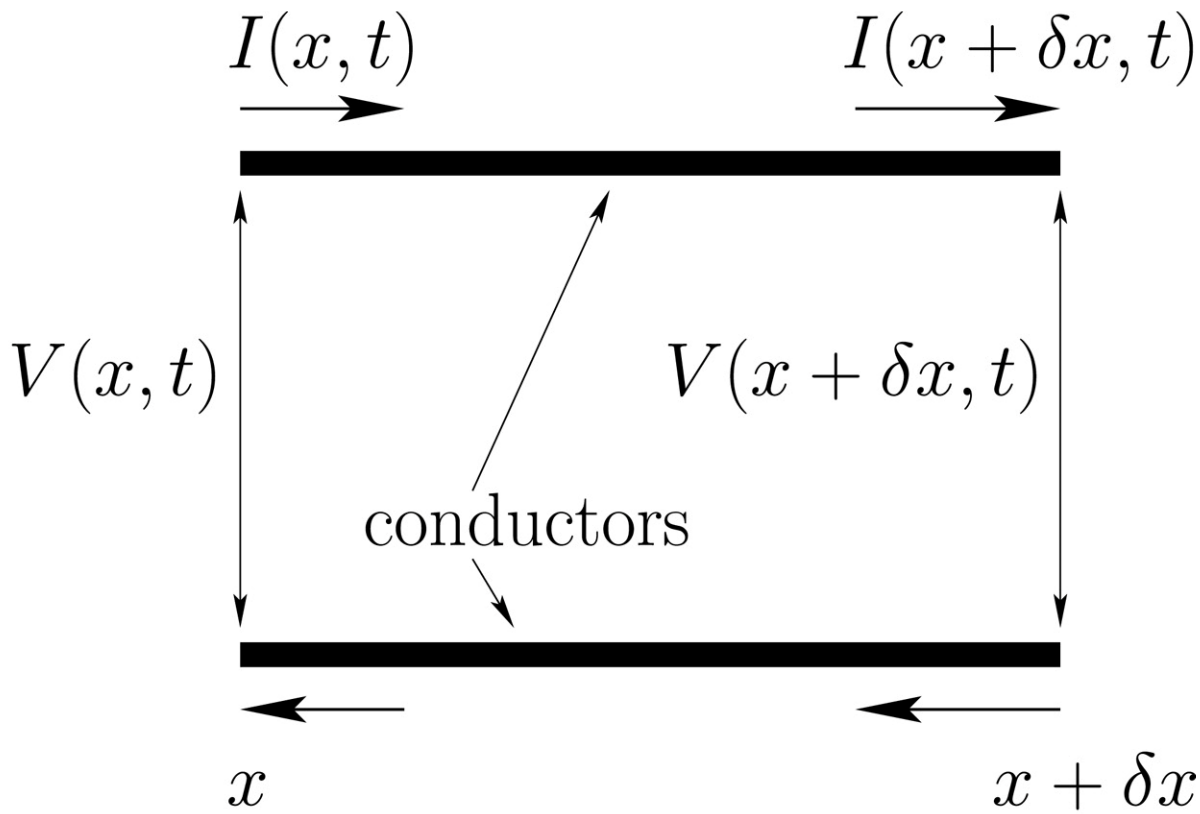

FIGURE 6.1
A section of a transmission line.

Oscillations and Waves

7 Multi-Dimensional Waves

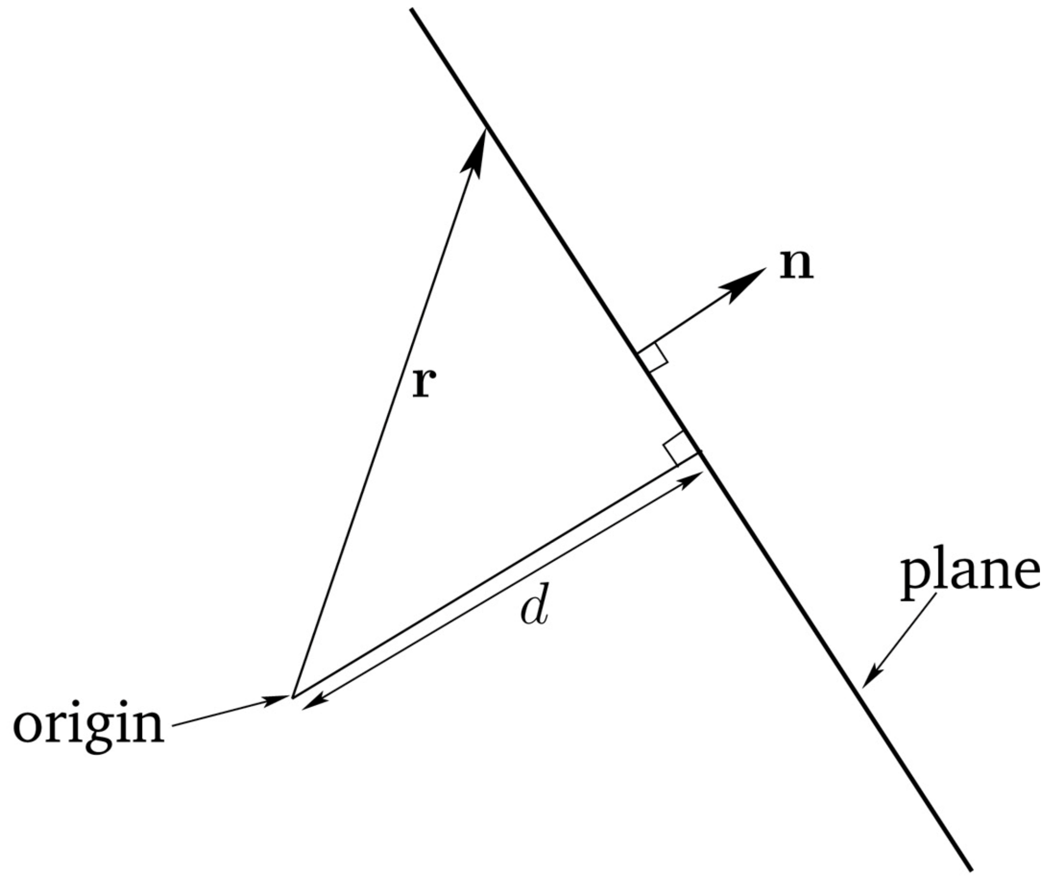

FIGURE 7.1
The solution of $\mathbf{n} \cdot \mathbf{r} = d$ is a plane.

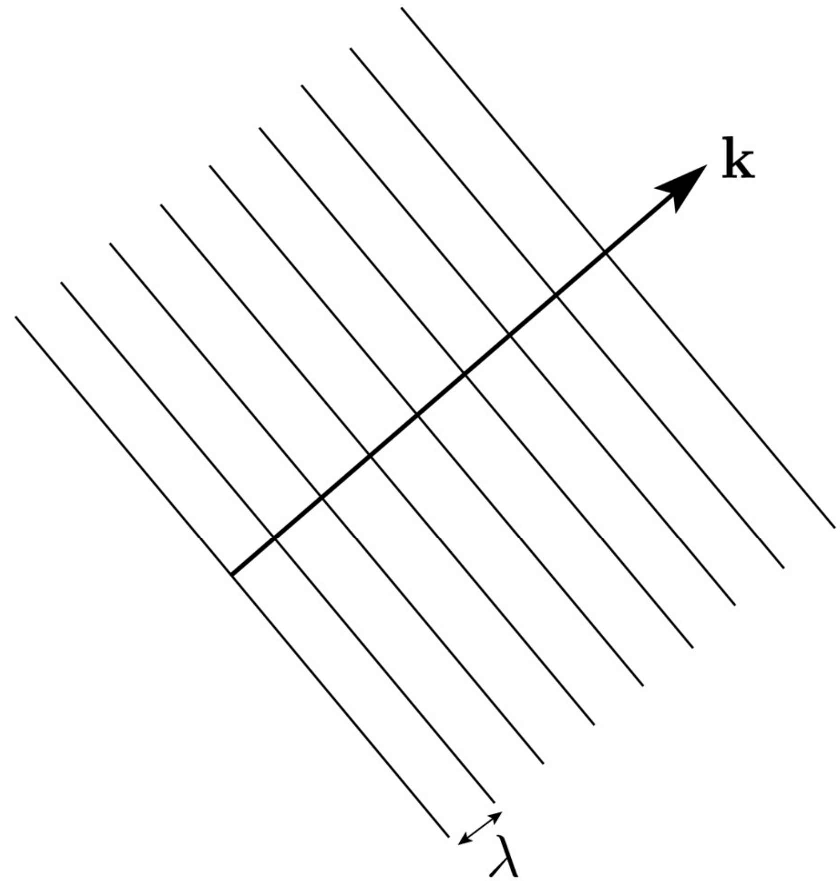

FIGURE 7.2
Wave maxima associated with a plane wave.

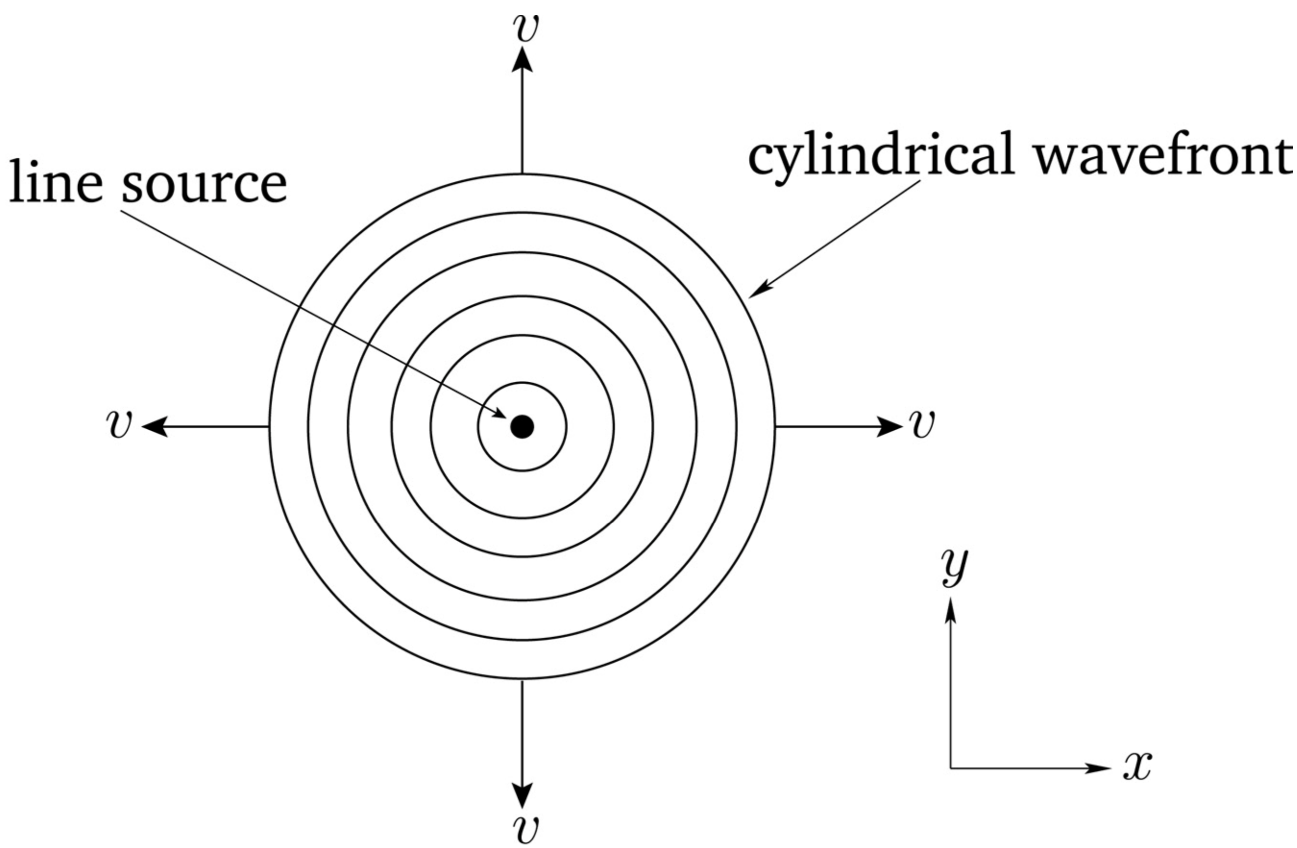

FIGURE 7.3
A cylindrical wave.

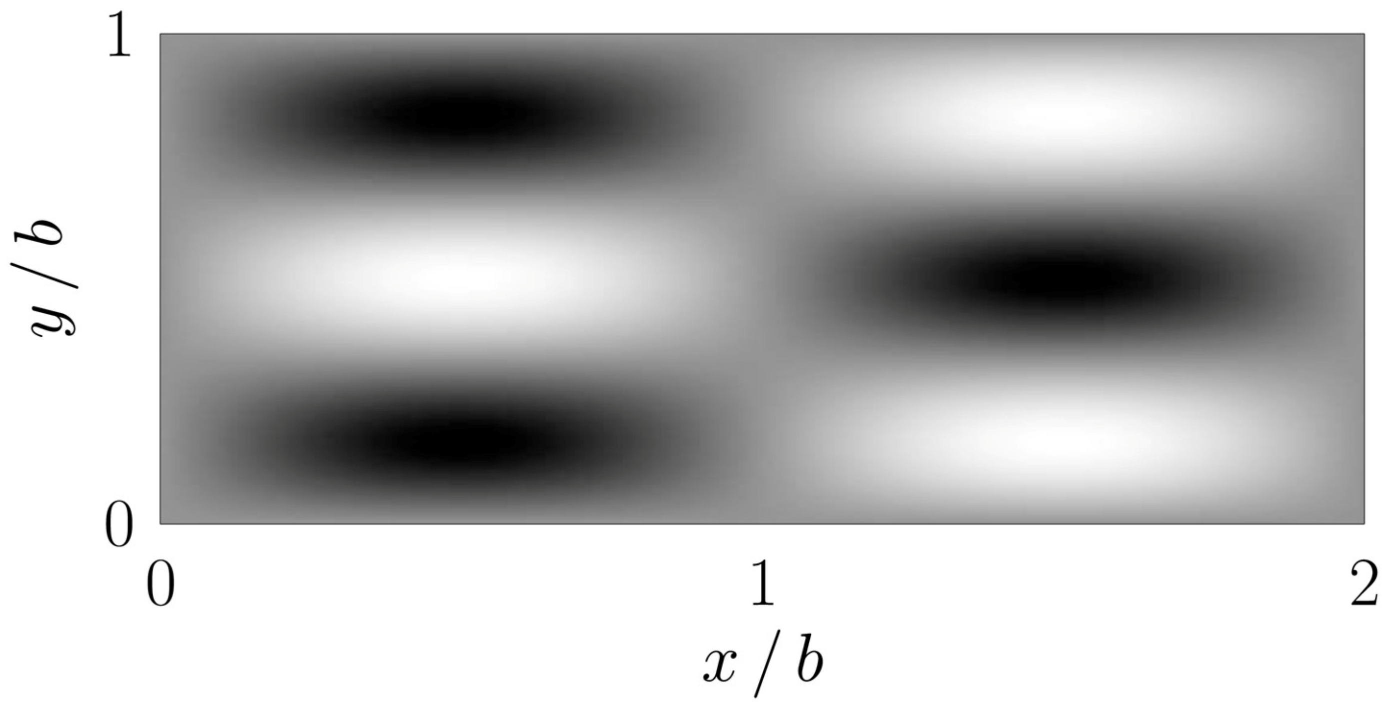

FIGURE 7.4
Density plot illustrating the spatial variation of the $m = 2$, $n = 3$ normal mode of a rectangular elastic sheet with $a = 2\,b$. Dark/light regions indicate positive/negative displacements.

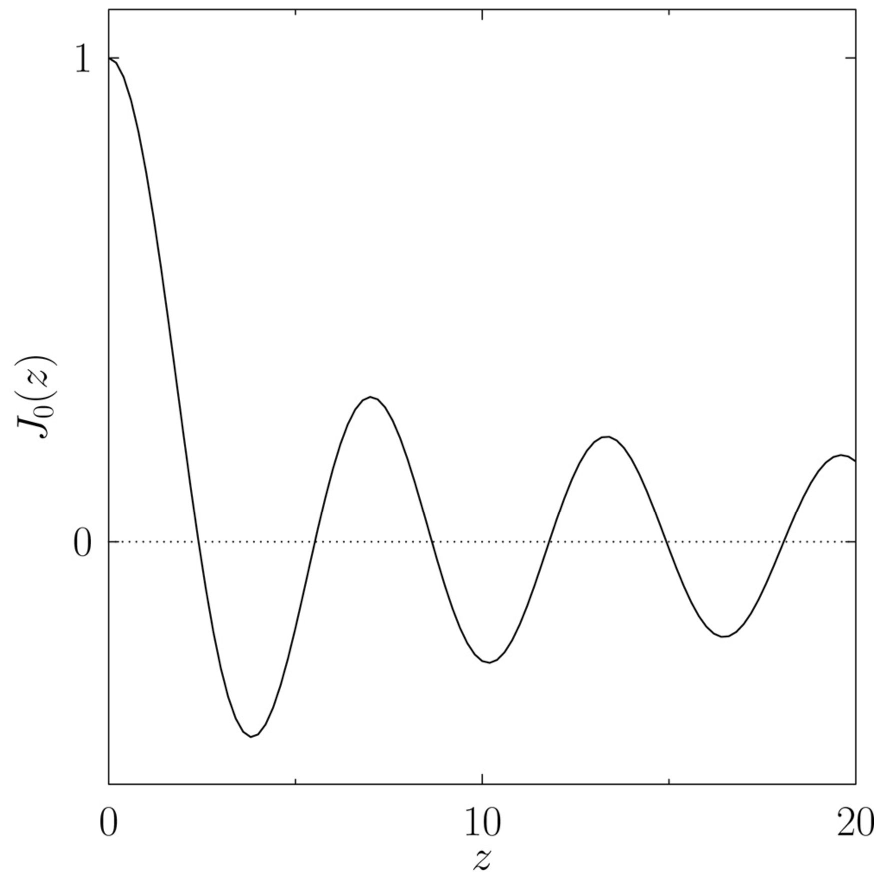

FIGURE 7.5
The Bessel function $J_0(z)$.

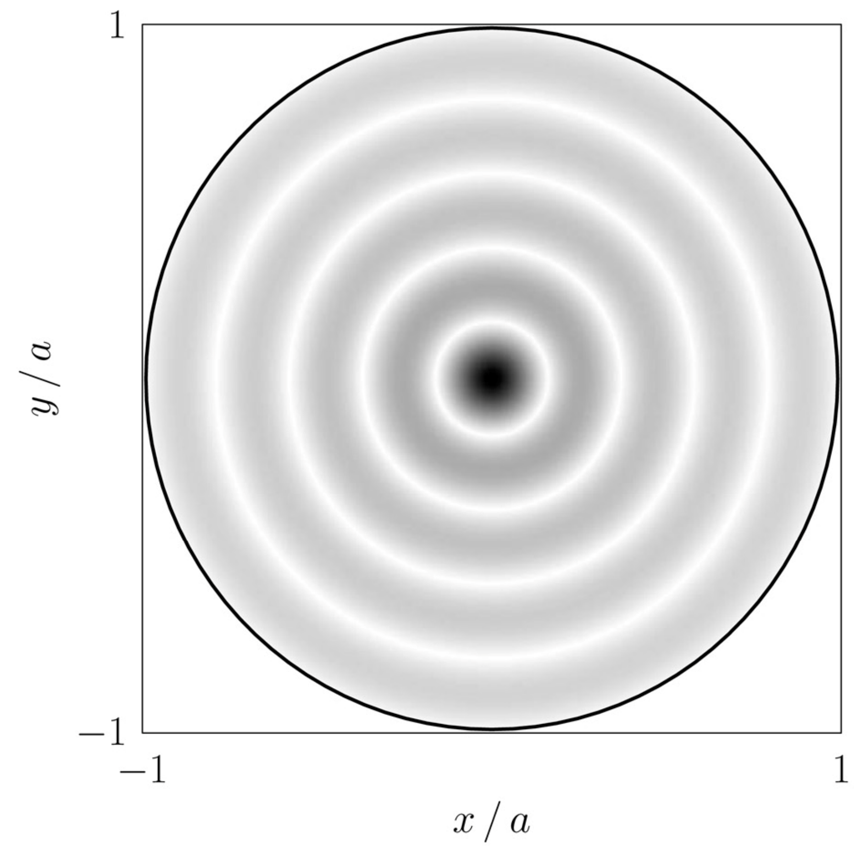

FIGURE 7.6
Density plot illustrating the spatial variation of the $j = 5$ normal mode of a circular elastic sheet of radius a. Dark/light regions indicate large/small displacement amplitudes.

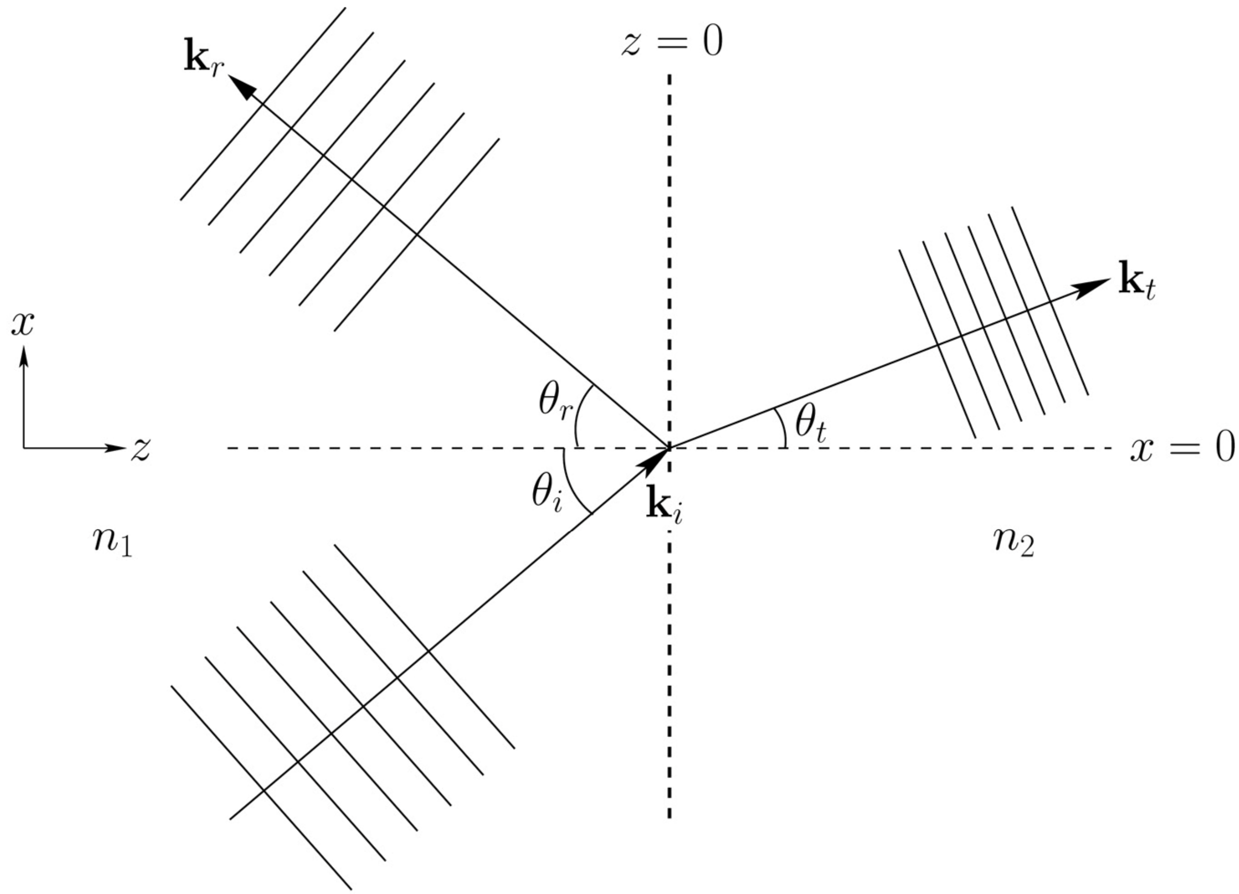

FIGURE 7.7
Reflection and refraction of a plane wave at a plane boundary.

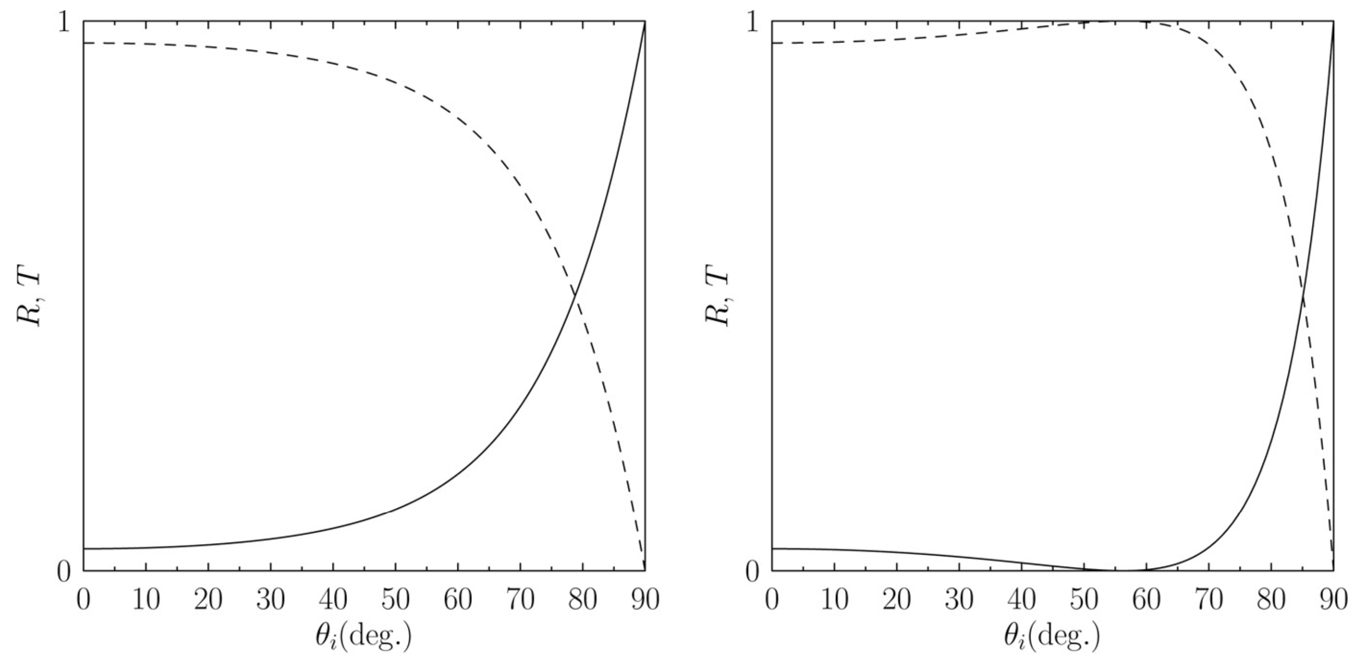

FIGURE 7.8
Coefficients of reflection (solid curves) and transmission (dashed curves) for oblique incidence from air ($n_1 = 1.0$) to glass ($n_2 = 1.5$). The left-hand panel shows the wave polarization for which the electric field is parallel to the boundary, whereas the right-hand panel shows the wave polarization for which the magnetic field is parallel to the boundary. The Brewster angle is 56.3°.

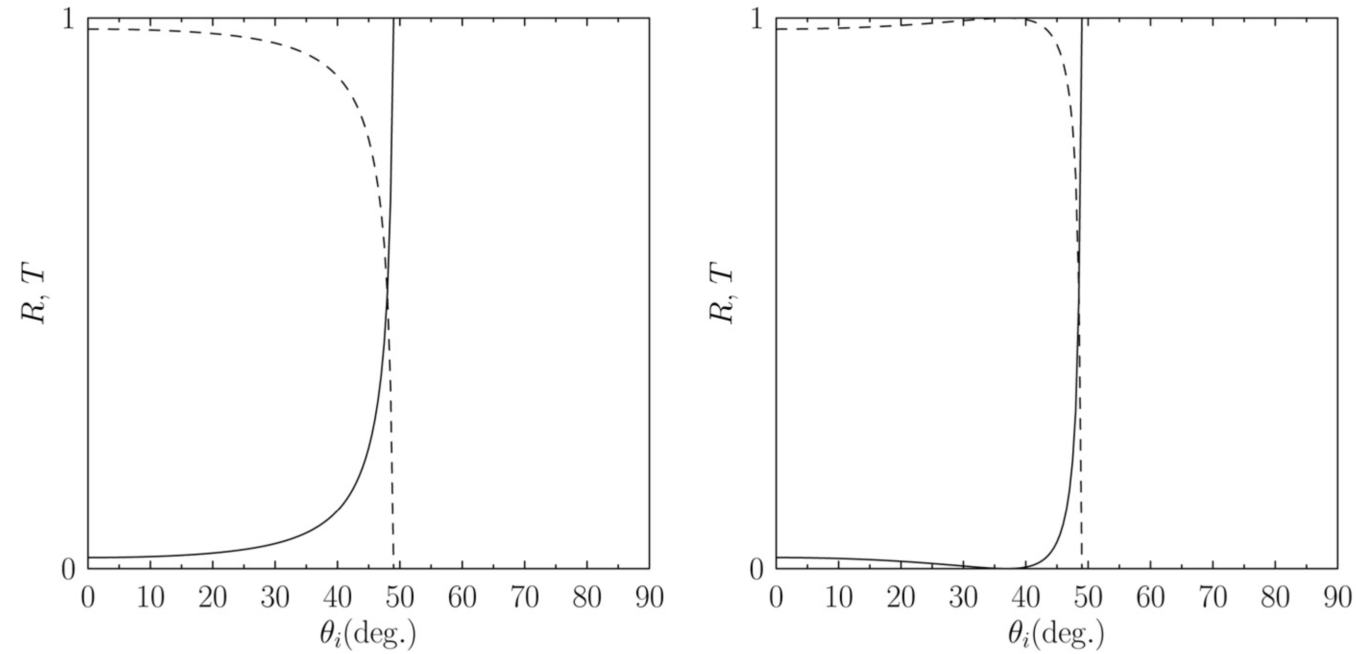

FIGURE 7.9
Coefficients of reflection (solid curves) and transmission (dashed curves) for oblique incidence from water ($n_1 = 1.33$) to air ($n_2 = 1.0$). The left-hand panel shows the wave polarization for which the electric field is parallel to the interface, whereas the right-hand panel shows the wave polarization for which the magnetic field is parallel to the interface. The critical angle is 48.8°.

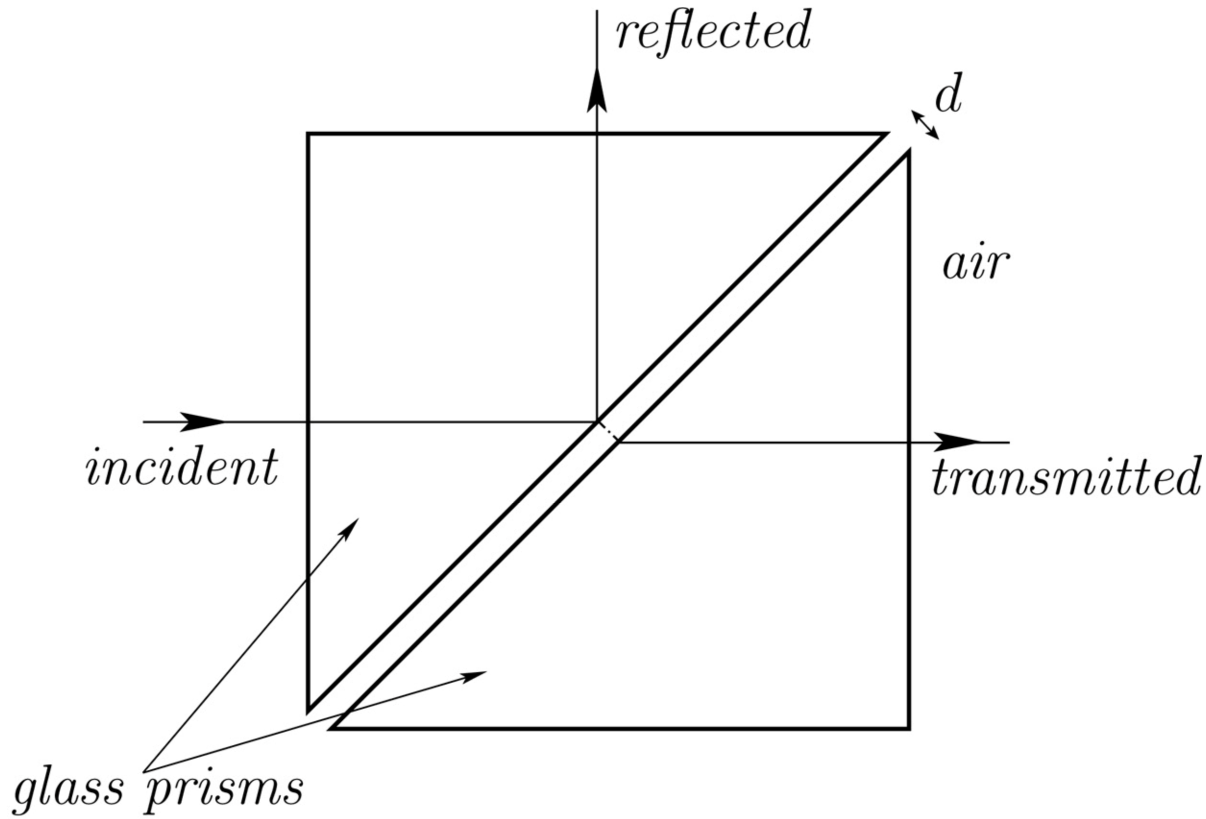

FIGURE 7.10
Frustrated total internal reflection.

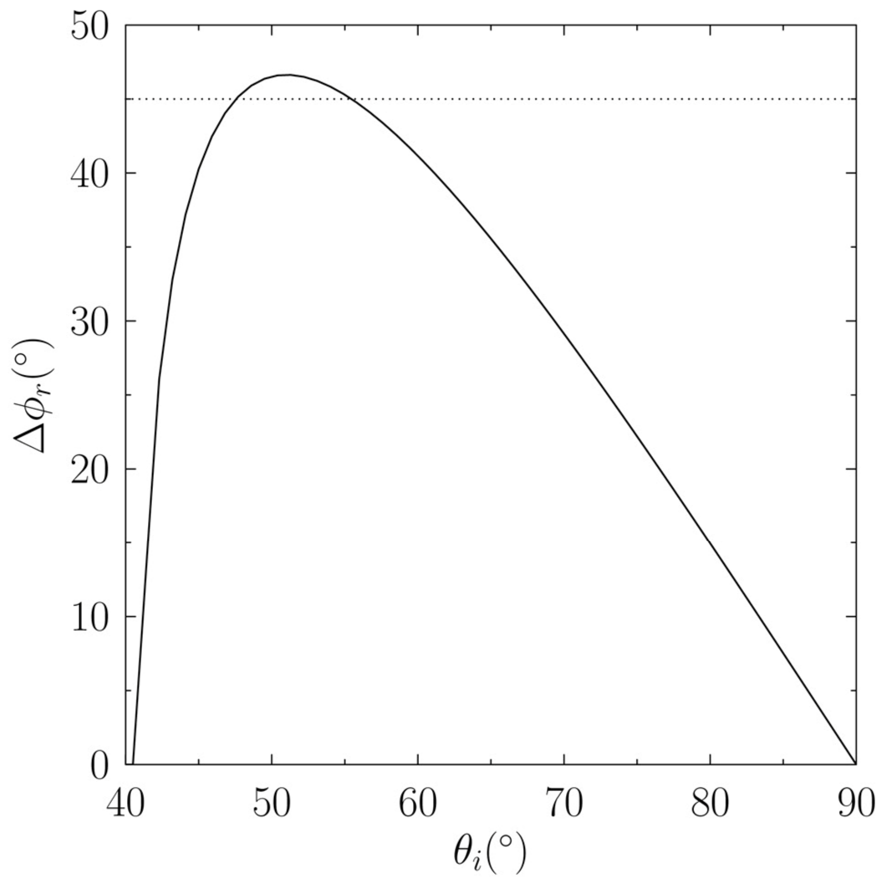

FIGURE 7.11
Phase advance introduced between the two different wave polarizations by total internal reflection at an interface between glass ($n_1 = 1.52$) and air ($n_2 = 1.0$).

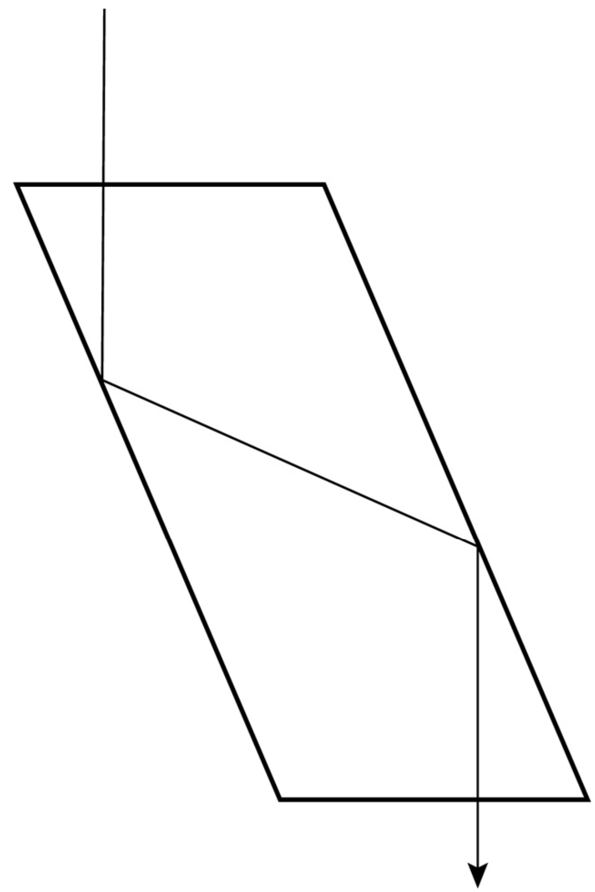

FIGURE 7.12
Path of light ray through Fresnel romb (schematic).

Oscillations and Waves

8 Wave Pulses

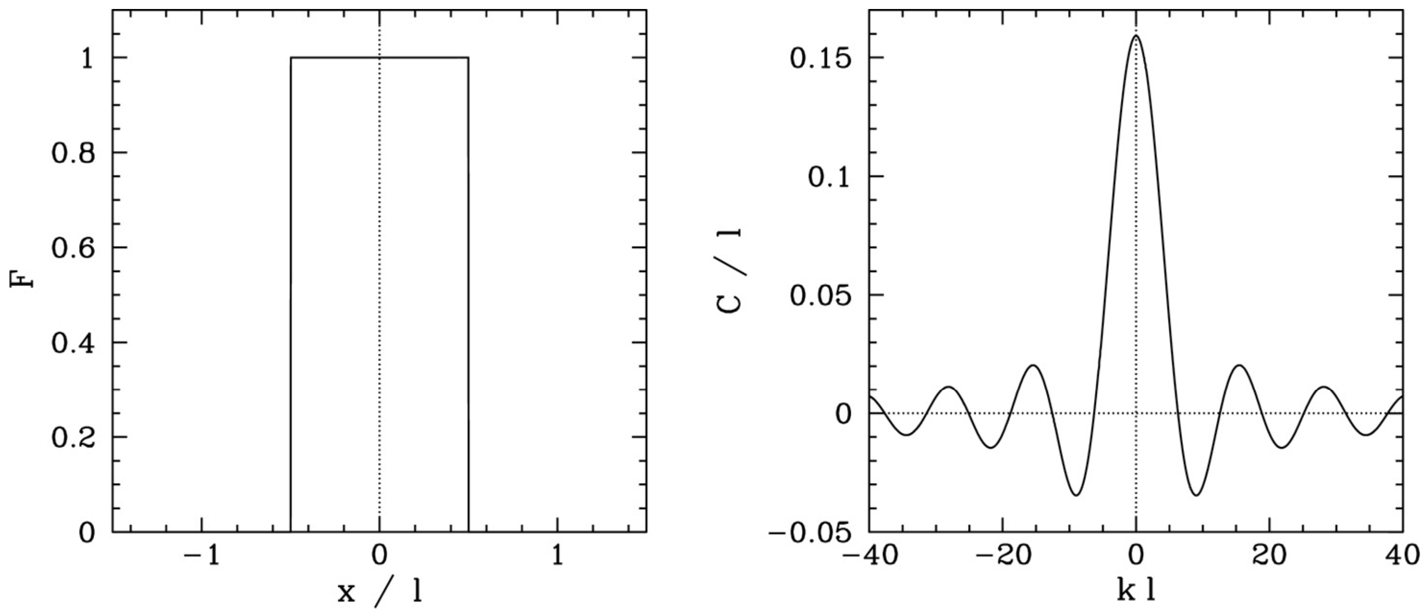

FIGURE 8.1
Fourier transform of a top-hat function.

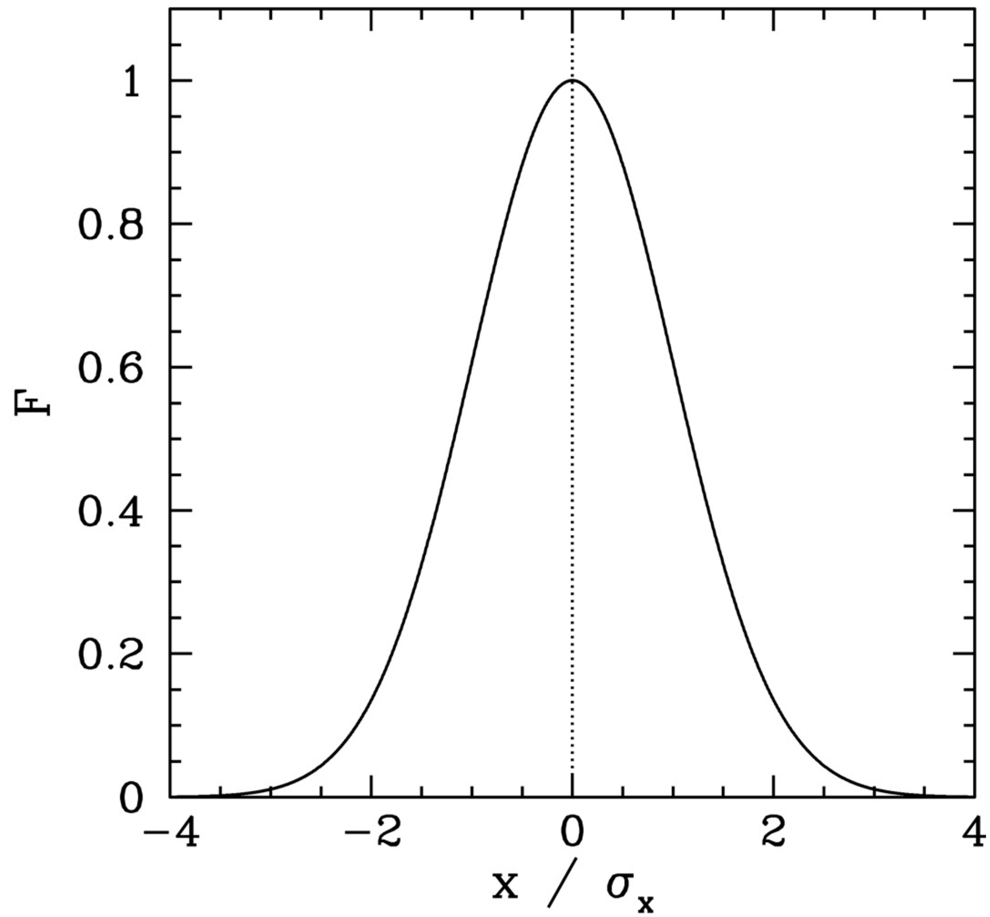

FIGURE 8.2
A Gaussian function.

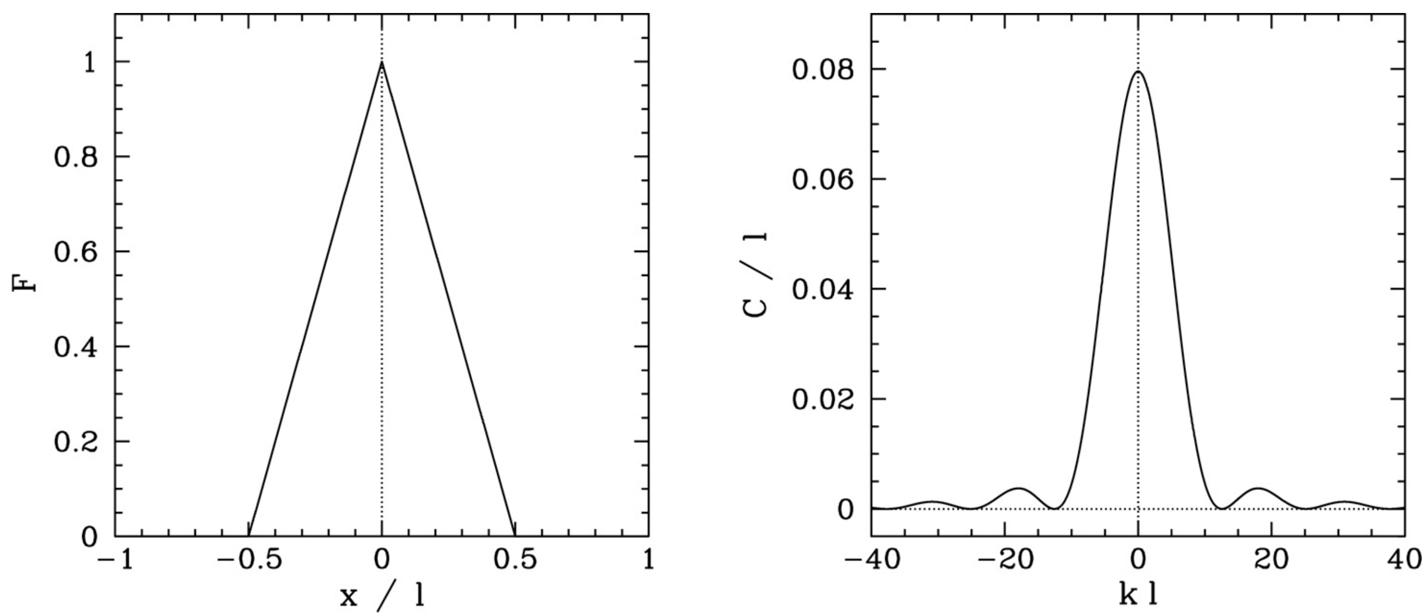

FIGURE 8.3
Fourier transform of a triangular wave pulse.

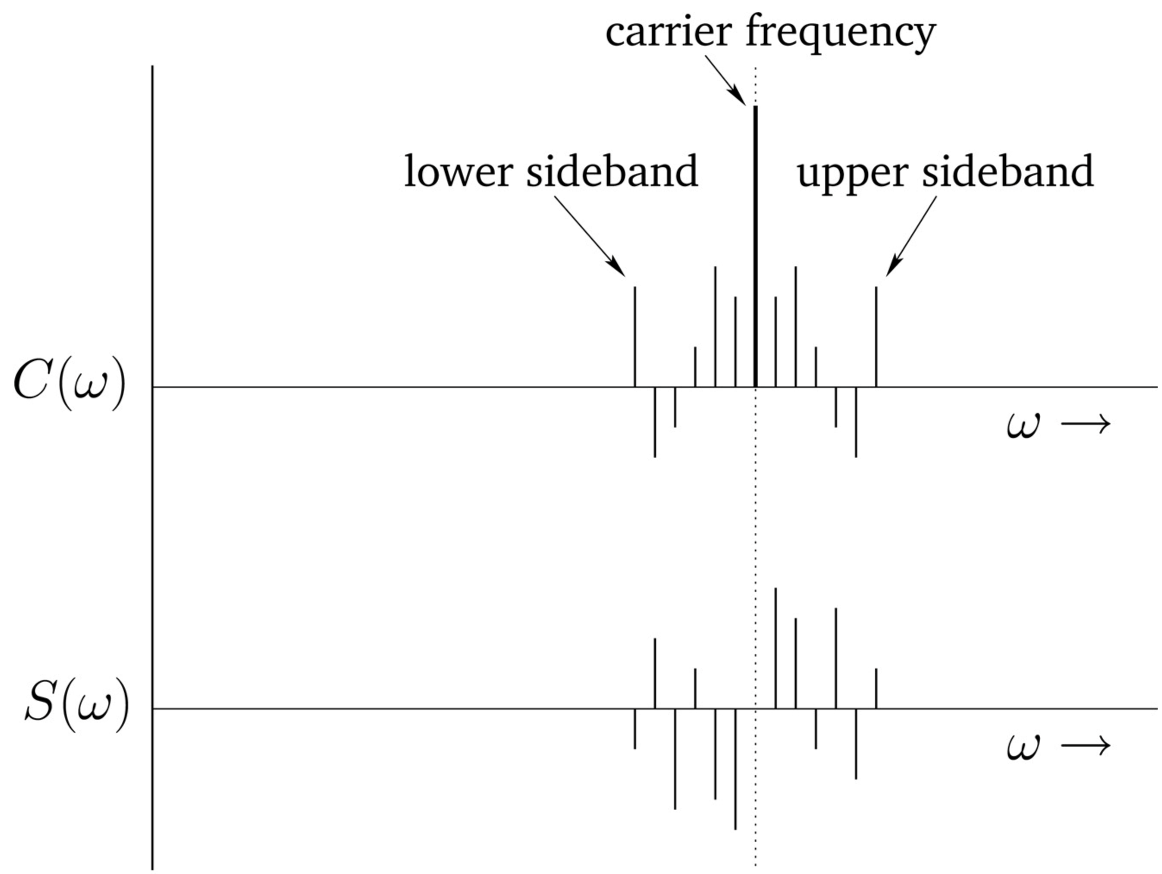

FIGURE 8.4
Frequency spectrum of an AM radio signal.

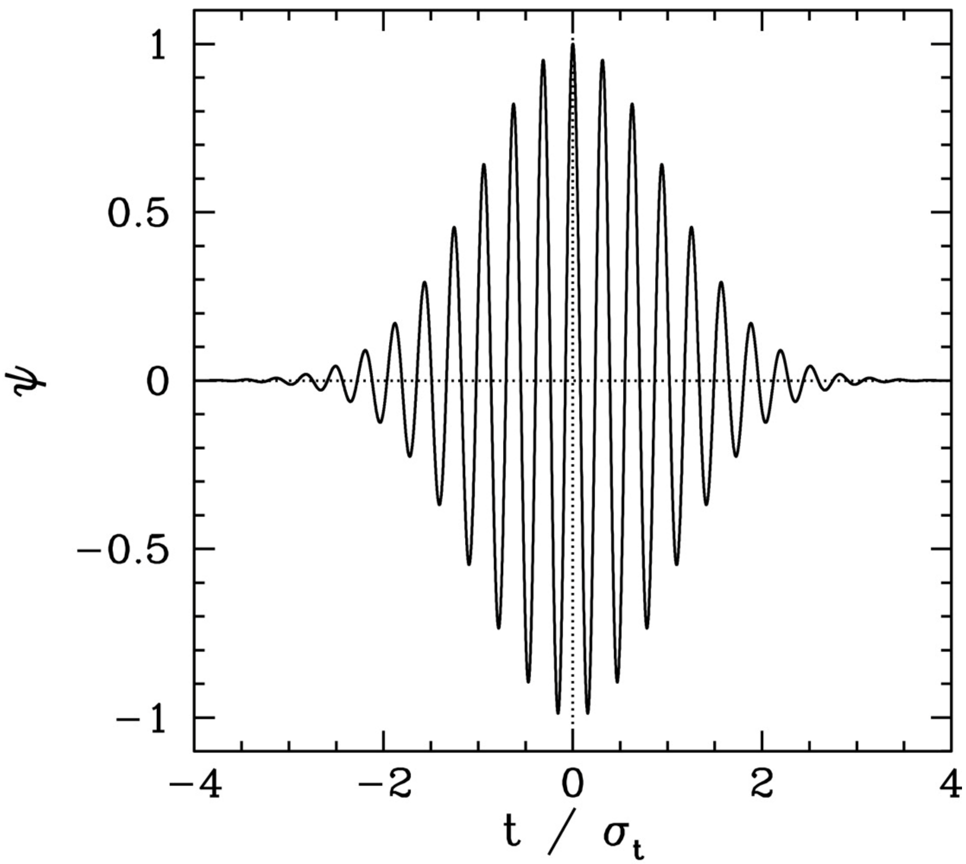

FIGURE 8.5
A digital bit transmitted over AM radio.

Oscillations and Waves

9 Dispersive Waves

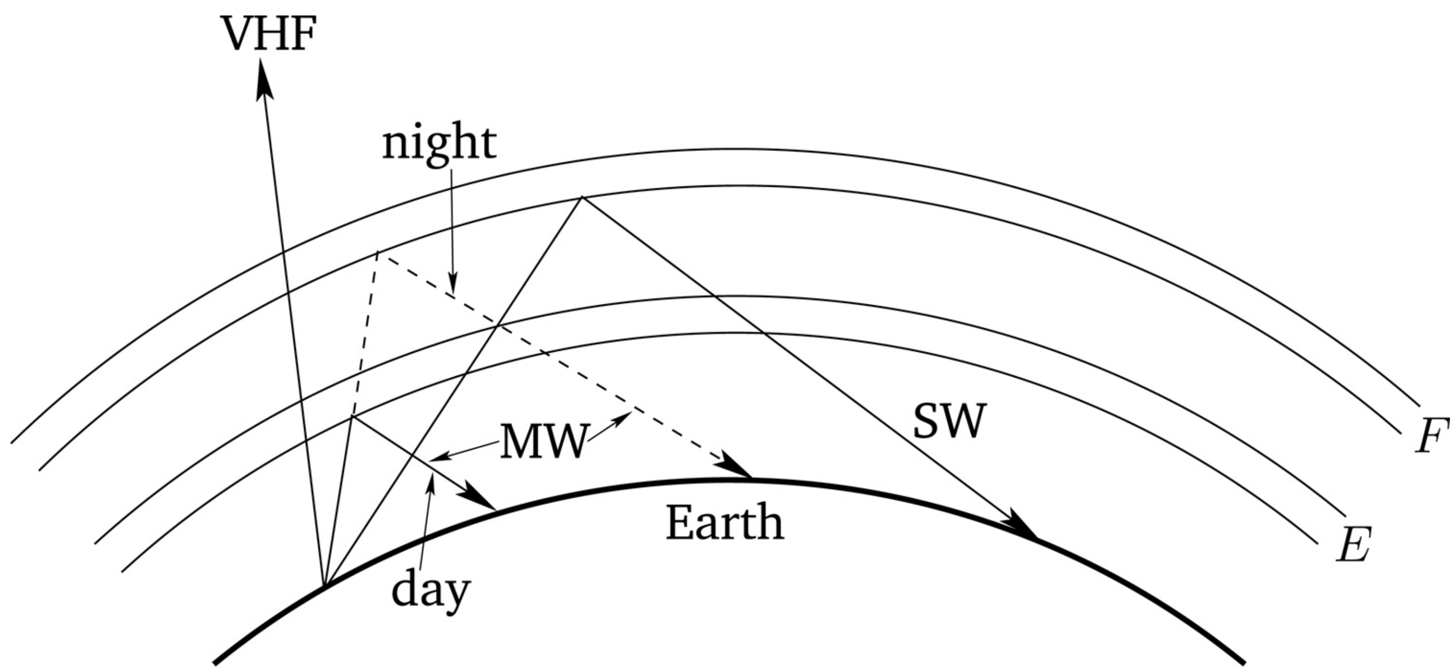

FIGURE 9.1
Reflection and transmission of radio waves by the ionosphere.

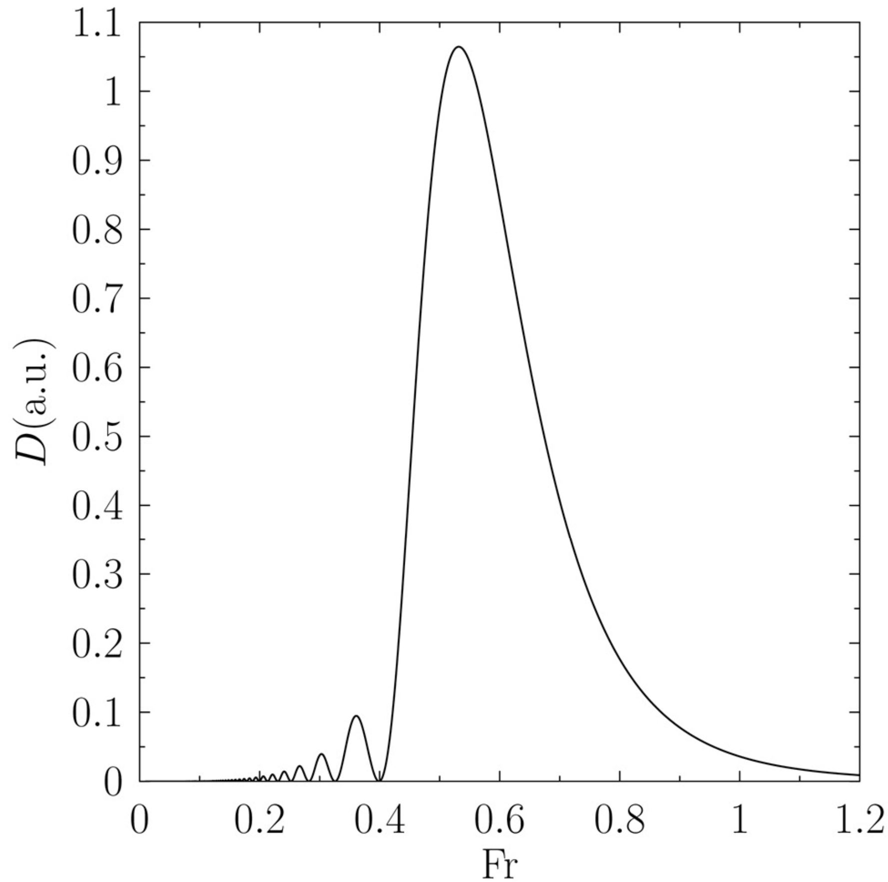

FIGURE 9.2
Variation of wave drag, D, with Froude number for a ship traveling through deep water.

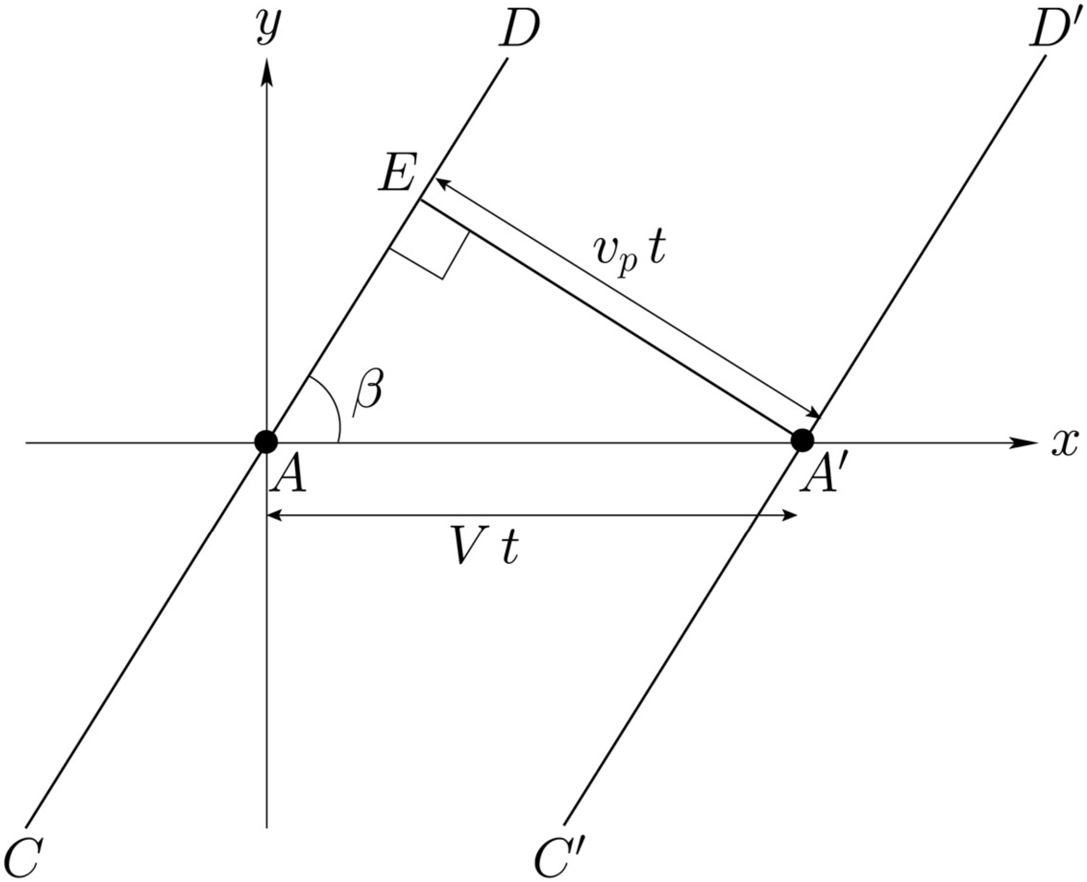

FIGURE 9.3
An oblique plane wave generated on the surface of the water by a moving ship.

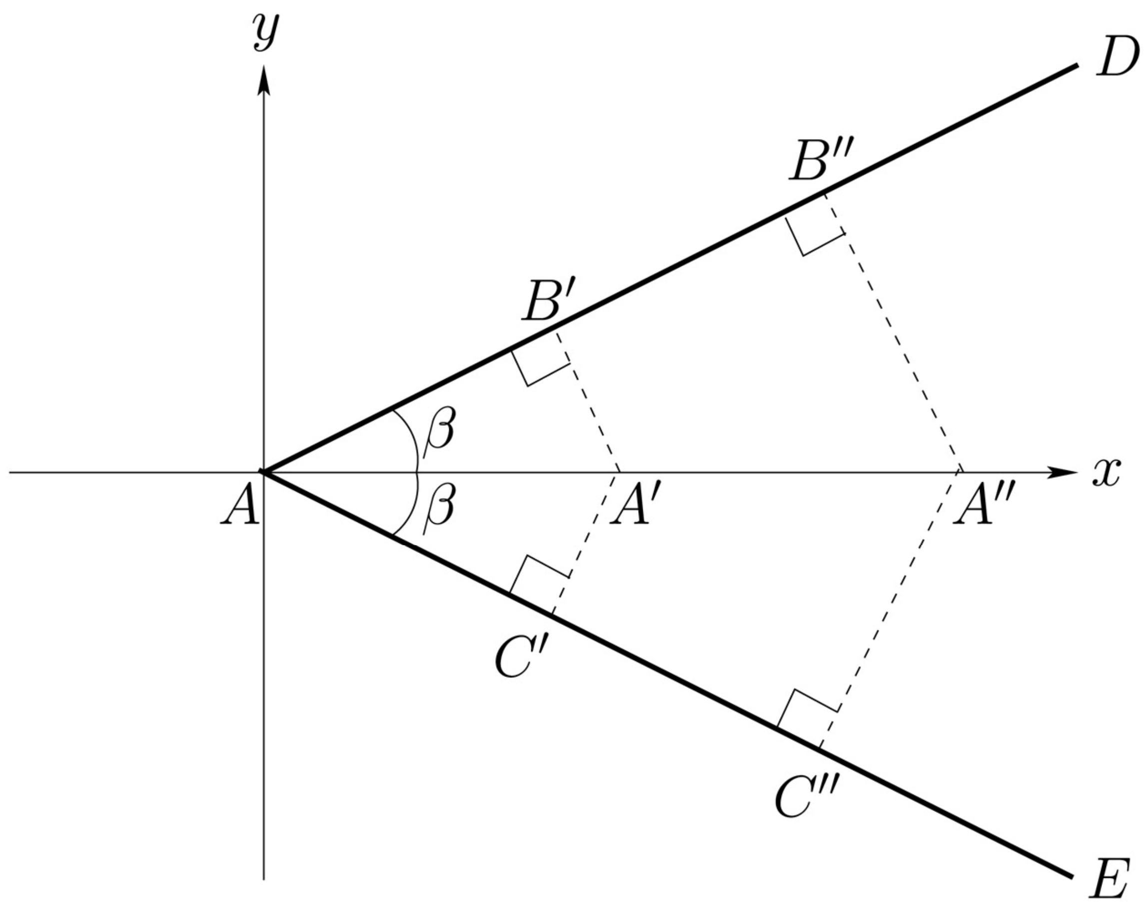

FIGURE 9.4
A shallow water wake.

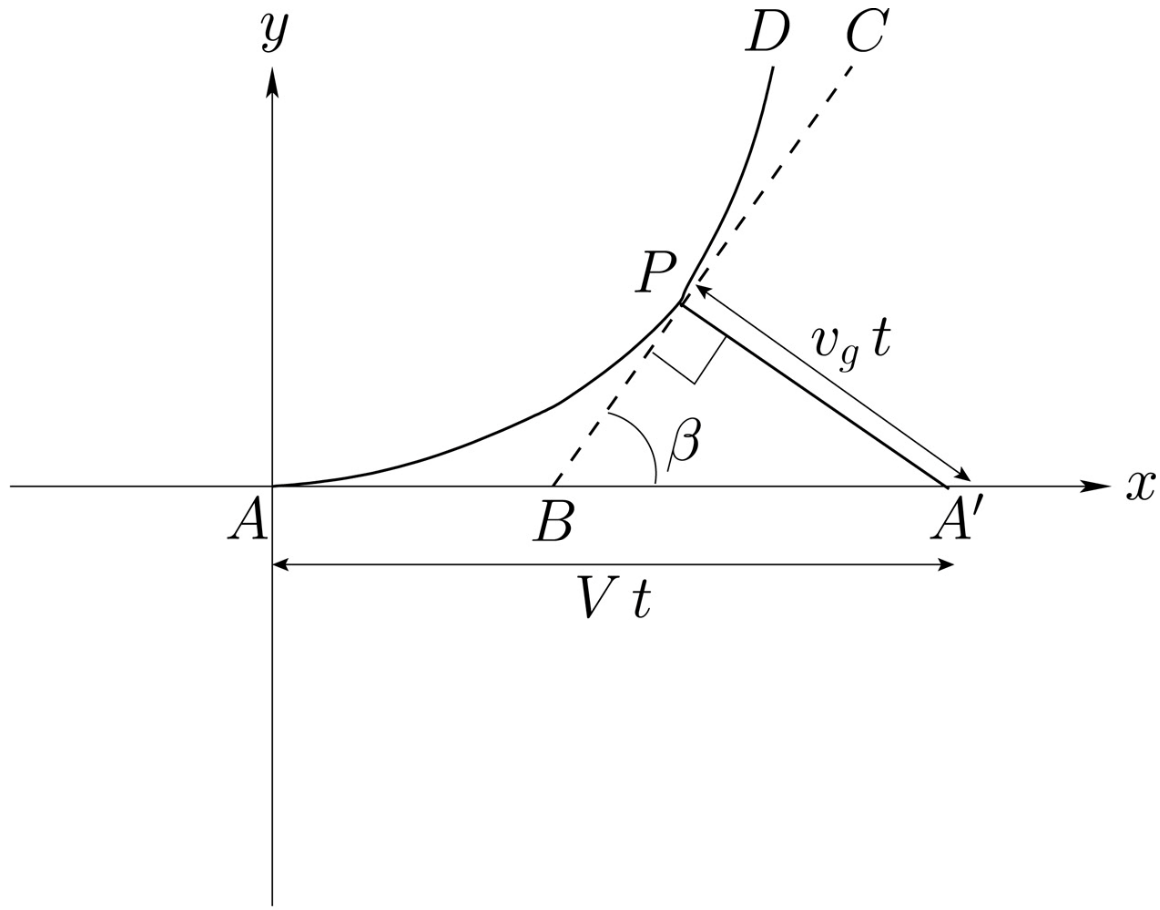

FIGURE 9.5
Formation of an interference maximum in a deep water wake.

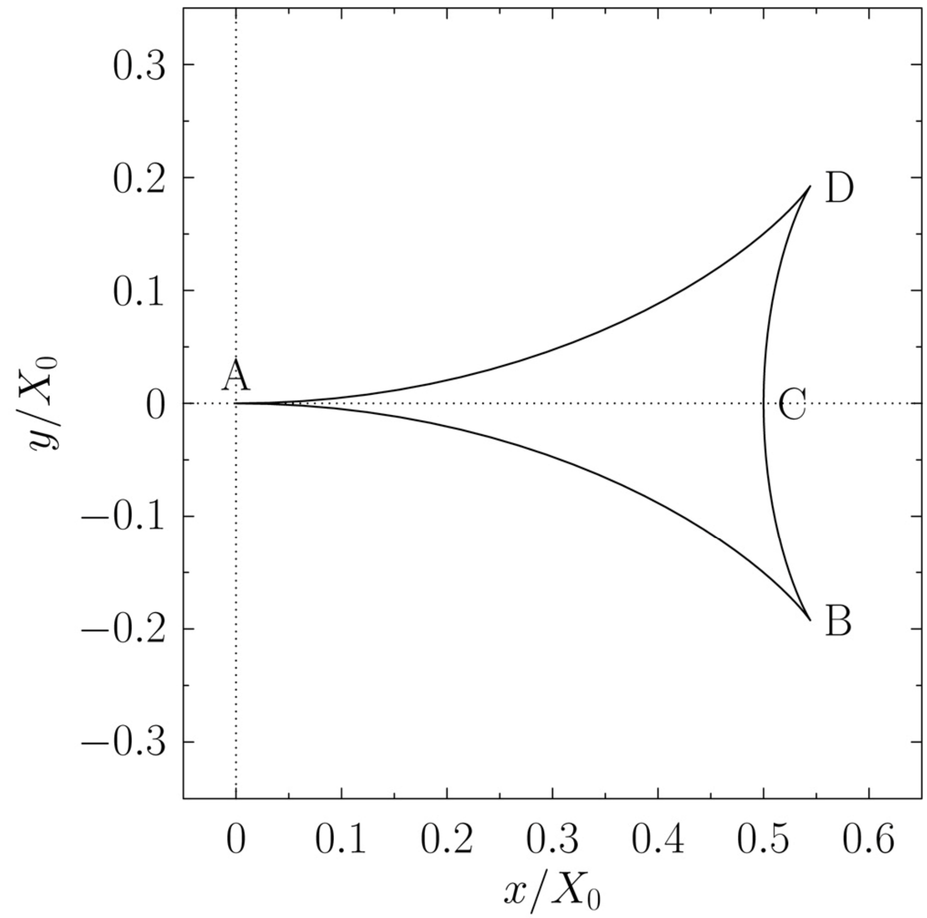

FIGURE 9.6
Locus of an interference maximum in a deep water wake.

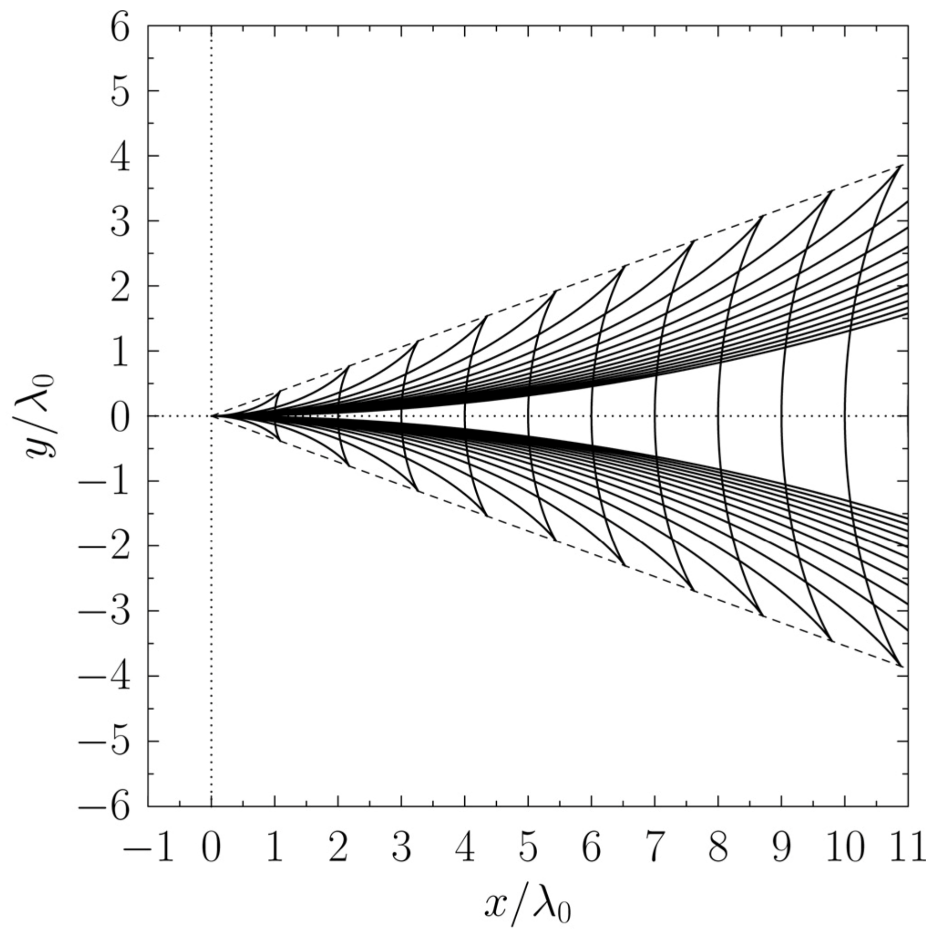

FIGURE 9.7
A deep water wake.

Oscillations and Waves

10 Wave Optics

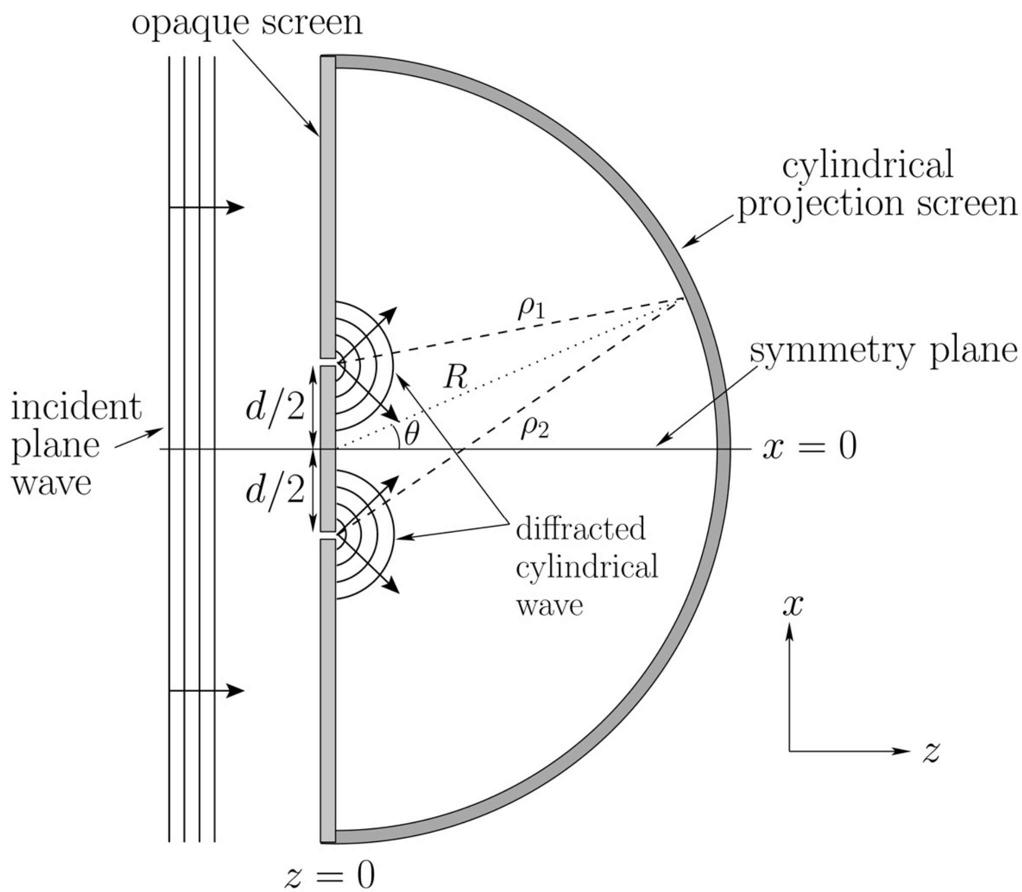

FIGURE 10.1
Two-slit interference at normal incidence.

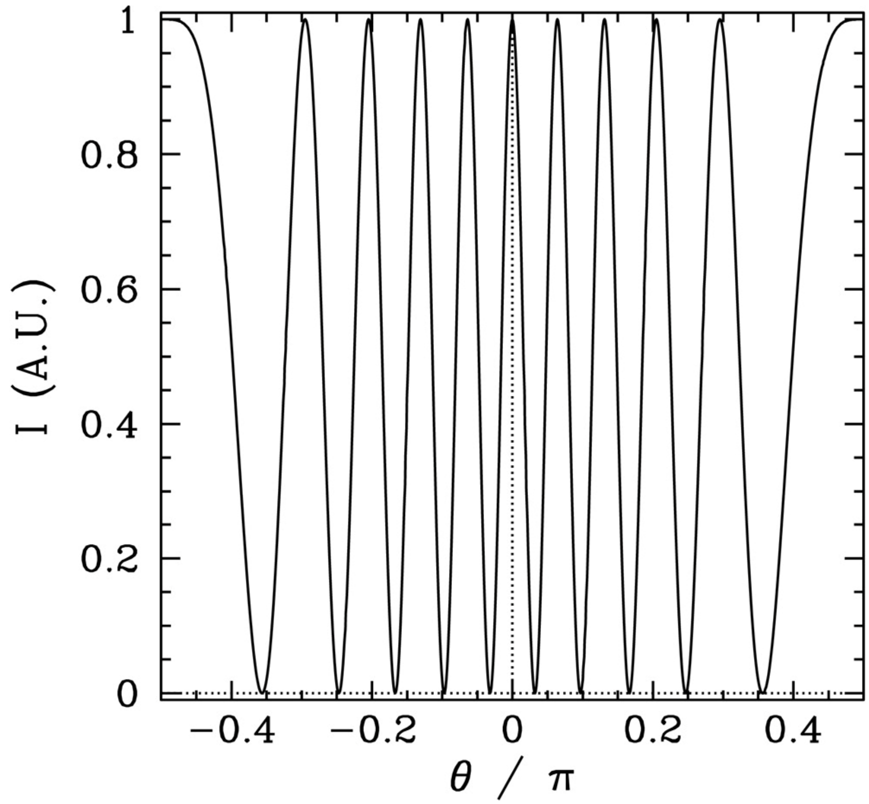

FIGURE 10.2
Two-slit far-field interference pattern calculated for $d/\lambda = 5$ with normal incidence and narrow slits.

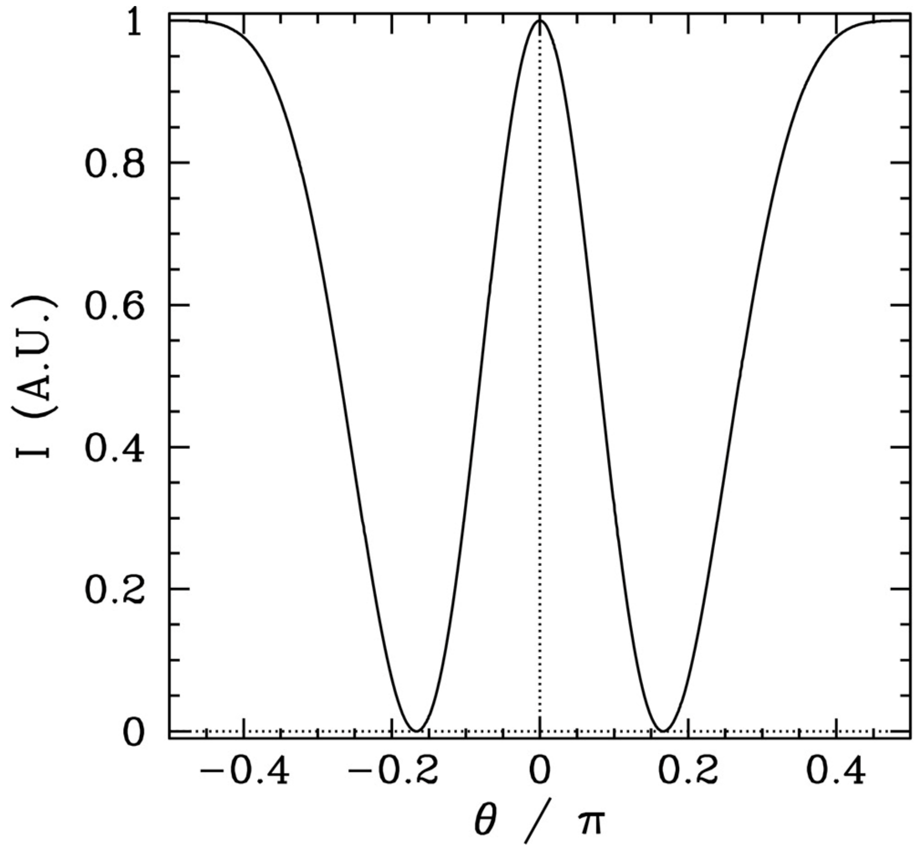

FIGURE 10.3
Two-slit far-field interference pattern calculated for $d/\lambda = 1$ with normal incidence and narrow slits.

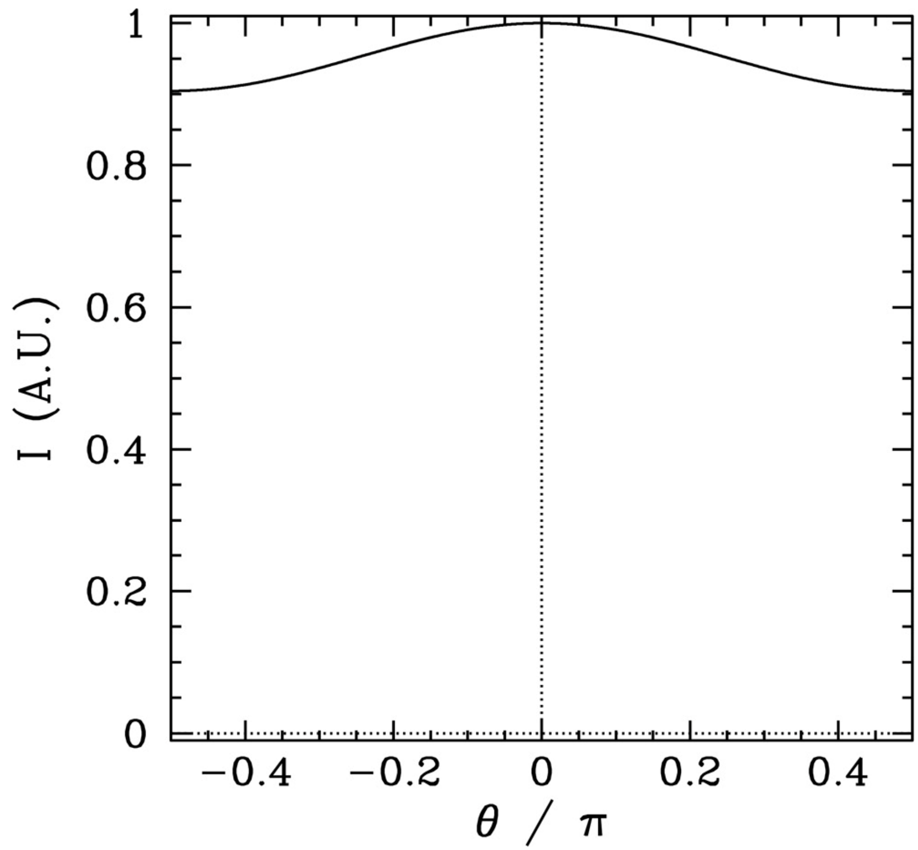

FIGURE 10.4
Two-slit far-field interference pattern calculated for $d/\lambda = 0.1$ with normal incidence and narrow slits.

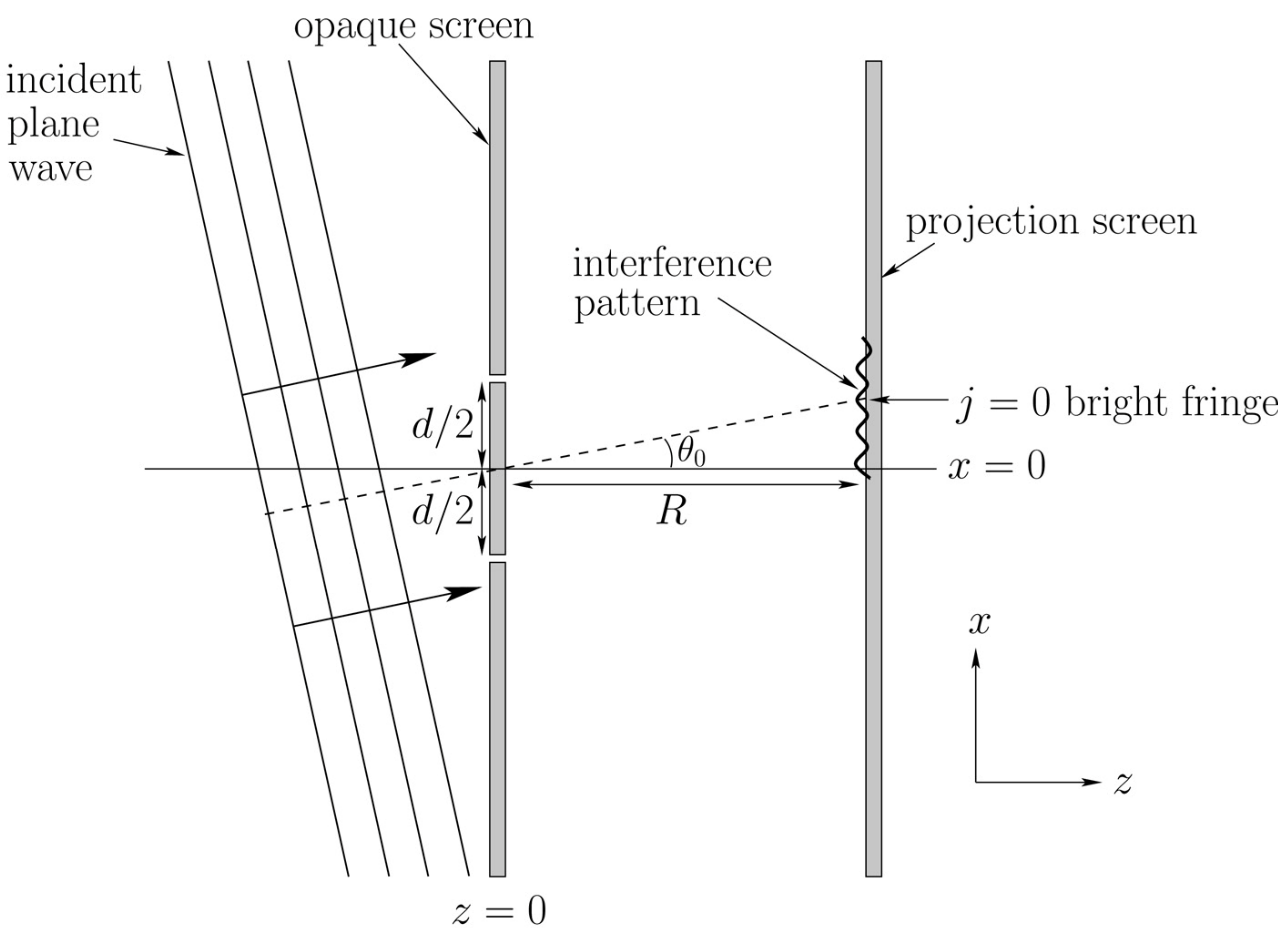

FIGURE 10.5
Two-slit interference at oblique incidence.

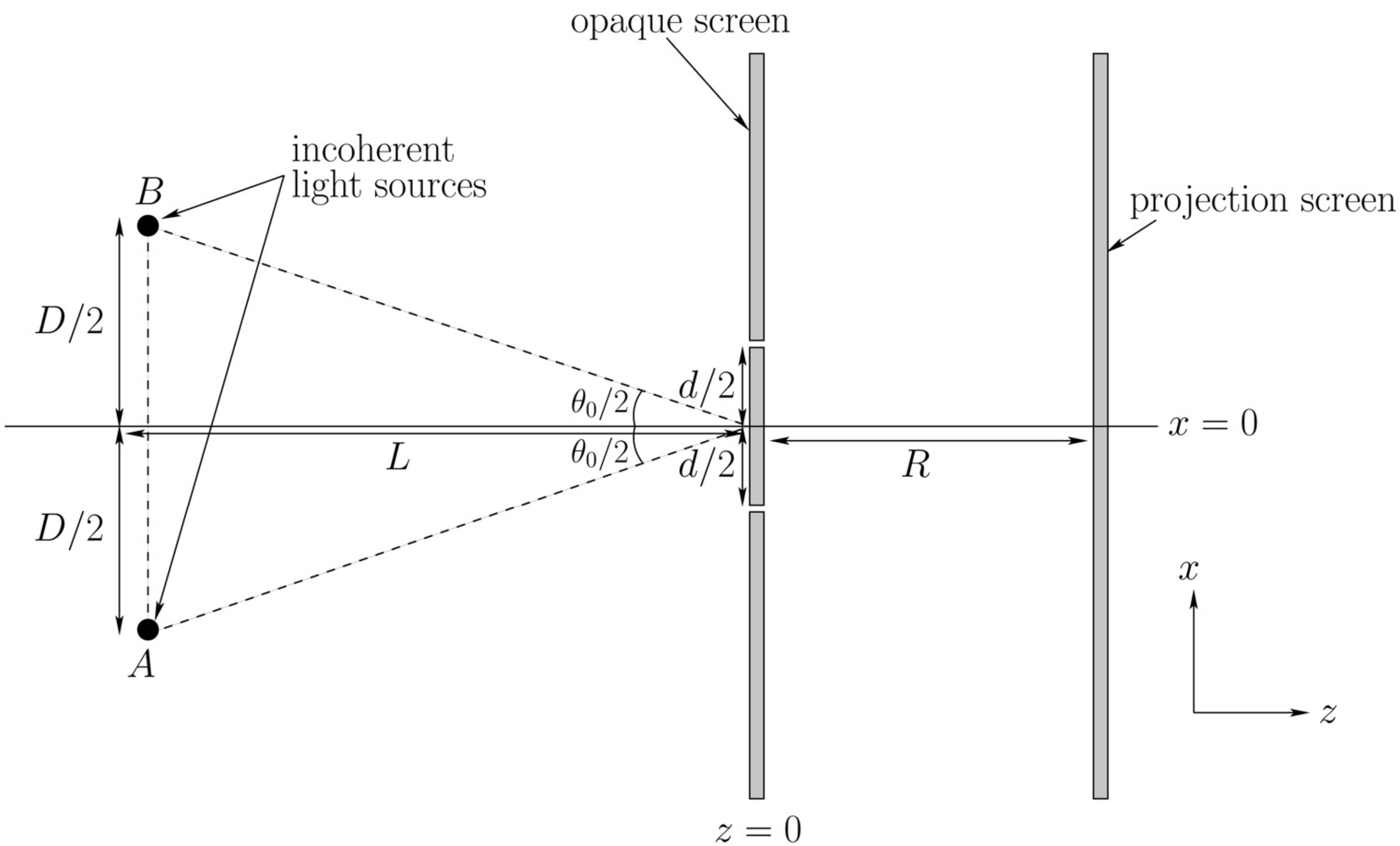

FIGURE 10.6
Two-slit interference with two line sources.

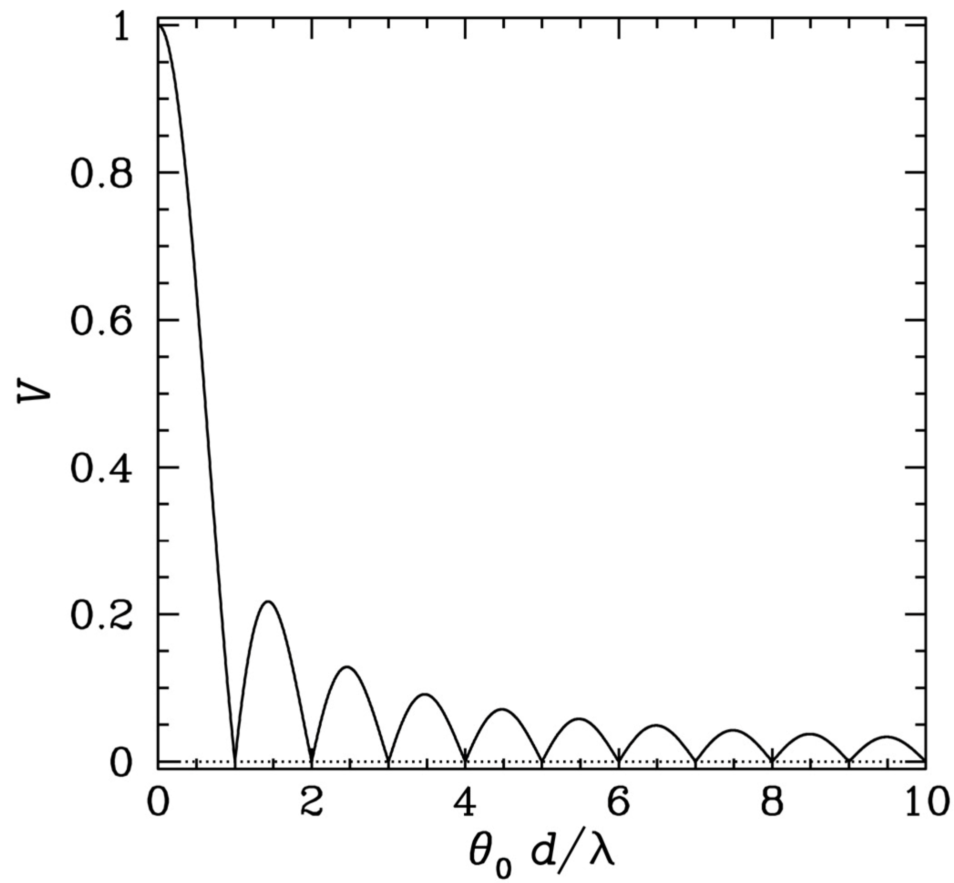

FIGURE 10.7
Visibility of a two-slit far-field interference pattern generated by an extended incoherent light source.

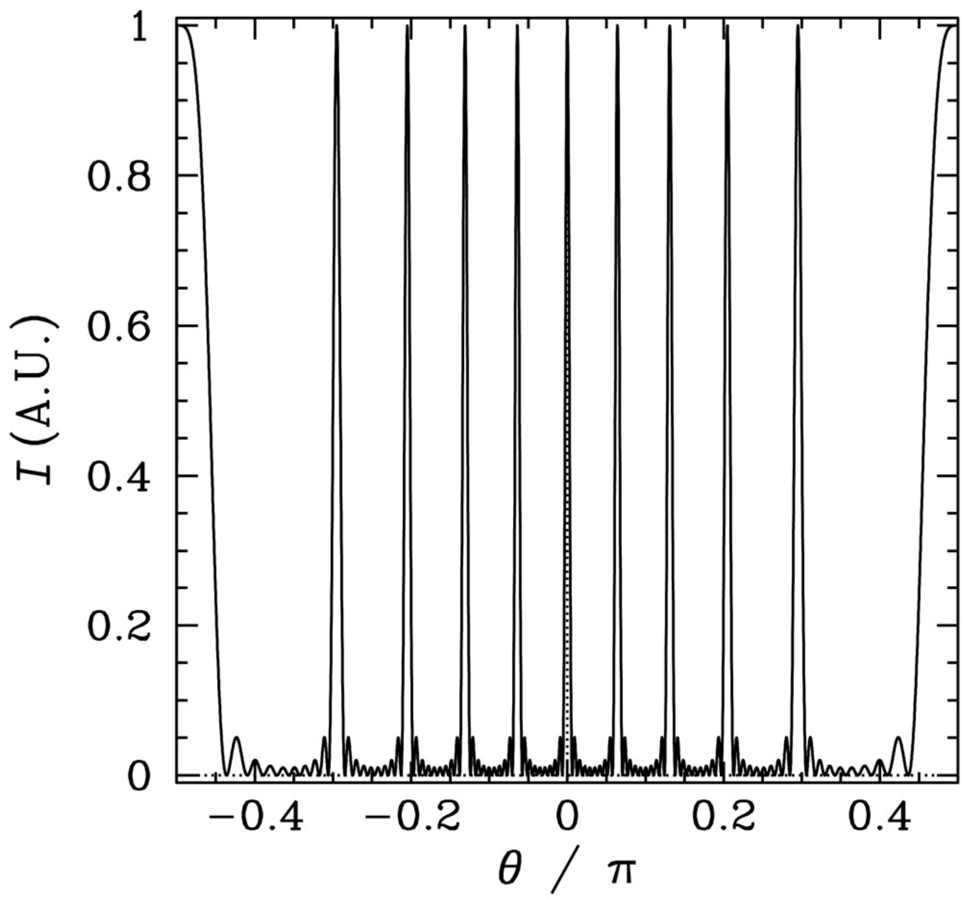

FIGURE 10.8
Multi-slit far-field interference pattern calculated for $N = 10$ and $d/\lambda = 5$ with normal incidence and narrow slits.

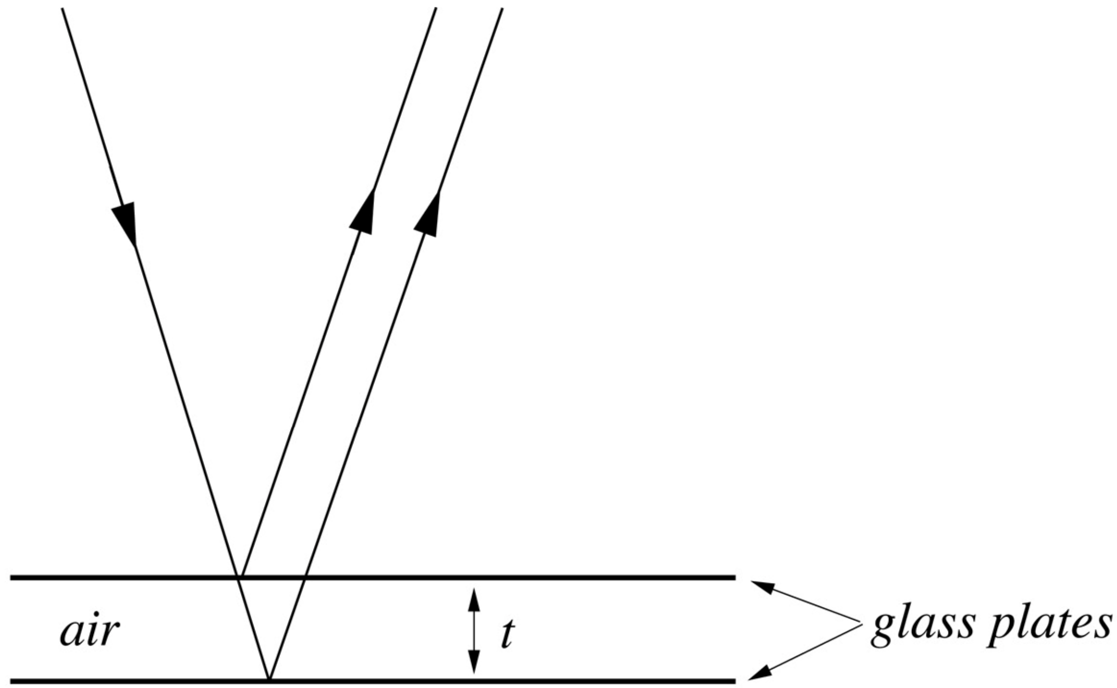

FIGURE 10.9
Interference of light due to a thin film of air trapped between two pieces of glass.

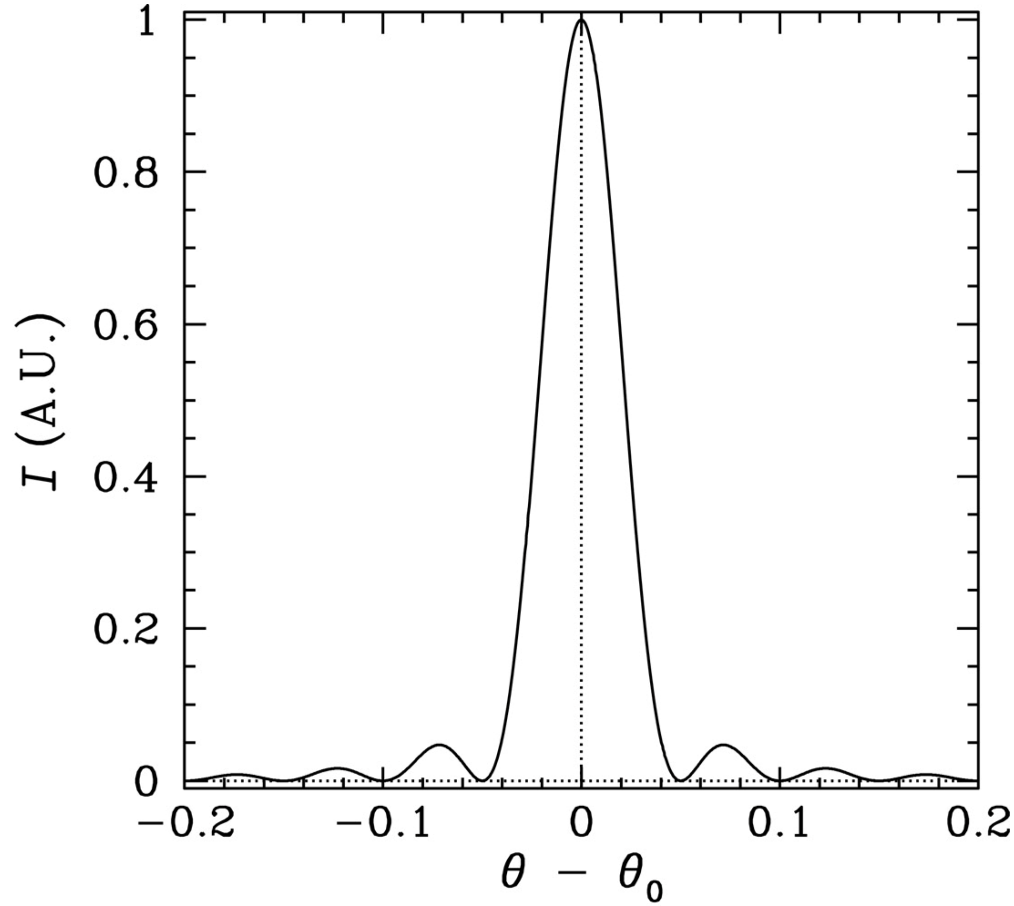

FIGURE 10.10
Single-slit far-field diffraction pattern calculated for $\delta/\lambda = 20$.

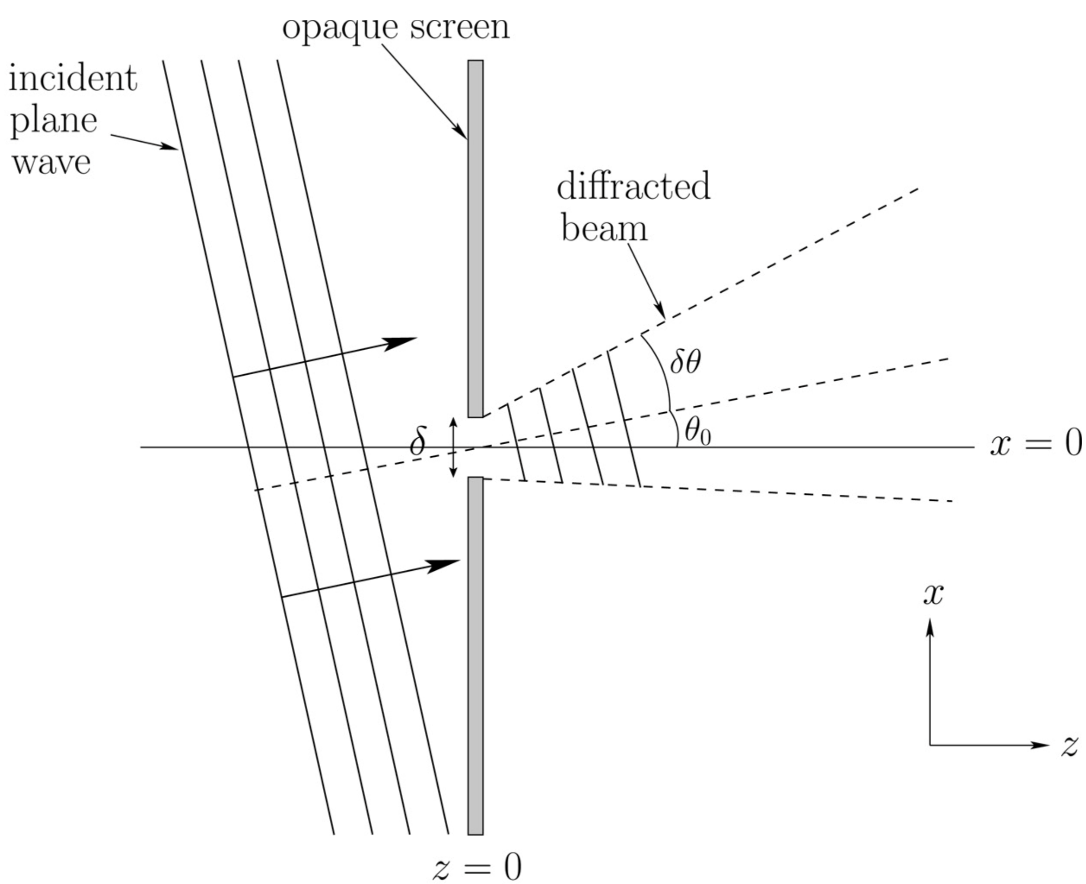

FIGURE 10.11
Single-slit diffraction at oblique incidence.

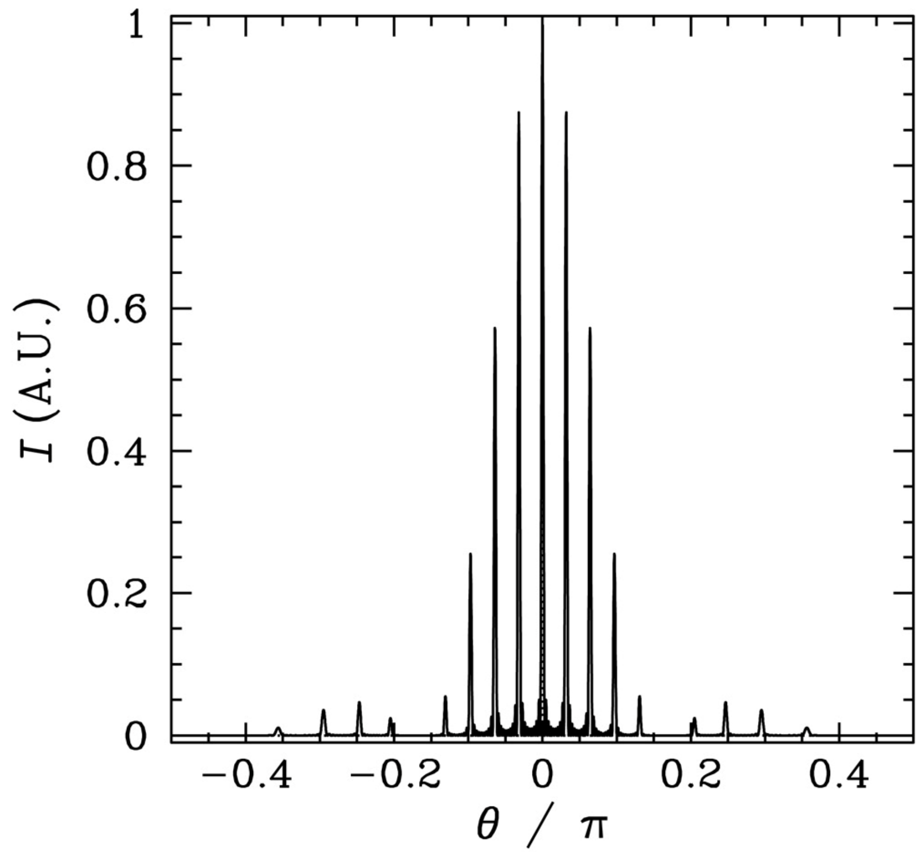

FIGURE 10.12
Multi-slit far-field interference pattern calculated for $N = 10$, $d/\lambda = 10$, and $\delta/\lambda = 2$, assuming normal incidence.

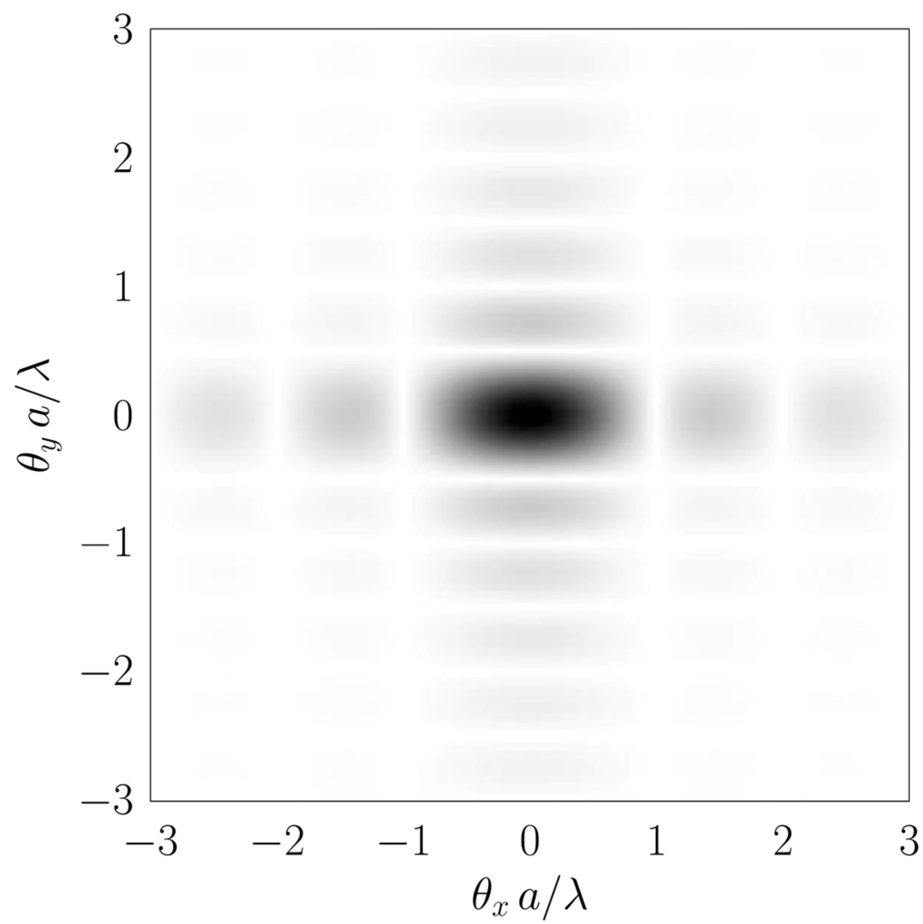

FIGURE 10.13
Far-field interference/diffraction pattern produced by a rectangular aperture for which $b = 2\,a$. Darker regions indicate higher light intensity.

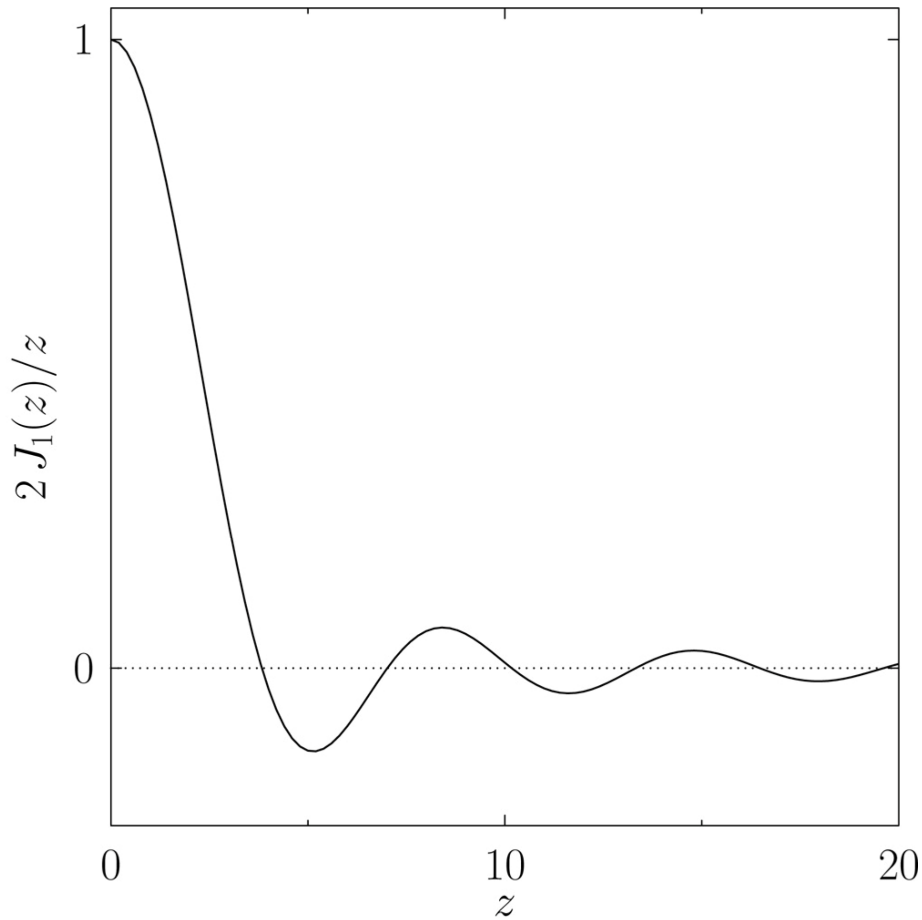

FIGURE 10.14
The function $2\,J_1(z)/z$.

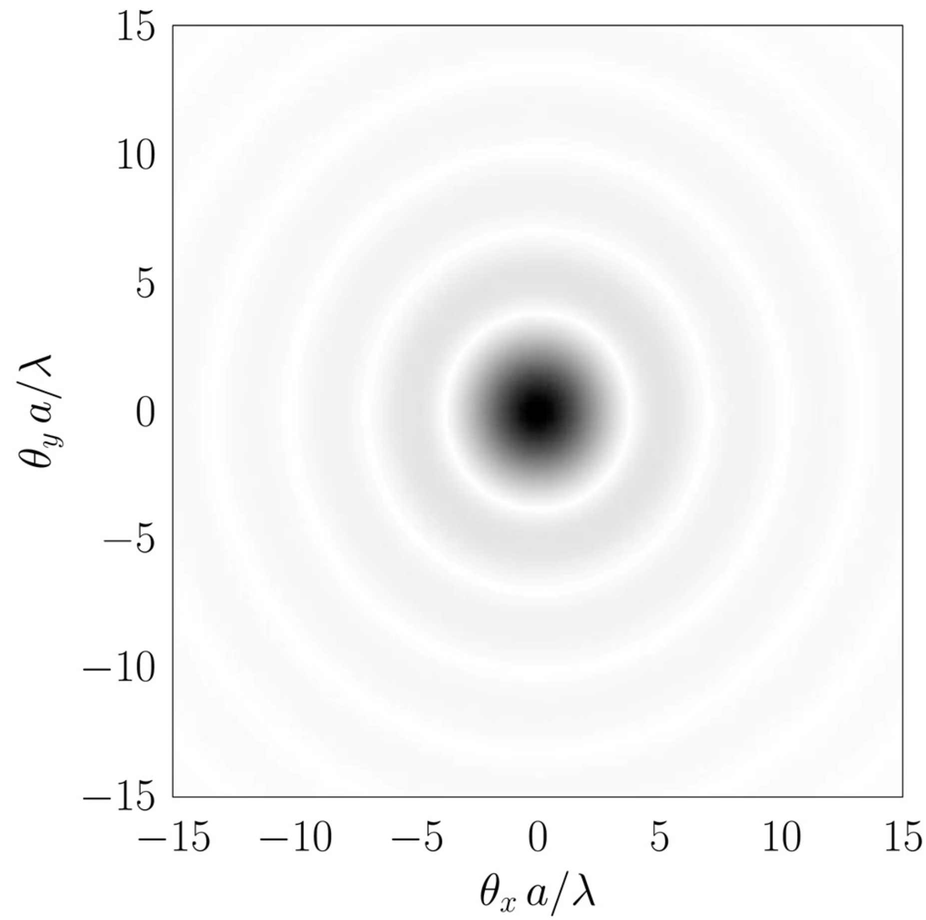

FIGURE 10.15
Far-field interference/diffraction pattern produced by a circular aperture of radius a. Darker regions indicate higher light intensity.

Oscillations and Waves

11 Wave Mechanics

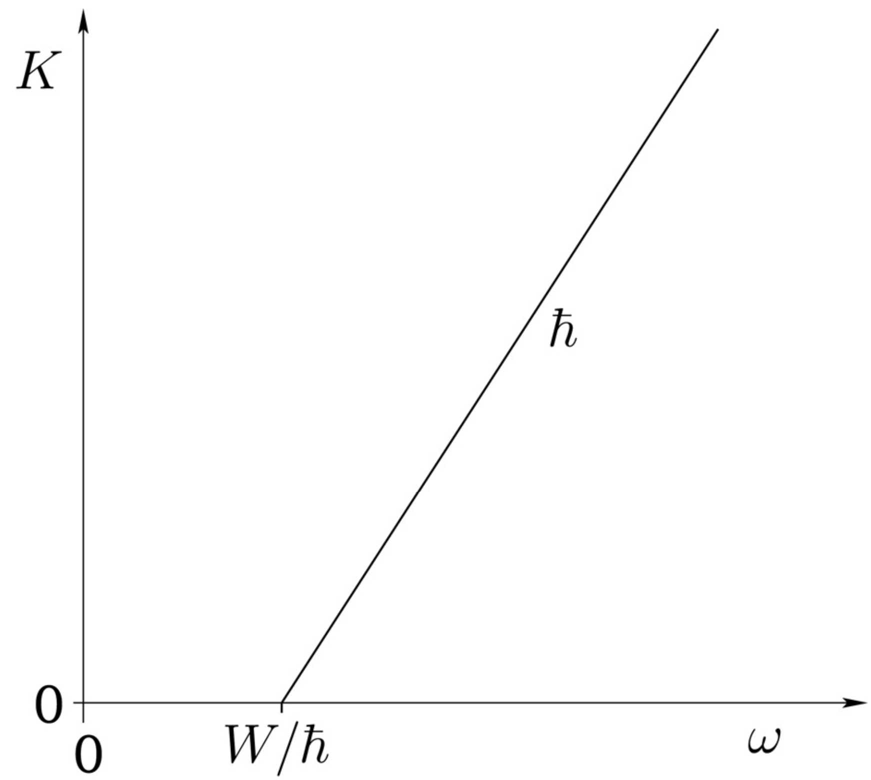

FIGURE 11.1
Variation of the kinetic energy K of photoelectrons with the wave angular frequency ω.

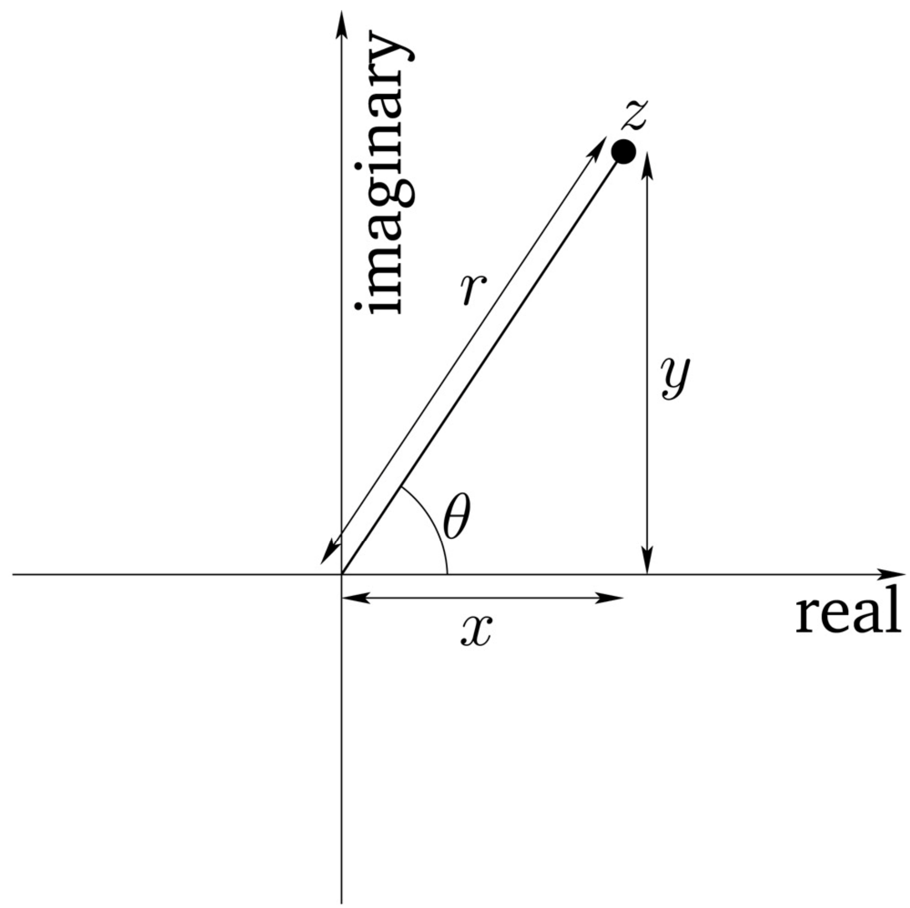

FIGURE 11.2
Representation of a complex number as a point in a plane.

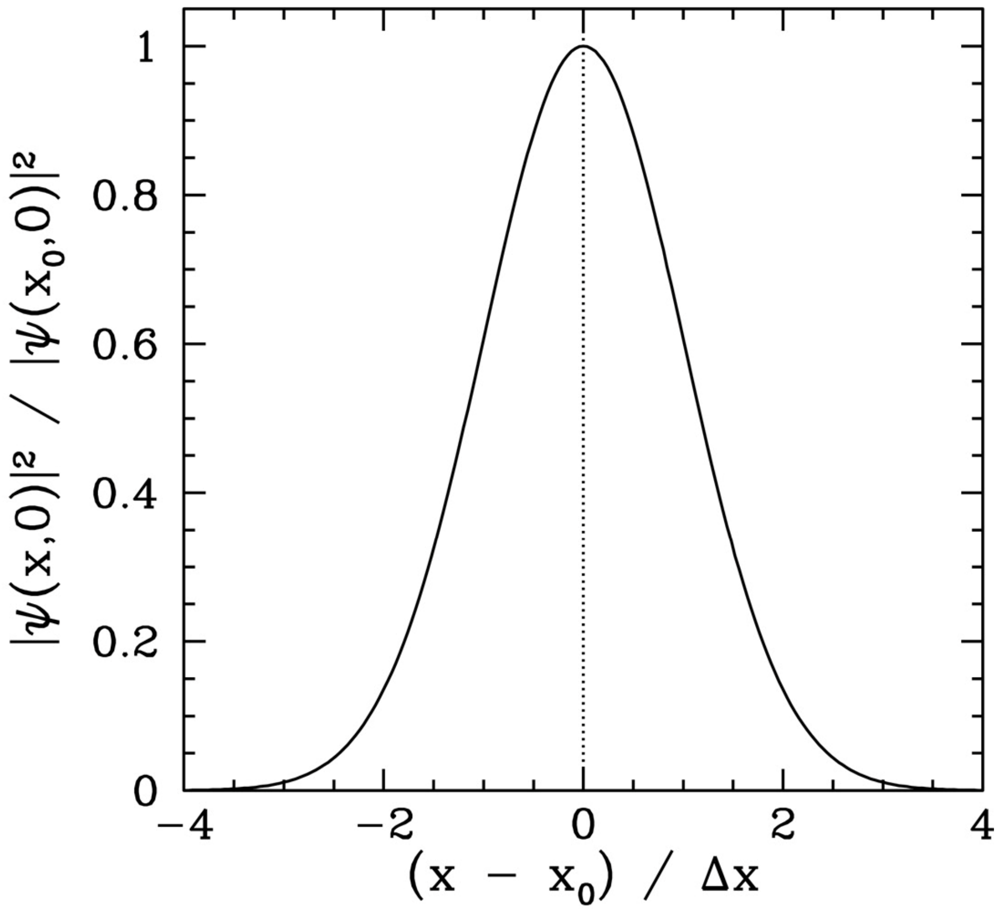

FIGURE 11.3
A one-dimensional Gaussian probability distribution.

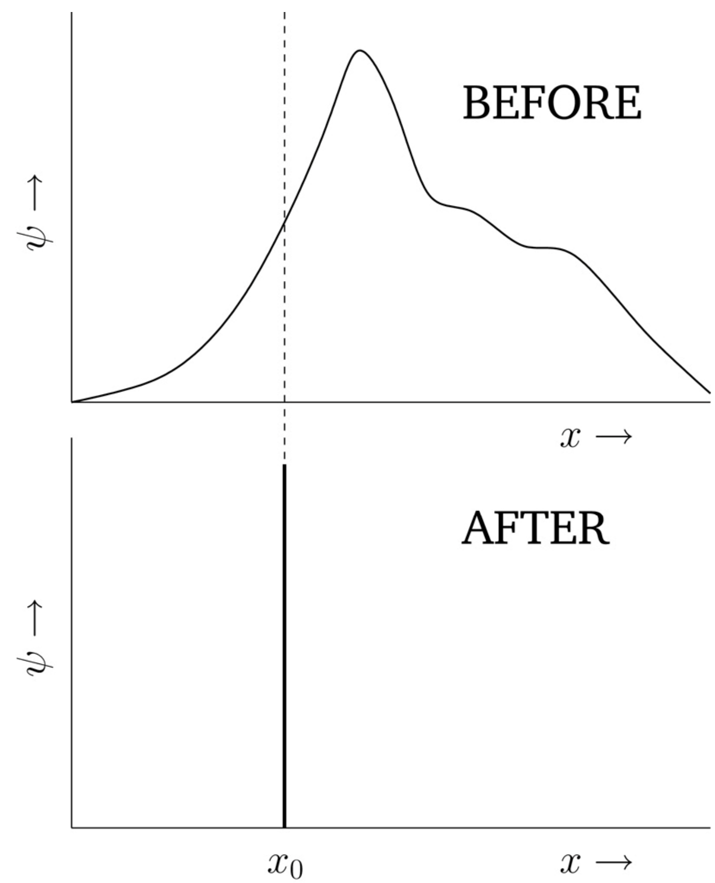

FIGURE 11.4
Collapse of the wavefunction upon measurement of *x*.

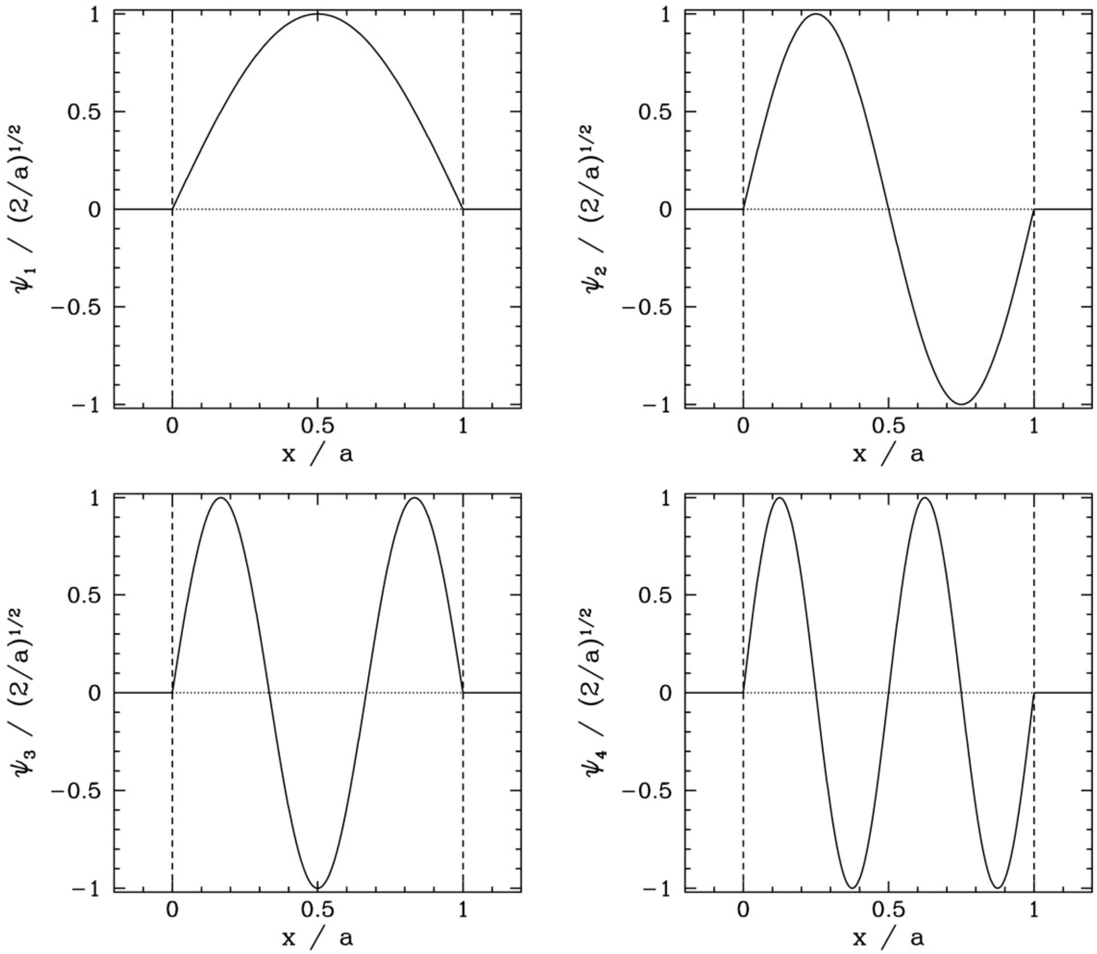

FIGURE 11.5
First four stationary wavefunctions for a particle trapped in a one-dimensional square potential well of infinite depth.

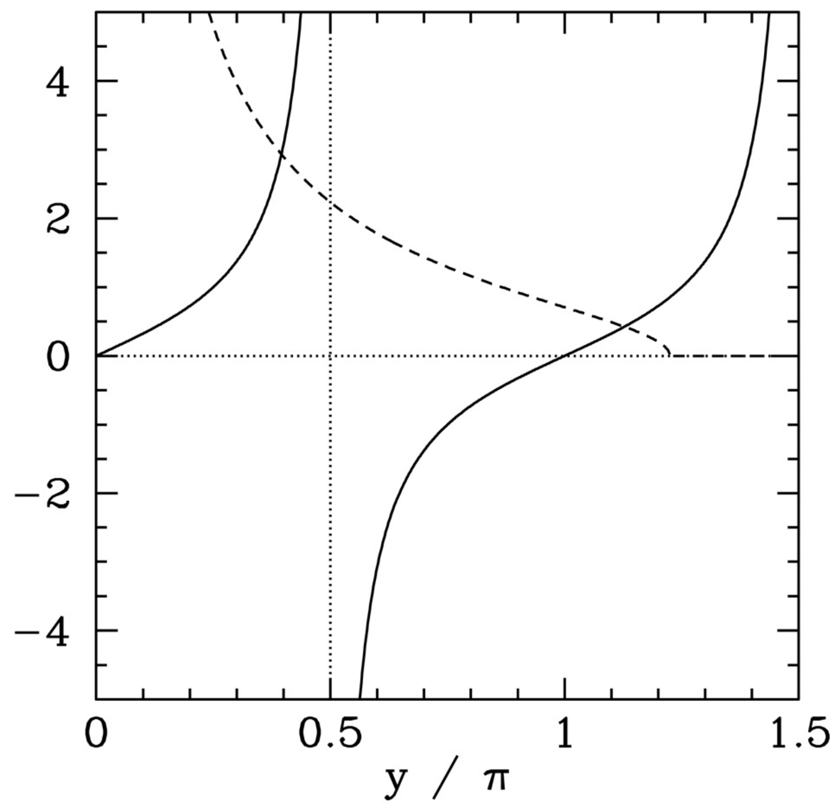

FIGURE 11.6
The curves $\tan y$ (solid) and $\sqrt{\lambda - y^2}/y$ (dashed), calculated for $\lambda = 1.5\,\pi^2$. The latter curve takes the value 0 when $y > \sqrt{\lambda}$.

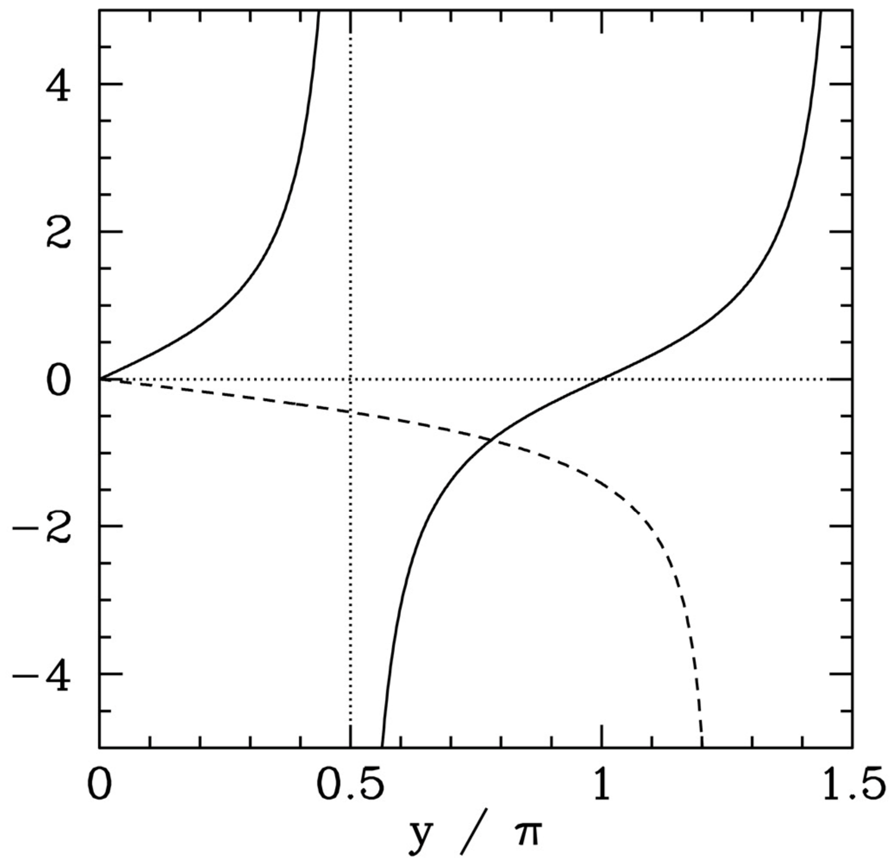

FIGURE 11.7
The curves $\tan y$ (solid) and $-y/\sqrt{\lambda - y^2}$ (dashed), calculated for $\lambda = 1.5\,\pi^2$.